

Evaluation of Pollutant Emissions from Portable Air Cleaners

Final Report: Contract No. 10-320

Prepared for the California Air Resources Board and
the California Environmental Protection Agency
Research Division
PO Box 2815
Sacramento CA 95812

Prepared by:
Hugo Destailats (principal investigator),
Mohamad Sleiman and William J. Fisk

Indoor Environment Group
Energy Analysis and Environmental Impacts Department
Environmental Energy Technologies Division
Lawrence Berkeley National Laboratory
1 Cyclotron Road
Berkeley, CA 94720

December 2014

Disclaimer

The statements and conclusions in this Report are those of the contractor and not necessarily those of the California Air Resources Board. The mention of commercial products, their source, or their use in connection with material reported herein is not to be construed as actual or implied endorsement of such products.

Table of Contents

List of Figures.....	vii
List of Tables.....	x
Abstract	xii
Executive Summary	xiii
Background.....	xiii
Methods.....	xiii
Results.....	xiv
Conclusions	xv
1. INTRODUCTION	1
1.1. Technologies considered in this study	2
1.2. Goals and scope of this study.....	5
MATERIALS AND METHODS.....	8
2. SELECTION AND PROCUREMENT OF AIR CLEANERS USED IN THIS STUDY.....	9
3. DEVELOPMENT OF A TESTING PROTOCOL FOR PORTABLE AIR CLEANERS.....	12
3.1. Room-Sized Experimental Chamber	12
3.2. Challenge pollutant mixture	14
3.3. Analytical methods for VOCs and aldehydes.....	15
3.4. Ozone Measurements and Ozone Chamber Deposition Rates	16
3.5. Ultrafine Particle Measurements	18
3.6. Analysis of Reactive Oxygen Species (ROS)	21
3.6.1. <i>Determination of ROS concentrations</i>	22
3.7. Preliminary Tests	26
RESULTS AND DISCUSSION.....	28
4. EXPERIMENTAL CHARACTERIZATION OF EMISSIONS FROM AIR CLEANERS	29
4.1. PAC1: PCO Air Cleaner	29
4.1.1. <i>Summary of observations</i>	29
4.1.2. <i>Ozone</i>	29
4.1.3. <i>VOCs</i>	31
4.1.4. <i>Ultrafine particles</i>	33

4.2. PAC2: Air Cleaner Combining HEPA / PCO / Catalyst	35
4.2.1. <i>Summary of observations</i>	35
4.2.2. <i>Ozone</i>	35
4.2.3. <i>VOCs</i>	37
4.2.4. <i>Ultrafine particles</i>	39
4.3. PAC3: PCO Air Cleaner with Ozone Generation.....	41
4.3.1. <i>Summary of observations</i>	41
4.3.2. <i>Ozone</i>	41
4.3.3. <i>VOCs</i>	43
4.3.4. <i>Ultrafine particles</i>	45
4.4. PAC4: Plasma Air Cleaner	47
4.4.1. <i>Summary of observations</i>	47
4.4.2. <i>Ozone</i>	47
4.4.3. <i>VOCs</i>	49
4.4.4. <i>Ultrafine particles</i>	51
4.5. PAC5: Ceramic Heater with Ionizer	53
4.5.1. <i>Summary of observations</i>	53
4.5.2. <i>Ozone</i>	56
4.5.3. <i>VOCs</i>	58
4.5.4. <i>Ultrafine particles</i>	61
4.6. PAC6: Heating Air Purifier	63
4.6.1. <i>Summary of observations</i>	63
4.6.2. <i>Ozone</i>	63
4.6.3. <i>VOCs</i>	65
4.6.4. <i>Ultrafine particles</i>	67
4.7. ROS measurements	69
5. EVALUATION OF THE IMPACTS OF AIR CLEANERS ON INDOOR AIR QUALITY	73
5.1. Determination of air flow in each device.....	73
5.2. Net Direct (Primary) Pollutant Emissions (Phase 1)	75
5.3. Net Pollutant Emissions or Removal in the Presence of Challenge Mixture (Phase 2)...	80
5.3.1. <i>Pollutant emission and removal rates in Phase 2</i>	80
5.3.2. <i>Yields of Byproducts Generated in the Air Cleaning Process</i>	84
5.3.3. <i>Evaluation of VOC removal effectiveness</i>	85
5.4. Predicted Impacts on Typical Indoor Scenarios	91
5.4.1. <i>Indoor Pollutant Levels Predicted through a Material-Balance Model</i>	91
5.4.2. <i>Potential Health Implications</i>	98

6. SUMMARY, CONCLUSIONS AND RECOMMENDATIONS	102
References	104
List of Publications Generated by this Study.....	112
Glossary of Terms, Abbreviations and Symbols.....	113
APPENDICES	115
APPENDIX 1. DEVELOPMENT OF SAMPLING AND ANALYTICAL METHODS FOR THE QUANTIFICATION OF ROS	116
<i>A.1.1. Development of calibration curves for the three fluorescent probes</i>	116
<i>A.1.2. Development of the ROS sampling method</i>	119
<i>A.1.3. Effect of ozone on ROS sampling</i>	122
APPENDIX 2. SUMMARY OF MEASUREMENTS OF EXPERIMENTS DESCRIBED IN SECTION 4.....	126
APPENDIX 3. CHAMBER CONCENTRATION REDUCTION FACTORS ω_i AND SINGLE-PASS REMOVAL EFFICIENCY $\phi_i^{p,ss}$ DESCRIBED IN SECTION 5.....	133

List of Figures

Figure 3.1.1. LBNL's 20-m ³ environmental chamber	12
Figure 3.1.2. Schematic representation of pollutant concentration profiles observed during Phase 1 and Phase 2.	13
Figure 3.4.1. Ozone decay curves in the LBNL environmental chamber	17
Figure 3.5.1: Concentration profiles of chamber ultrafine particle (UFP, >5 nm) background levels	18
Figure 3.5.2: Daily average ultrafine particle (UFP, >5 nm) concentration (\pm standard deviation).	19
Figure 3.5.3: Chamber experimental parameters during the same studied period: Daily and whole-period average.	20
Figure 3.6.1: Experimental setup to sample directly from the air cleaner's outlet	23
Figure 3.6.2: Equivalent aqueous H ₂ O ₂ and HTPA concentrations determined for the air cleaners (green) and for an ozone generator (blue).	24
Figure 4.1.1: Ozone concentration profiles for Phase 1	30
Figure 4.1.2: Ozone concentration profiles for Phase 2	30
Figure 4.1.3: Average ozone chamber concentrations during periods with air cleaner off and on in Phase 1 and Phase 2.	31
Figure 4.1.4: Individual VOC & aldehyde concentrations measured in Phase 1 experiments.	32
Figure 4.1.5: Individual VOC & aldehyde concentrations measured in Phase 2 experiments	32
Figure 4.1.6: Ultrafine particle (UFP, >5 nm) concentration profiles for Phase 1.	33
Figure 4.1.7: Ultrafine particle (UFP, >5 nm) concentration profiles for Phase 2.	34
Figure 4.1.8: Average ultrafine particle (UFP, >5 nm) concentration during periods with air cleaner off and on	34
Figure 4.2.1: Ozone concentration profiles for Phase 1	36
Figure 4.2.2: Ozone concentration profiles for Phase 2	36
Figure 4.2.3: Average ozone chamber concentrations during periods with air cleaner off and on in Phase 1 and Phase 2.	37
Figure 4.2.4: Individual VOC & aldehyde concentrations measured in Phase 1 experiments.	38
Figure 4.2.5: Individual VOC & aldehyde concentrations measured in Phase 2 experiments	38
Figure 4.2.6: Ultrafine particle (UFP, >5 nm) concentration profiles for Phase 1.	39
Figure 4.2.7: Ultrafine particle (UFP, >5 nm) concentration profiles for Phase 2.	39
Figure 4.2.8: Average ultrafine particle (UFP, >5 nm) concentration during periods with air cleaner off and on	40
Figure 4.3.1: Ozone concentration profiles for Phase 1	42
Figure 4.3.2: Ozone concentration profiles for Phase 2	42
Figure 4.3.3: Average ozone chamber concentrations during periods with air cleaner off and on in Phase 1 and Phase 2.	43
Figure 4.3.4: Individual VOC & aldehyde concentrations measured in Phase 1 experiments.	44
Figure 4.3.5: Individual VOC & aldehyde concentrations measured in Phase 2 experiments	44

Figure 4.3.6: Ultrafine particle (UFP, >5 nm) concentration profiles for Phase 1.	45
Figure 4.3.7: Ultrafine particle (UFP, >5 nm) concentration profiles for Phase 2.	46
Figure 4.3.8: Average ultrafine particle (UFP, >5 nm) concentration during periods with air cleaner off and on	46
Figure 4.4.1: Ozone concentration profiles for Phase 1	48
Figure 4.4.2: Ozone concentration profiles for Phase 2	48
Figure 4.4.3: Average ozone chamber concentrations during periods with air cleaner off and on in Phase 1 and Phase 2.	49
Figure 4.4.4: Individual VOC & aldehyde concentrations measured in Phase 1 experiments.	50
Figure 4.4.5: Individual VOC & aldehyde concentrations measured in Phase 2 experiments	50
Figure 4.4.6: Ultrafine particle (UFP, >5 nm) concentration profiles for Phase 1.	51
Figure 4.4.7: Ultrafine particle (UFP, >5 nm) concentration profiles for Phase 2.	52
Figure 4.4.8: Average ultrafine particle (UFP, >5 nm) concentration during periods with air cleaner off and on	52
Figure 4.5.1: Chamber temperature measured for the operation of PAC5 as a heater/ionizer during Phase 1 and Phase 2.	54
Figure 4.5.2: Chamber relative humidity measured for the operation of PAC5 as a heater/ionizer during Phase 1 and Phase 2	55
Figure 4.5.3: Ozone concentration profiles for Phase 1 (ionizer only)	56
Figure 4.5.4: Ozone concentration profiles for Phase 2 (ionizer only)	57
Figure 4.5.5: Average ozone chamber concentrations during periods with air cleaner off and on in Phase 1 and Phase 2. (ionizer only)	57
Figure 4.5.6: Individual VOC & aldehyde concentrations measured in Phase 1 experiments.	59
Figure 4.5.7: Individual VOC & aldehyde concentrations measured in Phase 2 experiments	60
Figure 4.5.8: Ultrafine particle (UFP, >5 nm) concentration profiles for Phase 1 (heater + ionizer)	61
Figure 4.5.9: Ultrafine particle (UFP, >5 nm) concentration profiles for Phase 2. (heater + ionizer)	62
Figure 4.5.10: Average ultrafine particle (UFP, >5 nm) concentration during periods with air cleaner off and on (heater + ionizer)	62
Figure 4.6.1: Ozone concentration profiles for Phase 1	64
Figure 4.6.2: Ozone concentration profiles for Phase 2	64
Figure 4.6.3: Average ozone chamber concentrations during periods with air cleaner off and on in Phase 1 and Phase 2.	65
Figure 4.6.4: Individual VOC & aldehyde concentrations measured in Phase 1 experiments.	66
Figure 4.6.5: Individual VOC & aldehyde concentrations measured in Phase 2 experiments	66
Figure 4.6.6: Ultrafine particle (UFP, >5 nm) concentration profiles for Phase 1.	67
Figure 4.6.7: Ultrafine particle (UFP, >5 nm) concentration profiles for Phase 2.	67
Figure 4.6.8: Average ultrafine particle (UFP, >5 nm) concentration during periods with air cleaner off and on	68
Figure 4.7.1: ROS concentrations determined in the chamber using the DCFH fluorescent probe	70
Figure 4.7.2: ROS concentrations determined in the chamber using the AuR fluorescent probe	71

Figure 4.7.3: ROS concentrations determined in the chamber using the TPA fluorescent probe.	72
Figure 5.1.1: Determination of air flow rate through devices	73
Figure 5.2.1: Parameters used in this study	75
Figure 5.2.2: Emission and removal rates of key VOCs, UFP and ozone for each device, Phase 1	79
Figure 5.3.1: Emission and removal rates of key VOCs, UFP and ozone for each device, Phase 2	83
Figure 5.3.2: VOC chamber concentration reduction factor ω_i as a function of the single-pass removal efficiency $\varphi^{p,ss}$	88
Figure 5.3.3: PM chamber concentration reduction factor ω_i as a function of the single-pass removal efficiency $\varphi^{p,s}$	90
Figure 5.4.1: Reported conversion of limonene and ozone in chamber studies	97
Figure A.1.1. Determination of the waiting period required for the reactions involving the probes DCFH and AuR.	117
Figure A.1.2. Calibration curves for ROS determined with the three fluorescent probes: (a) DCFH; (b) AuR; and (c) TPA	118
Figure A.1.3. Experimental setup used to develop the ROS sampling method	120
Figure A.1.4. Equivalent H ₂ O ₂ and HTPA concentrations determined in the presence of ozone	122
Figure A.1.5. Schematic representation of chemical processes in aqueous solution leading to formation of ROS from ozone decomposition	124
Figure A.1.6: Equivalent H ₂ O ₂ determined with the DCFH method at three collection temperatures, by sampling 50 L of air containing 470 ppb O ₃ (g)	125

List of Tables

Table 1.2.1: Indoor VOC concentrations reported in the literature.	7
Table 2.1.1: Air cleaners tested in this study.	11
Table 3.2.1: Pollutants used in the challenge mixture used in Phase 2	15
Table 3.6.1: Fluorescent probes used in ROS measurements	21
Table 3.6.2: Determination of ROS levels emitted by PAC4	25
Table 4.1.1: Experimental conditions used in experiments with PAC1	29
Table 4.2.1: Experimental conditions used in experiments with PAC2	35
Table 4.3.1: Experimental conditions used in experiments with PAC3	41
Table 4.4.1: Experimental conditions used in experiments with PAC4	47
Table 4.5.1: Experimental conditions used in experiments with PAC5	53
Table 4.6.1: Experimental conditions used in experiments with PAC6	63
Table 4.7.1: Blank levels determined during OFF periods in the determination of ROS concentrations	69
Table 5.1.1: Air flow through each air cleaner considered in this study	74
Table 5.2.1: Net emission rates (E_i , in red) or removal rates (R_i , in black) determined in Phase 1	78
Table 5.3.1: Net emission rates (E_i , in red) or removal rates (R_i , in black) determined in Phase 2	82
Table 5.3.2: Yield of byproducts observed in Phase 2	85
Table 5.3.3: Determination of the recycle ratio for each experiment in Phase 2	87
Table 5.4.1: Parameters used to model the two indoor scenarios	91
Table 5.4.2: Values reported in the literature for ozone deposition velocities, v_d^o	93
Table 5.4.3: Pollutant concentration change ΔC_i ($\mu\text{g m}^{-3}$) in Scenario 1 based on results from Phase 2	95
Table 5.4.4: Pollutant concentration change ΔC_i ($\mu\text{g m}^{-3}$) in Scenario 2 based on results from Phase 2.	96
Table 5.4.5: Health-based reference levels for pollutants studied in this study	99
Table 5.4.6: Indoor and outdoor UFP particle sizes reported in recent studies	100
APPENDICES	
Table A.1.1: Analytical figures of merit for ROS quantification using DCFH, AuR and TPA.	119
Table A.1.2: Experimental conditions and results for H_2O_2 collection efficiency with each fluorescent probe.	121
Table A.2.1: Pollutant concentrations measured in PAC1 experiments	126
Table A.2.2: Pollutant concentrations measured in PAC2 experiments	127
Table A.2.3: Pollutant concentrations measured in PAC3 experiments	128
Table A.2.4: Pollutant concentrations measured in PAC4 experiments	129

Table A.2.5: Pollutant concentrations measured in PAC5 experiments with heating and ionizer	130
Table A.2.6: Pollutant concentrations measured in PAC5 experiments with only ionizer	131
Table A.2.7: Pollutant concentrations measured in PAC6 experiments	132
Table A.3.1: VOC removal efficiency parameters corresponding to four air cleaners that showed net VOC elimination.	133
Table A.3.2: UFP removal efficiency parameters corresponding to two air cleaners that showed net elimination of particulate matter.	133

Abstract

A new generation of portable standalone air cleaners relies on photocatalytic oxidation, plasma generation and microbial thermal inactivation. These technologies can generate potentially harmful byproducts, including volatile organic compounds (VOCs), ozone, ultrafine particles (UFP) and/or reactive oxygen species. Emissions originating from six portable air cleaners were investigated using a 20-m³ room-sized environmental chamber under realistic conditions. Pollutant concentrations were determined with the air cleaners operating in clean air and in the presence of a challenge VOC mixture. Four devices removed between 8% and 29% of VOCs at rates between 600 and 1700 µg h⁻¹, while the other two emitted VOCs at rates of 300 – 1400 µg h⁻¹. Two devices showed good particle removal efficiency, reducing the UFP number concentration by 35% to 90%. Primary emissions (e.g., 85 µg h⁻¹ toluene) and secondary oxidation byproducts (e.g., 16 µg h⁻¹ formaldehyde) were observed. One device emitted very high ozone levels (up to 6 mg h⁻¹), which also produced UFP in the presence of VOCs, reaching concentrations of 3 x 10³ particles per cm³. Modeling results using chamber-derived emissions rates suggested that ozone emitted by one device can exceed regulatory levels. Formaldehyde emissions were predicted to exceed California reference exposure levels for three devices, and benzene emissions were predicted for two devices to exceed Proposition 65 risk levels.

Executive Summary

Background

Due to the lack of prior research, standards or regulations pertaining to the pollutant emissions by indoor air cleaners, there is a poor understanding of the effectiveness of most devices and little information on emissions from a diverse set of products available in the market. In some cases, indoor air quality (IAQ) benefits claimed by manufacturers may be overstated, or air cleaners may pose risks as a result of pollutant emissions. Nearly one million Californians may be exposed to potentially harmful pollutants emitted by these devices. Poorly engineered portable air cleaners may negatively impact IAQ through emissions of ozone, volatile organic compounds (VOCs), particulate matter (PM) and/or reactive oxygen species (ROS). Several products often integrate filtration and other conventional approaches with emerging technologies for which emissions have not been fully characterized. The objective of this study is to evaluate the primary and secondary emissions of indoor air pollutants by devices commercialized as portable air cleaners in California, with emphasis on a new generation of equipment integrating several emerging technologies. Emissions from photocatalytic oxidation (PCO) devices were evaluated. PCO air cleaners rely on oxidation of VOCs in contact with a titanium dioxide catalyst irradiated with UV light. This reaction initiates a series of sequential oxidation steps that form intermediate organic species and final inorganic products such as CO₂ and water. Partially oxidized byproducts may be emitted by the device during the PCO treatment of indoor air. The application of non-thermal plasma to air cleaning was also evaluated. This technology has shown promise in the elimination of indoor air pollutants, but with simultaneous formation of ozone. Other technologies evaluated in this study include the use of heated ceramics and ionizers, and microbial inactivation technologies applying fast heating processes, all of which may be a source of VOCs, ozone and aerosol particles. Emissions were determined in realistic indoor conditions in clean air and in the presence of a challenge VOC mixture. The resulting impacts of emitted pollutants on indoor air quality were assessed for model residential scenarios.

Methods

This study assessed primary and secondary pollutant emissions from six portable air cleaners that included three PCO devices (in some cases combined with filtration), a plasma generator, a ceramic heater/ionizer and an antimicrobial heating device. The devices were selected in consultation with ARB, and purchased from online vendors or directly from the manufacturers. Laboratory methods were developed to characterize pollutant emissions from air cleaners, building upon the previous work performed in this area by LBNL. The primary emissions from the devices were determined in a 20-m³ stainless-steel environmental chamber in clean air (Phase 1), and originated in off-gassing from electronic and plastic materials, as well as in the release of ozone and reactive oxygen species by some of the devices. Emissions of primary and secondary pollutants were also determined in the presence of a challenge VOC mixture (Phase 2). The challenge mixture included 11 VOCs that are typically found indoors, at realistic levels (low ppb range), corresponding to a range of chemical functionalities that

included aldehydes, alcohols, aromatic hydrocarbons, aliphatic hydrocarbons and terpenes among others. Samples were collected from the chamber during periods in which the air cleaner was turned off and turned on, and emissions were determined using a mass-balance model. Volatile carbonyls, VOCs, ozone and ultrafine particles (UFPs) were determined using established methods that have been used previously in our laboratory. Carbonyls were collected in dinitrophenyl hydrazine (DNPH)-coated silica cartridges that were subsequently extracted and analyzed by liquid chromatography. Sorbent tubes were used to collect VOC samples, and were analyzed by thermal desorption/gas phase/mass spectrometry (TD/GC/MS). Ozone and UFPs were measured continuously using a photometric analyzer and a water-based condensation particle counter (W-CPC), respectively. Three methods to sample and analyze ROS relying in their reaction with a fluorometric probe were developed for this study. In each case, air samples were collected in an impinger filled with buffer and reacted with a probe yielding a fluorescent byproduct, analyzed spectrophotometrically.

Results

In Phase 1, net pollutant emission and removal rates were determined for the studied devices operating under a clean air atmosphere. Very high ozone emissions were observed from one of the PCO air cleaners (6 mg h^{-1}), and lower but measureable ozone emissions from the plasma device (0.07 mg h^{-1}). The three methods developed in this study to detect ROS were successfully used, with consistent results. The devices did not appear to emit ROS in measurable levels, except for the plasma air cleaner when sampling directly at the air outlet. Two devices removed particulate matter (a PCO provided with HEPA filtration and the plasma device), and four showed a net emission of VOCs higher than $10 \text{ } \mu\text{g h}^{-1}$ (two PCO devices and two ceramic heaters). Emission rates of individual compounds were in the range $5 - 90 \text{ } \mu\text{g h}^{-1}$. In Phase 2, net pollutant emission and removal rates were determined in the presence of the challenge VOC mixture. Ozone and ROS emission trends, as well as particulate matter removal trends, were similar to those observed in Phase 1. Due to the presence of ozone-reacting VOCs (limonene and styrene), the device that emitted high levels of ozone became a source of ultrafine particles due to the nucleation of oxidation byproducts and agglomeration of new particles, with chamber concentrations of $3 \times 10^3 \text{ particles cm}^{-3}$. Four of the six air cleaners removed a measurable amount of VOCs present in the challenge mixture (removal rates in the range $600 - 1700 \text{ } \mu\text{g h}^{-1}$), while the other two devices (a PCO air cleaner and a ionizer/ceramic heater) emitted VOCs with emission rates of $300 - 1400 \text{ } \mu\text{g h}^{-1}$. Comparing with Phase 1 results, both VOC emission and removal rates were roughly one order of magnitude higher in Phase 2 due to the presence of higher levels in the challenge mixture. In the case of devices that removed VOCs in Phase 2 experiments, the fraction of those compounds eliminated from indoor air was between 8 and 29%. Considering emissions of individual VOCs, formaldehyde is produced as a byproduct by two of the three PCO devices, and also as a byproduct of the plasma air cleaner. The formaldehyde emission rates were between 25 and $33 \text{ } \mu\text{g h}^{-1}$ in Phase 2. Other VOCs emitted at high levels by at least one air cleaner in Phase 2 include toluene and benzaldehyde, presumably due to emissions from plastic constituents.

The emission rates and byproduct yields determined in this study were used to predict the expected indoor concentration changes for each pollutant due to operation of each air cleaner under two model scenarios. A first-order material-balance model was applied to establish pollutant levels in each case. The two typical residential scenarios considered were (1) three air cleaners operating simultaneously in different rooms of a 1,500-ft² house ventilated according to ASHRAE 62.2 ventilation rates, and (2) a single air cleaner operating in a small furnished bedroom with door closed and minimum ventilation. Potential health implications were evaluated by comparing predicted pollutant levels in both scenarios with reference exposure levels (RELs) listed by the California EPA's Office of Environmental Health Hazard Assessment, with the State's air quality standards for ozone, with the ARB's regulation for ozone-emitting air cleaners, and with Proposition 65 "safe harbor" levels for no significant risk levels (NSRLs) of carcinogens and maximum allowable dose levels (MADLs) for chemicals causing reproductive toxicity. By comparing those reference levels with those predicted in the two model scenarios we observed that most VOCs were either emitted or removed in amounts that were far smaller than health-based exposure levels, and likely did not contribute to any major change in indoor air quality. However, hazardous levels were exceeded by ozone, formaldehyde and benzene in one of the scenarios. In the case of UFPs, while there are no similar guidelines, the emissions arising from ozone reaction with reactive VOCs led to chamber levels that were comparable to those measured in California homes.

Conclusions

This study showed emissions of primary and secondary pollutants from portable air cleaners, which in some cases may lead to indoor levels that can affect occupant's health. In particular, one device emitted extremely high levels of ozone, which in the presence of reactive VOCs led also to the formation of ultrafine particulate matter. Operation of this device in a poorly ventilated room was predicted to exceed regulatory ozone levels. Several air cleaners emitted formaldehyde at rates that could contribute to indoor concentrations of this harmful indoor pollutant. ROS emissions were detected from a plasma air cleaner, and two devices (a PCO and a ionizer/ceramic heater) resulted in net emissions, rather than removal, of VOCs. These findings will help the State assist the public in making informed decisions when purchasing and using portable air cleaners, and will help ARB identify which health and indoor air quality concerns associated with new technologies need to be further addressed. These results, along with those from other recent studies, can contribute to the development of effective standard testing procedures, such as ASTM or ISO methods, which are needed to control harmful emissions and verify the validity of marketing claims. The implementation and adoption of widely accepted testing and rating methods can develop over time the comprehensive body of evidence required to determine whether regulation is needed. In addition, this research may help manufacturers develop the appropriate engineering controls needed to prevent harmful pollutants from being released indoors. Those controls may include, for example, removing the sources of ozone, or the use of filters and/or catalysts to maximize VOC abatement.

[This page is intentionally left blank]

1. INTRODUCTION

In a 2006 survey, 14% of California's 12 million households reported ownership or use of portable air cleaner during the previous five years (Piazza et al, 2006), which included a majority of electrostatic precipitators (ESPs), ionizers and ozone generators (OGs). Another study of 108 new California homes found that portable air cleaners were regularly used in 17% of them (Offermann, 2009). Some of those devices may negatively impact indoor air quality (IAQ) through emissions of ozone (O₃) (Phillips and Jakober, 2006; Jakober and Phillips, 2008). Nearly one million Californians may be exposed to potentially harmful pollutants emitted by poorly engineered air cleaning devices. Increasing public awareness of the deleterious health effects of indoor ozone is likely driving consumers to seek alternative products available in a dynamic multi-million dollar market. Several new products combine new technologies such as plasma, photocatalytic oxidation (PCO) and other technologies in integrated devices. While ozone emissions remain a concern, formaldehyde and other partially oxidized VOCs may be generated as undesired byproducts of chemical processes taking place inside the air cleaner unit.

A recent review of portable air cleaning technologies available in North America, Europe and Asia (Zhang et al, 2011) reached the following conclusions:

- (1) no single technology is able to remove all indoor pollutants;
- (2) in many cases undesirable by-products were generated during the operation of the devices;
- (3) filtration is efficient in removing particles, but used filters can be a source of sensory pollution;
- (4) sorption of some gaseous pollutants (VOCs, formaldehyde, O₃, NO₂, SO₂, and H₂S) is efficient if the system is properly designed and operated, but it may produce byproducts if ozone reacts with adsorbed contaminants.
- (5) UV germicide inactivation (UVGI) is an effective method to inactivate some airborne microorganisms, but ozone may be produced in some cases;
- (6) PCO can reduce concentrations of some VOCs and formaldehyde, but may also generate harmful by-products that need to be controlled; catalyst poisoning is a long-term problem that needs to be understood;
- (7) plasma can reduce concentrations of particulates and some VOCs, but can also produce harmful byproducts including ozone and oxidation intermediates. In addition, its energy consumption can be high;
- (8) ozone is not recommended due to the formation of harmful by-products;

- (9) not enough information is available on the long-term performance and required maintenance of most air cleaning systems;
- (10) better performance criteria and standardization methods to evaluate air cleaners should be developed, including labeling systems.

1.1. Technologies considered in this study

Photocatalytic oxidation (PCO) devices typically utilize a honeycomb monolith or other high-surface area support, coated with titanium dioxide (TiO_2 or titania). The support is irradiated with fluorescent bulbs with peak irradiance near either 254 nm (UVC) or 365 nm (UVA). The choice of the lamp used in PCO air cleaners is critical to avoid simultaneous emissions of ozone. Light emission from the fluorescence of mercury vapor inside the lamps comprises various lines, from which the most intense are the one at 254 nm (also called often "germicidal") and at 185 nm (also called vacuum ultraviolet, or VUV). Quartz is used to build the lamp due to its excellent UV transparency. However, various modifications are implemented on the quartz to influence the spectrum and intensity of the light transmitted through the material, including:

- (1) An internal protective coating that extends the lamp's lifetime by reducing the amounts of mercury oxide (HgO) that deposits on the inner surfaces, thus slowing down lamp aging. Materials used for these coatings include transparent metal oxide layers of yttrium (Y_2O_3) or aluminum (Al_2O_3), both of which have good transmittance in the UV-region, and can effectively protect the quartz wall against adsorption and reaction of mercury. Y_2O_3 can be used only for lamps emitting primarily at 254 nm, because its transmission in the VUV-region is too low. Hence, it may filter effectively the ozone-forming radiation. On the other hand, Al_2O_3 has an excellent transmittance at both 254 nm and 185 nm (Voronov, 2008).
- (2) The composition of the quartz itself can be "tuned" to enable more or less VUV light to be transmitted through it. This can be achieved by doping the quartz with metals. The doped quartz is often referred to as "ozone-free quartz" by manufacturers, and can effectively filter UV light of wavelength < 220 nm (e.g., Shin-Etsu Quartz Products Co., 2014).
- (3) Several PCO units use UVA light (also called "blacklight"), rather than UVC light. The basic design of UVA lamps is the same, except that these lamps are coated with phosphors that absorb the 185 nm and 254 nm mercury lines and emit a broader spectrum centered around 365 nm (Forbes et al, 1976). The composition of the phosphors used for UVA lamps currently includes either europium-doped strontium fluoroborate or lead-activated calcium metasilicate. These coatings prevent effectively the formation of ozone.

In PCO air cleaners, air flows through the monolith, where the VOCs adsorb reversibly on the catalyst and are oxidized by reactive surface species formed upon irradiation. Briefly, the semiconductor acts as a sensitizer for light-induced redox processes through an electron–hole separation upon absorption of a photon of energy that equals or exceeds the semiconductor bandgap energy. Excited-state electrons and holes can recombine, or else be trapped in metastable surface states and react with electron donors and acceptors adsorbed on the catalyst surface. In many cases, oxidation proceeds through the formation of surface-bound hydroxyl (OH) radicals upon trapping of a hole by a TiOH hydrated surface functionality of TiO₂. These surface groups are highly reactive towards the adsorbed VOCs, initiating a series of oxidation steps conducive to the production of intermediate organic species and final inorganic products such as CO₂ and water (a process often referred to as *mineralization*) (Hoffmann et al, 1995). Effective and fast photocatalytic oxidation of several VOCs has been reported (Boularnanti et al, 2008; Ao and Lee, 2005; Cheng and Zhang, 2008; Yu et al, 2006). PCO and other technologies using short-wave UV radiation (wavelength < 300 nm) may generate highly reactive species, such as hydroxyl and peroxy radicals (Thiebaud, 2010; Bahrini et al, 2010). Those short-lived species are very effective oxidizing agents towards target VOCs inside the air cleaner. Fine and ultrafine particles are also expected to be emitted from air cleaners using new technologies such as the ceramic heating. The potential health effects of these oxidizing agents are associated with irritation of the respiratory tract. Integrated devices are capturing a growing market share; the results from this study will help evaluate potential IAQ and public health impacts of these new generation devices. In addition, this research may help the development of appropriate engineering controls to prevent these pollutants being released to the gas phase (e.g., use of filters or catalysts downstream of the PCO stage).

There is a growing interest in the use of non-thermal plasma for air cleaning applications. Microplasma systems of small size and low discharge voltage have shown good efficiency in the elimination of indoor air pollutants such as formaldehyde, albeit with simultaneous formation of ozone (Shimizu et al, 2011). In general plasma is effective in removing aerosol particles, but it has only limited efficiency in the elimination of VOCs, and the formation of ozone and NO_x limits its applicability (Zhang et al, 2011). However, the combination of plasma with photocatalysis shows an interesting synergism by integrating the fast kinetics of chemical processes initiated by the plasma with the more complete mineralization achieved by photocatalytic mechanisms (Thevenet et al, 2007). In addition, combined plasma and PCO systems were shown to be effective in the combined elimination of particulates (by the plasma) and gaseous pollutants (by the PCO, including ozone produced by the plasma) (Park et al, 2008). The proposed mechanisms for the degradation of toluene by non-thermal plasma (DC corona discharge) showed the predominant role of hydroxyl radicals in the initiation and propagation steps through addition to the aromatic ring and H-atom abstraction (Van Durme et al, 2007). Plasma air cleaners were also shown to be effective in microbial inactivation (Liang et al, 2012; Nishikawa and Nojima, 2003).

Other technologies of interest include the use of ceramic and transition metal oxides that adsorb and/or remove formaldehyde at room temperature (Yu et al, 2013; Sidheswaran et al, 2011) and microbial inactivation technologies in ultra-high temperature processes in short residence times (Damit et al, 2013; Jung et al, 2010; Jung et al, 2009), often in combination with ceramic and zeolite surfaces (Ji et al, 2007; Cheng et al, 2012).

Characterization of ozone emissions by OGs, ESPs and ionizers has been carried out by ARB staff and other investigators (Phillips and Jakober, 2006; Jakober and Phillips, 2008; Tung et al, 2005; Britigan et al, 2006). Several other studies on portable air cleaners evaluated their effectiveness at removing aerosol particles (Britigan et al, 2006; Ward et al, 2005; Shaughnessy et al, 1994; Shaughnessy et al, 2006), microbes (Macintosh et al, 2008) and VOCs (Cheng et al, 1998; Howard-Reed et al, 2008a; Howard-Reed et al, 2008b). However, little attention has been paid to the generation of secondary organic pollutants formed during the operation of portable air cleaning devices. Ultrafine particles have been observed to be formed by operation of OGs and ESPs (Alshawa et al, 2007; Hubbard et al, 2005; Waring et al, 2008). In recent work, our group at LBNL has investigated the performance of a prototype in-duct whole-building photocatalytic oxidation (PCO) air cleaner. We observed and quantified the formation of volatile aldehydes and carboxylic acids as partial oxidation byproducts upon challenging the device with realistic indoor VOC mixtures (Hodgson et al, 2007a; Hodgson et al, 2007b). Using the same approach, the performance of a TiO₂-coated PCO quartz fiber filter was optimized to maximize pollutant removal and minimize byproduct formation (Destailats et al, 2012). Those results, together with more recent bench-scale studies performed in our laboratory (Quici et al, 2010; Kibanova et al, 2012; Kibanova et al, 2009), suggested that PCO air cleaners, when operated under certain conditions and in the absence of additional downstream treatment, may constitute a significant source of harmful byproducts such as formaldehyde. Similar results have also been described by other authors (Ginestet et al, 2005; Sun et al, 2008; Mo et al, 2009), further illustrating that the yield of secondary pollutants is highly dependent on experimental conditions, including the composition of the VOC mixture and the concentration of key constituents. In recent CARB-funded projects, our group has characterized secondary pollutants from ozone-initiated indoor chemistry (Nazaroff et al, 2006; Destailats et al, 2006; Singer et al, 2006; Coleman et al, 2008) and emissions from office electronic equipment under idle and active cycles (Maddalena et al, 2009; Destailats et al, 2008), gaining valuable insight on the key physical-chemical phenomena involved and the experimental and analytical tools used in this study. To evaluate the total emission impacts of these portable air cleaning devices, the primary emissions of the devices are reported in the absence of a challenge VOC mixture. Primary emissions can be high due to off-gassing from electronic and plastic materials, and may also include reactive oxygen species released by the air cleaner. Characterizing these emissions can also help us to interpret the secondary emission results.

1.2. Goals and scope of this study

Primary and secondary emissions from portable air cleaners may lead to poor IAQ and associated health effects for a significant number of Californians. The reported research will help the State assist the public in making informed decisions when purchasing and using these devices, and help ARB determine whether there are any health or indoor air quality concerns associated with new technology air cleaners that need to be addressed. Information generated in this work will also contribute to the broader research and regulatory effort that the ARB has been carrying out in this field over the past years.

Due to the lack of prior research, standards or regulations pertaining to the pollutant emissions by devices that are supposed to improve indoor air quality, we have a poor understanding of the effectiveness of most devices and little information on emissions from a diverse set of products available in the market. In some cases, IAQ benefits claimed by manufacturers may be overstated or air cleaners may pose risks as a result of pollutant emissions. This study assessed the primary and secondary pollutant emissions from a range of air cleaners other than those producing ozone. Innovative experimental methods have been developed in this study to address the characterization of pollutant emissions from air cleaners, building upon the previous work performed in this area by LBNL scientists. The data set and exposure assessment presented here, obtained from the experimental characterization of a portfolio of air cleaners available in the State, will indicate the extent of the pollutant emissions problems. The information produced by this study will enable the development of effective standard testing procedures, in concert with results from studies carried out in recent years addressing other complementary aspects, such as the removal of ultrafine particles (Sultan et al, 2011; Zuraimi et al, 2011).

A major focus of our study is the characterization of the impact of portable air cleaners on indoor VOCs. Those pollutants constitute a complex mixture that presents a wide range of chemical functionalities, including aldehydes, alcohols, aromatic hydrocarbons, aliphatic hydrocarbons and terpenes among others. Several surveys reported typical levels found in commercial and residential indoor environments, including new homes (Hodgson and Levin, 2003; Offermann, 2009; Shimer et al, 2005). A summary of reported indoor pollutant levels is presented in Table 1.2.1. This information constitutes the basis on which the challenge mixture used in this study was developed. Other pollutants considered in this study are ozone, ultrafine particles (UFPs) and reactive oxygen species (ROS). Specific methods to detect low-level ROS based on sensitive fluorescent probes (Zhao and Hopke, 2012; Hasson and Paulson, 2003; Sleiman et al, 2013) were developed and are described in detail in Section 3.

The objectives of the study are:

- Evaluate the primary and secondary emissions of indoor air pollutants
- Evaluate the devices' pollutant removal efficiencies

This study will focus on a new generation of air cleaning equipment, including the following emerging technologies: photocatalytic oxidation (PCO), non-thermal plasma and microbial thermal inactivation.

The technical tasks of this study included:

- Selection of air cleaners to be studied (Task 2)
- Development of a laboratory testing protocol (Task 3), comprising the following sub-tasks:
 - setting up a room-sized environmental chamber
 - developing a challenge pollutant mixture
 - adapting analytical methods for VOCs and aldehydes
 - setting up ozone and ultrafine particle continuous monitoring equipment
 - determining ozone deposition rates
 - developing a novel method to determine ROS concentrations, and
 - performing preliminary tests.
- Characterizing emissions from air cleaners (Task 4), including determination of VOC, volatile aldehyde, ozone, UFP and ROS concentrations with each air cleaner turned off and on, under two different conditions: clean chamber air (Phase 1) and in the presence of the challenge mixture (Phase 2)
- Evaluating the impacts of air cleaners on indoor air quality (Task 5), comprising the following sub-tasks:
 - determining air flow through each device
 - calculating net pollutant direct primary emission rates in clean air (Phase 1)
 - calculating net pollutant emission or removal rates in the presence of the challenge mixture (Phase 2)
 - determining removal efficiencies and yields of secondary pollutant emissions
 - predicting impacts of emissions on typical indoor scenarios

Table 1.2.1. Indoor VOC concentrations reported in the literature

Compound	Hodgson and Levin, 2003 (ppb)				Shimer et al, 2005 ($\mu\text{g}/\text{m}^3$)		Offermann, 2009 ($\mu\text{g}/\text{m}^3$)	
	median		95%-ile		mean	90%-ile	mean	90%-ile
	residential	office	residential	office	residential		new homes	
2-Butoxyethanol		0.65	3.6				2.0	14
1,4-Dioxane	0.03		0.11					
Formaldehyde	17		61				36	86
Acetaldehyde	3.0		11				19	55
Acrolein	1.8		6.5					
n-Nonane	0.25	0.36	0.90	1.3				
1,3-Butadiene	0.23		0.83					
Benzene	0.90	1.0	3.2	3.6	4.7	8.3	0.8	4.3
Toluene	3.3	2.1	12	7.6			9.5	42
Ethylbenzene	0.53	0.48	1.9	1.7				
m/p-Xylene	1.3	1.4	4.7	5.1	6.3	13	4.2	15
o-Xylene	0.51	0.66	1.8	2.4			1.1	4.7
Styrene	0.23	0.40	0.83	1.4	2.8	3.9	0.9	2.8
Isopropylbenzene	0.07		0.25					
1,3,5-Trimethylbenzene	0.25	0.38	0.90	1.4				
1,2,4-Trimethylbenzene	0.79	0.88	2.9	3.2			1.0	3.8
1,2,3-Trimethylbenzene	0.20	0.29	0.72	1.0				
Naphthalene	0.09		0.32				0.2	0.6
1,4-Dichlorobenzene	0.09	0.03	0.32	0.11	18	36	0.2	1.7
Vinyl chloride	0.01		0.04					
Dichloromethane	1.4	0.40	5.1	1.4				
Chloroform	0.22		0.79				0.4	1.8
1,1,1-Trichloroethane	0.35	1.6	1.3	5.8	6.5	11		
Carbon tetrachloride	0.09		0.32					
1,2-Dichloroethane	0.01		0.04					
Trichloroethene	0.07	1.8	0.25	6.5	0.68	2.0		
Tetrachloroethene	0.14	0.47	0.51	1.7	1.1	2.3	0.3	0.6
Pyridine	0.17		0.61					
Ethylene glycol							3.2	36
Hexanal							7.0	22
n-hexane							0.9	5.2
d-limonene							7.6	37
Phenol							1.6	3.9
Alpha-pinene							9.3	33
Total identified VOCs	33	13	123	44	40	77	105	369



**MATERIALS
AND
METHODS**

2. SELECTION AND PROCUREMENT OF AIR CLEANERS USED IN THIS STUDY

A set of six air cleaners with significant presence in the California market was identified in consultation with ARB staff, procured and used in this study. Given the large number and diversity of portable air cleaners currently marketed, we focus on devices that utilize photocatalytic oxidation (PCO), formation of radical species in a non-thermal plasma, and microbial inactivation by heated ceramics. Among the devices considered but not included in the final set were additional PCO air cleaners, electrostatic precipitators and a generator of “electrolyzed water mist”. We selected air cleaners designed for residential room-sized applications, rather than large-scale applications (e.g., casinos, warehouses, offices, health care facilities). We generated an initial list of potential candidates for testing, and consulted with ARB staff to narrow down this selection to a final list of six devices. We conducted web-based research, including on-line information from manufacturers and consumers, as well as the products’ brochures and specifications. The devices were purchased from on-line retailers (such as Amazon.com or Target.com), or else directly from the manufacturers. The purchase was carried out through the regular LBNL procurement process, without indicating that the purpose was its use in an emission testing study. Given the size and scope of this study, only one device per model was studied.

Table 2.1.1 presents the information available for the six devices tested in this study. Three of the six devices utilize photocatalytic oxidation (PCO). In two of those three air cleaners, PCO is used in combination with other technologies (filtration, germicidal lamps and catalysts). The other three devices correspond to the following categories: plasma generators, ceramic heater with ionizer and heated microbial inactivation. All devices are marketed for residential room-sized applications, and are of roughly similar dimensions and power, compatible with the dimensions of our test chamber (20 m³).

We do not identify the brand names or models for the tested devices, but rather use a naming convention by numbering each Portable Air Cleaner (PAC) from 1 to 6. The goal is not to single out any particular device, but rather to identify the main features of these technologies that may lead to potentially harmful emissions.

The rationale for selecting these six air cleaners is the following:

- (1) Device PAC1 is a PCO air cleaner operating with UVA light (wavelength 365 nm), that claims to be ozone-free and to produce hydroxyl radicals. It was selected because of its relatively simple design and the use of UVA lamp (different from most other reviewed units). Its price is in the mid- to high-end range, which presumably correlates with better-than-average performance.
- (2) In device PAC2, the PCO stage is preceded by a HEPA filter and is also provided by an “oxygenating catalyst”, presumably to remove ozone that may form during the air cleaning process inside the device. The specifications do not clarify this

point, which is our best guess of the role of this catalyst. The unit is a relatively inexpensive “tower”-type device.

- (3) The PAC3 device is advertised as a PCO air purifier and sanitizer. It’s UV lamp produces very high ozone levels. It is a “tower”-type device. Its price is in the mid-to high-end range, which presumably correlates with better-than-average performance.
- (4) Device PAC4 is a plasma generator that claims production of hydrogen, superoxide and hydroperoxyl radical (HOO), and is marketed primarily as an anti-microbial air cleaner. It is a small-sized, table-top device, of relatively low price.
- (5) Device PAC5 is a ceramic room heater with ionizer, that operates either as an ionizer (with no heating) or with both functions simultaneously. It is an inexpensive “tower”-type device. The fan operated both during heating periods and also in conditions during which only the ionizer was operating.
- (6) Device PAC6 employs heating element, but it is not designed for room heating. It only increases the temperature of the airflow inside the device up to 400 °C for a very short time to inactivate microorganisms. This device only claims antimicrobial activity and ozone removal, but not VOC removal.

Table 2.1.1. Air cleaners tested in this study

ID	CARB-certified	Marketing/ manufacturer description ⁽¹⁾	Description	Principle of operation	Dimensions	Weight	Maximum volume or area treated	Retail price
PAC1	No	Hydroxyl generator. Targets microorganisms, odors and VOCs	Forced air circulation through PCO air cleaner	Photocatalyst (TiO ₂) irradiated by UVA lamp (365 nm)	12 x 9 x 6"	8 lb	10,000 ft ³	\$ 450
PAC2	Yes	Room air purifier. Targets PM, airborne germs, viruses, mold, mildew and VOCs	Forced air circulation through combined HEPA / PCO / catalyst	Photocatalyst irradiated by UV lamp (254 nm) + HEPA filter + "oxygenating catalyst"	11 x 14 x 30"	13 lb	room ⁽²⁾	\$ 130
PAC3	No	Residential air purifier and sanitizer. Targets mold, bacteria, viruses, odors and VOCs	Forced air circulation through PCO device using ozone generating UV lamp	Photocatalyst irradiated by UV lamp (254 nm)	4" x 4" x 16"	5 lb	3000 ft ²	\$500
PAC4	No	Air purifier. Targets airborne microorganisms	Forced air circulation through a plasma air cleaner	Non-thermal plasma with generation of reactive oxygen species	6" height; 2.4" dia.	0.5 lb	173 ft ² (16 m ²)	\$ 170
PAC5	Yes	Room air heater with ionizer. Targets dust, pollen, smoke and pet dander.	Forced air circulation through a ceramic heater with ionizer	Ionizer charges particulate matter to remove it from room air.	9 x 9 x 24"	8 lb	room ⁽²⁾	\$ 95
PAC6	Yes	Air purifier. Targets airborne microorganisms	Air circulation through internal heating device	Localized high temperatures (400 F) kills microorganisms, does not change room temperature	10" height 8" diameter	3.2 lb	550 ft ² (51 m ²)	\$ 230

(1) language used in advertising and/or technical specifications

(2) the manufacturer does not specify room area or volume

3. DEVELOPMENT OF A TESTING PROTOCOL FOR PORTABLE AIR CLEANERS

3.1. Room-Sized Experimental Chamber

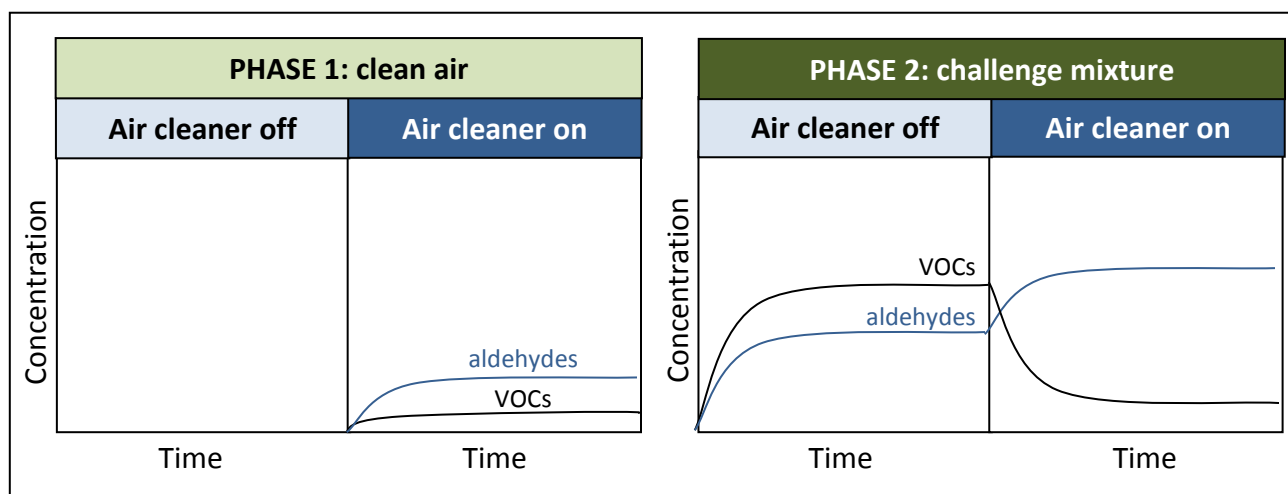
A test protocol was developed to evaluate the primary and secondary emissions from portable air cleaners, drawing on our previous experience in the evaluation of air cleaning devices as well as emission tests carried out in the LBNL room-sized chamber. The basic approach consisted in placing the air cleaners inside our 20-m³ stainless-steel chamber (Figure 3.1.1), which is ventilated with clean air at a stable rate that is representative of air exchange rates found in homes. Clean air was provided by circulating laboratory air through a 1-m³ container containing granulated activated carbon and a chemisorbent (Purafil SP) to remove VOCs. This system also reduced chamber particle concentrations.

Figure 3.1.1. LBNL's 20-m³ environmental chamber



All tested units were brand-new, and have been used for the first time in this experiment. We performed in each case an initial 2-day operation period outside of the chamber to allow venting of an initial burst of VOCs that, in our experience, are often released by previously-unused manufactured electronic devices. In Phase 1, we measured the primary emissions of air cleaners placed in a clean-air environment. Levels of VOCs, volatile carbonyls, ultrafine particulate matter, ozone and ROS were recorded inside the chamber with the air cleaner turned off and turned on. In Phase 2, we injected pollutants into the chamber at a constant rate, waiting until concentrations had stabilized. Once concentrations were stable, we turned on the air cleaner, and operated it continuously until pollutant levels had stabilized and reached a steady-state. Also in Phase 2, pollutant levels were measured with the air cleaner off and on. Figure 3.1.2 illustrates the experimental phases involved in the evaluation of each unit, illustrating representative qualitative examples of anticipated VOC and aldehyde concentration profiles that may be found during the experiments. In most cases, only one on/off cycle was performed in Phases 1 and 2 for each air cleaner. For a subset of devices, more than one cycle was performed to verify reproducibility of results.

Figure 3.1.2. Schematic representation of pollutant concentration profiles observed during Phase 1 and Phase 2



The chamber is provided with sampling ports placed on a lateral wall, designed to sample from a distance of at least 30 cm from the internal chamber walls. The same sampling locations were used throughout the experiments. Integrated VOC and volatile carbonyl samples were collected using peristaltic pumps which draw air through the samplers and ROS were sampled in impingers, as described below. Sampling flows were determined with a calibrated flow meter for each sample. The air cleaners were placed in the same location near the chamber's center.

3.2. Challenge pollutant mixture

In Phase 2, each device was operated inside the LBNL stainless steel 20-m³ chamber under controlled atmospheres generated by continuous injection of a challenge VOC mixture, at an air exchange rate in the low to typical range of air exchange rates in residential buildings, in the range 0.3 to 0.5 h⁻¹. A key parameter optimized during the development of the method was the composition of the challenge pollutant mixture used in the tests. For the selection of these pollutants, we evaluated the following considerations:

- (1) Total number of VOCs injected: in order to perform a realistic evaluation, we included a number of VOCs, rather than using a single compound to represent the complex mixture typically found indoors (Hodgson and Levin, 2003; Offerman 2009; Shimer et al, 2005). We decided to use a mixture of 11 compounds, to represent the complexity of the problem;
- (2) Total VOC (TVOC) concentration: In Phase 2, we maintained the total VOC (TVOC) concentration in the range 100 – 150 ppb, to be consistent with TVOC levels reported in the literature (see Table 1.2.1);
- (3) Relative concentration among VOCs: In Phase 2, some compounds that are known to be present at higher levels than others in homes, such as toluene and formaldehyde, were injected at higher rates to reproduce not only realistic levels but also realistic relative concentrations with respect to other compounds in the mixture;
- (4) Chemical functionalities considered: The VOC mixture included all relevant chemical functionalities relevant to indoor air, including alcohols, alkanes, alkenes, aromatic hydrocarbons, terpenoids, chlorinated compounds, aldehydes and nitrogenated hydrocarbons.
- (5) Presence of secondary byproduct precursors: In prior research we observed that upon challenging an air cleaner with a pollutant mixture, secondary aldehydes were formed (Hodgson et al, 2007a; Hodgson et al, 2007b; Destailats et al, 2012). Also, it is well known that the presence of ozone leads to the formation of volatile byproducts and secondary organic aerosols (SOA) (Singer et al, 2006; Destailats et al, 2006). For that reason, the challenge mixture was not only designed to mimic typical pollutants present in office buildings at levels that are also commonly encountered in those settings, but also included precursors that were identified in those studies to lead to the formation of secondary byproducts (both in the gas phase and aerosols). For example, limonene and styrene were SOA precursors by reaction with ozone.

Table 3.2.1 lists the eleven compounds included in the model indoor pollutant mixture used in Phase 2, as well as the target concentration range for those pollutants. All chemicals were procured from Sigma-Aldrich and were of high purity (>97%). Except

for formaldehyde, all other compounds, which are liquids, were mixed and injected using a syringe pump placed inside the chamber at an injection rate in the range 5-10 $\mu\text{L h}^{-1}$. A fan was pointed to the end of the needle to facilitate evaporation of the liquid droplets. Formaldehyde was injected separately using a different syringe pump, from a ~37% w/w aqueous solution that was introduced into a heated tube and carried into the chamber on an air flow.

Table 3.2.1. Pollutants used in the challenge mixture used in Phase 2

Compound	Target chamber level (ppb)
formaldehyde	10 – 40
butanal	1 – 10
benzene	1 – 10
toluene	10 – 30
pyridine	1 – 10
trichloroethylene (TCE)	1 – 10
limonene	1 – 15
ethanol	1 – 20
hexane	10 – 40
o-xylene	1 – 10
styrene	1 – 10

3.3. Analytical methods for VOCs and aldehydes

Most of the analytical methods used in this project have been used in our laboratory for a long time, and did not require preliminary evaluation. Only one new analytical approach was developed in this project: the evaluation of reactive oxygen species (ROS) present in chamber air. This method development is described in detail in Section 3.6.

Samples of VOC and volatile carbonyls were collected simultaneously during periods in which the air cleaners were turned off and turned on, through chamber ports. The duration of each period was approximately 24 hours, which allowed for sufficient time for equilibration of pollutant concentrations. VOC samples were collected in Tenax-TA®/Carbosieve® dual sorbent tubes (Supelco, PA) over periods of 60 min at flows of

~100 mL min⁻¹. The concentration value reported in each case corresponds to a time-integrated average over the sampled period. Air was drawn through the sorbent tubes using peristaltic pumps that were connected to the sampling tubes on one end, and to a flow calibrator on the other. The flow corresponding to each sample was measured using a primary air flow calibrator (Giliberator®) with a precision better than 1%. The start and end time for each sample was recorded. Sorbent tubes were analyzed by thermal desorption/gas chromatography/mass spectrometry (TD/GC/MS, Gerstel/Agilent) operated in electron impact mode, following the standard TO-1 EPA method (US EPA, 1984). A DB-5 chromatographic column (Agilent J&W) was used with TD desorption at 250 °C and trapping at -10 °C. The GC temperature program consisted on a 5 °C min⁻¹ ramp between 1 °C and 220 °C. Bromofluorobenzene was added to each tube and used as internal standard for quantification. Calibration curves for each analyte were performed in the range 5–150 ng, using characteristic MS ions of each analyte by injecting known amounts of authentic standards in precleaned Tenax tubes. The detection limit for each VOC was typically 1 ng or lower, corresponding to chamber concentrations <0.1 µg m⁻³.

Volatile carbonyl samples were collected using dinitrophenyl hydrazine (DNPH)-coated silica samplers (Waters, MA) over periods of identical duration as those of the VOC samples. The concentration reported in each case corresponds to a time-integrated average over the sampled period. Air was drawn through the aldehyde samplers by means of peristaltic pumps operating at ~1 L min⁻¹. The flow corresponding to each sample was measured using a primary air flow calibrator (Giliberator®) with a precision better than 2%. DNPH cartridges were extracted with 2-mL aliquots of acetonitrile, and the extracts were analyzed by HPLC with UV detection at 360 nm following a US EPA method (US EPA, 1999). A calibration curve for quantification was carried out using authentic standards of the DNPH hydrazone of formaldehyde, acetaldehyde and acetone. The detection limit for each volatile carbonyl determined by the DNPH/HPLC method was typically 10 ng or lower, corresponding to chamber concentrations <0.1 µg m⁻³.

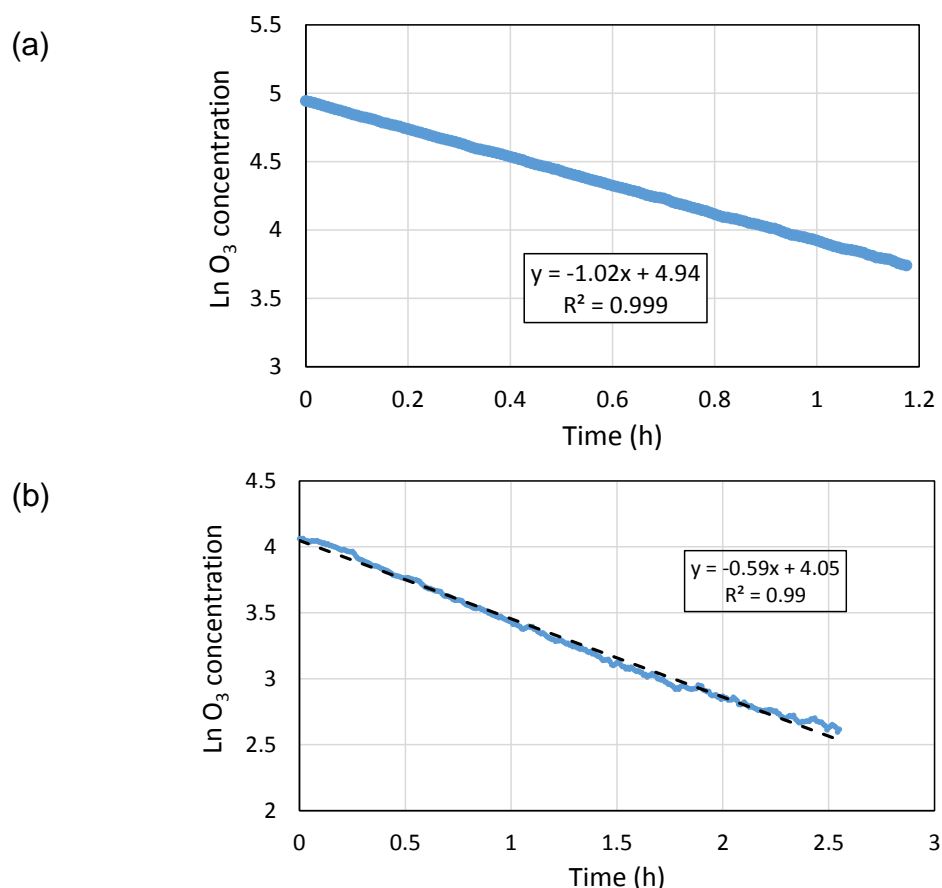
In both cases (for VOC and volatile aldehyde samples), each sample concentration was determined as the average of two parallel samples collected simultaneously. The experimental error was determined as the difference between that duplicate determination. Laboratory and reactant blanks were analyzed regularly, along with batches of samples analyzed.

3.4. Ozone Measurements and Ozone Chamber Deposition Rates

Ozone concentrations in the chamber were measured continuously using a photometric detector (API 400), with a precision of ± 2 ppb. The instrument was calibrated prior and immediately after experiments by ARB personnel.

The rate of ozone deposition to chamber surfaces was determined experimentally prior and after the experiments, by following the loss rate immediately after an ozone source was turned off. The corresponding curves are shown in Figure 3.4.1. In the first case, with the chamber operating at an air exchange rate of 0.3 h^{-1} , the measured decay rate was 1.02 h^{-1} . By difference, the ozone deposition rate was estimated as 0.72 h^{-1} . In the determination carried out at the end of the experiments, with the chamber operating at an air exchange rate of 0.03 h^{-1} , the measured decay rate was 0.59 h^{-1} . Hence, the ozone deposition rate in the second determination, calculated by difference of those two values, was 0.56 h^{-1} . Both determinations are close, so we will use for the ozone deposition rate in the chamber, an average value of $D_{\text{ozone}} = (0.64 \pm 0.08) \text{ h}^{-1}$.

Figure 3.4.1. Ozone decay curves in the LBNL environmental chamber
(a) before experiments; (b) after experiments

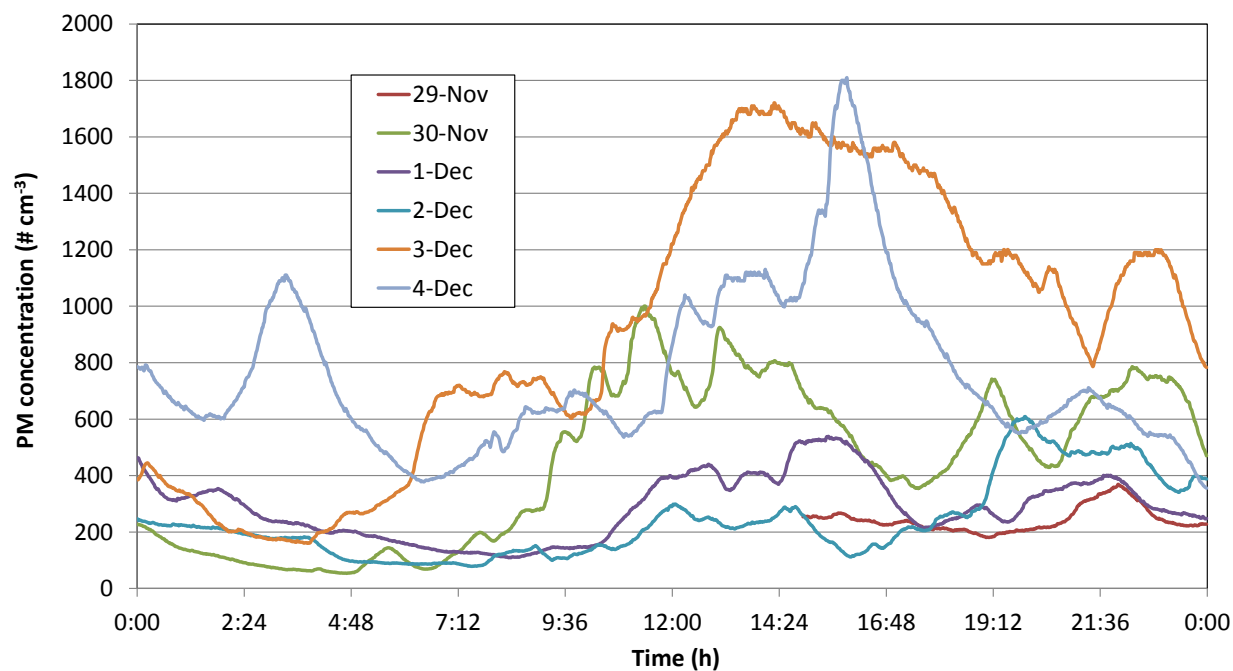


3.5. Ultrafine Particle Measurements

Ultrafine particles (UFPs) were measured continuously during the experiments using a water-based Condensation Particle Counter (W-CPC, TSI Inc model 3787). The paper wick was replaced regularly to ensure proper functioning of the instrument.

Chamber background UFP levels were measured over a week. The curves corresponding to those measurements are reported in Figure 3.5.1. Overall, we observed fluctuations, with higher levels of particles associated with periods of higher building occupancy and operation of the ventilation system. By contrast, nighttime periods had in general lower UFP levels.

Figure 3.5.1: Concentration profiles of chamber ultrafine particle (UFP, >5 nm) background levels



Daily UFP concentration averages are represented in Figure 3.5.2, with the error bars corresponding in each case to the corresponding standard deviation of the data. On the basis of these results, the background UFP concentration in the LBNL chamber was

determined to be $(530 \pm 290) \# \text{ cm}^{-3}$. Simultaneously, other chamber parameters were determined:

- Temperature: $22.4 \pm 0.5 \text{ }^\circ\text{C}$
- Relative humidity: $51 \pm 6 \%$
- Ozone concentration: $2 \pm 1 \text{ ppb}$
- Air exchange rate: $0.28 \pm 0.05 \text{ h}^{-1}$

The corresponding daily values for these parameters are reported in Figure 3.5.3. The UFP and ozone background values were consistent with those measured in each experiment when the air cleaner was turned off, as reported in Section 4. In each experiment, the background chamber values correspond to the measurement carried out with the air cleaner OFF.

Figure 3.5.2: Daily average ultrafine particle (UFP, >5 nm) concentration (\pm standard deviation). Measured in November/December 2012.

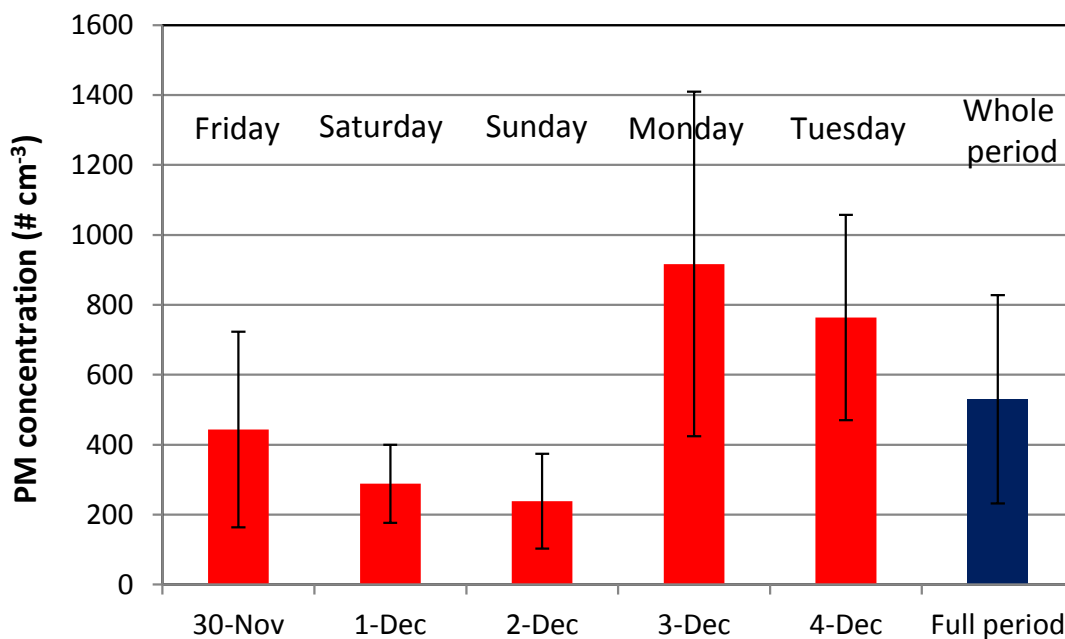
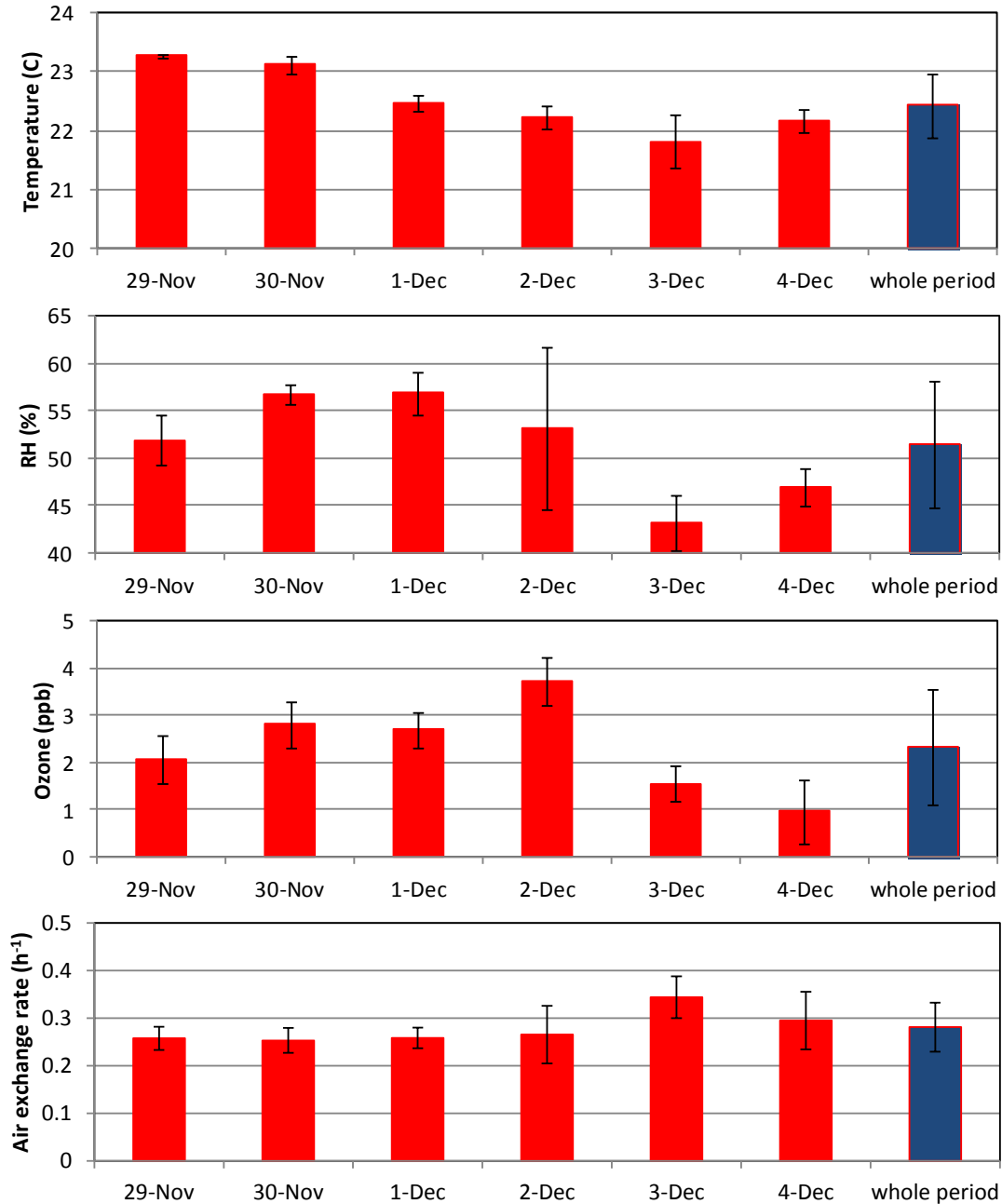


Figure 3.5.3: Chamber experimental parameters during the same studied period: Daily and whole-period average. Measured in November/December 2012.

The error bars correspond to the standard deviation of the data



3.6. Analysis of Reactive Oxygen Species (ROS)

A novel methodology to determine ROS concentration was developed in this project, with the purpose of measuring levels emitted that may potentially affect human health, as well as validating manufacturers' ROS generation claims. Several sampling and analytical methods use fluorescent probes to identify and quantify ROS in air samples (Hasson and Paulson, 2003; Arellanes et al, 2006; Wang et al, 2011; Venkatachari and Hopke, 2008; Zhou et al, 1997; Linxiang et al, 2004; Hong et al, 2008; Zhao et al, 2012; Sleiman et al, 2013). In this project, we developed three different methods to determine trace ROS levels using the fluorescent probes described in Table 3.6.1. One of the probes (DCFH) was sensitive to a broad spectrum of ROS, while the other two were specific to either peroxides (AuR) or hydroxyl radical (TPA). All chemicals used were of analytical grade or superior, and solutions were prepared using HPLC grade water. The fluorescent probes 2',7'-dichlorodihydrofluorescein diacetate (H₂DCFDA) and Amplex® ultra Red (AuR) were purchased from Invitrogen™ (Carlsbad, CA). Terephthalic acid (TPA), 2-hydroxyterephthalic (HTPA) and other chemicals and solvents used in these tests were purchased from Sigma-Aldrich (St Louis, MO). Those chemicals included Type VI-A horseradish peroxidase (HPR), a hydrogen peroxide solution (30 % wt), dimethyl sulfoxide (DMSO) and phosphate buffers.

Table 3.6.1. Fluorescent probes used in ROS measurements

Fluorescent probe	ROS detected	ROS-induced chemical change	Excitation/emission wavelength (nm)	Reported detection limit	Ref
2',7'-dichlorofluorescein (DCFH) MW: 487 CAS: 4091-99-0	H ₂ O ₂ , HO·, ROO·, ONOO ⁻	Production of the fluorescent 2,7-dichlorofluorescein	485/530	50 nM	(1)
Amplex® ultra Red (AuR) MW : 257 CAS : 119171-73-2	H ₂ O ₂	Production of a highly fluorescent byproduct resorufin	563/587	50 nM (10 pmoles)	(2)
Terephthalic acid (TPA) MW : 166 CAS : 100-21-0	OH·	Production of the fluorescent 2-hydroxy-terephthalate (HTPA)	310/412	5 nM (100 fmol)	(3)

(1) Venkatachari and Hopke, 2008

(2) Zhou et al, 1997

(3) Linxiang et al, 2004

For the DCFH test, a 400 μM 2',7'-dichlorodihydrofluorescein (H_2DCF) solution was prepared by mixing 0.5 mL of a 10 mM H_2DCFDA ethanolic stock solution with 2 mL of NaOH 0.01 M. The hydrolyzed H_2DCF was kept at room temperature during 30 minutes and the neutralized with 10 mL of 50 mM phosphate buffer (pH 7.2). This solution was freshly prepared and kept on ice prior to use, together with a 100 U mL^{-1} HPR solution and 1:1000 H_2O_2 stock solution.

For the AuR test, a 10 mM AuR stock solution was prepared in DMSO and stored at -20°C prior to use. For each experiment, this stock solution was diluted to prepare a fresh 150 μM AuR solution, which was stored on ice during each experiment.

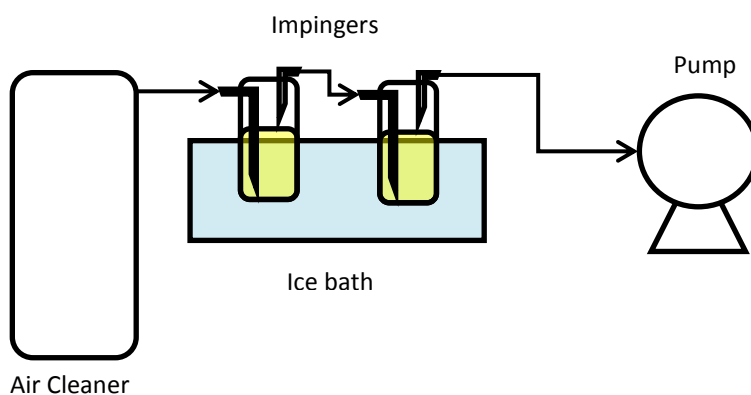
For the TPA test, stock solutions for 2.5 mM HTPA and 0.5 M TPA in NaOH 0,1M were prepared by directly dissolving the solid reactants.

All stock solutions (except 1 mM AuR) were stored in a refrigerator at $2\text{-}6^\circ\text{C}$ without showing appreciable changes after a month. The fluorescence intensity of all standards and samples collected in the tests was measured using a filter spectrofluorimeter (TD7000, Turner Design, San Jose CA) at the corresponding emission and excitation wavelengths summarized in Table 3.6.1, using 20-nm bandwidth filters. Blanks were carried out and their fluorescence intensity was deducted from calibration levels on each test.

Further details on method development, calibration and evaluation of ozone interferences are described in Appendix 1.

3.6.1. Determination of ROS concentrations

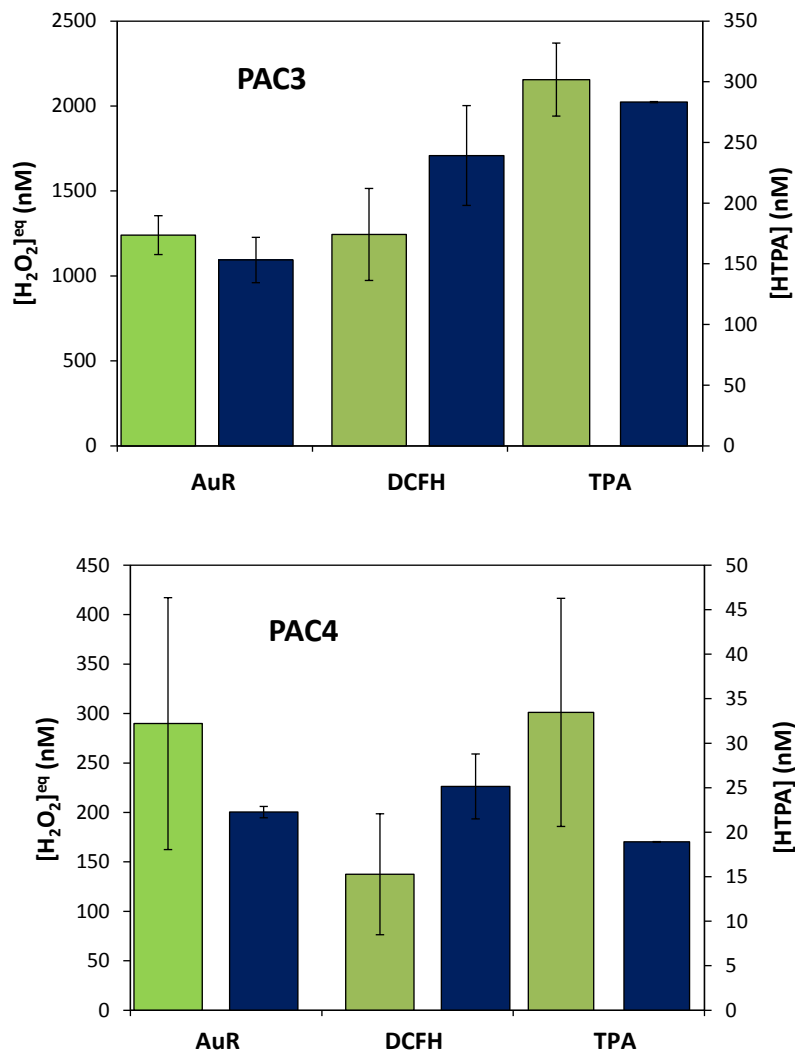
Two devices, PAC3 and PAC4, were identified in preliminary tests as a strong and a weak ozone emitters, respectively. We sampled simultaneously ROS and ozone under identical conditions at the outlet of both air cleaners, and also at the outlet of a laboratory ozone generator operated with "zero" quality clean air that reproduced the same ozone level generated by each air cleaner. Two impingers in series were placed directly at the outlet of each device, and out coming air was sampled at flow rates between 0.5 and 1 L min^{-1} , as illustrated in Figure 3.6.1.

Figure 3.6.1: Experimental setup to sample directly from the air cleaner's outlet

A 3-mL aliquot of the collected sample was used at the end of each test to determine the amount of ROS emitted by each air cleaner and by the ozone generator as described above. Results are presented in Figure 3.6.2.

In the case of the PAC3 air cleaner, although the overall response was higher, all the ROS signal could be attributed to the formation of these reactive species in solution due to the presence of ozone. Given the high level of ozone emitted by this device and the relatively high “background ROS” signal, this method was not able to quantify ROS that are emitted simultaneously with ozone. The DCFH method yielded a higher signal for the ozone generator than for the air cleaner. While the other two methods showed a slightly higher signal for the air cleaner than for the ozone generator, the relative differences were only 6% for TPA and 11% for AuR, which were of the same order of the experimental error.

Figure 3.6.2: Equivalent aqueous H₂O₂ and HTPA concentrations determined for the air cleaners (green) and for an ozone generator (blue)



In the case of the PAC4 air cleaner (plasma generator), the signal measured for DCFH was also higher for the ozone generator than for the air cleaner, similar to results observed for PAC3. However, measurements for the other two probes (TPA and AuR) showed ROS levels for emissions from the air cleaner that were significantly higher than background levels measured from the ozone generator (43% and 31% higher, respectively). In consequence, the contribution of airborne ROS from PAC4 could be estimated by subtracting the value determined with the air cleaner from that from the ozone generator.

The results, summarized in Table 3.6.2, were determined by:

- (1) adding the aqueous concentrations determined in impinger 1 and 2 for each determination (expressed in nM), to account for breakthrough (if $RE < 100\%$)
- (2) subtracting the value of the ROS aqueous concentration measured with the ozone generator from that obtained with the air cleaner
- (3) calculating the corresponding number of moles of ROS emitted, by multiplying the aqueous concentration determined in (a) times the volume of buffer used to collect the sample (10 mL) and the analysis dilution factor (3/5)
- (4) dividing the number of moles calculated in (c) by the volume of air circulated through the impingers, and
- (5) converting from mole L^{-1} units to part-per-billion units, multiplying by the molar volume of air at standard conditions of temperature and pressure ($22.4 L mol^{-1}$)

Table 3.6.2. Determination of ROS levels emitted by PAC4

AuR	$[H_2O_2]_{\text{aqueous}}^{\text{eq}}$ (nM)			$[H_2O_2]_{\text{gas}}^{\text{eq}}$ (ppb)
	air cleaner	ozone generator	difference	
	290 ± 130	200 ± 10	90 ± 140	0.3 ± 0.3
TPA	$[HTPA]_{\text{aqueous}}$ (nM)			$[OH]_{\text{gas}}^{\text{eq}}$ (ppt)
	air cleaner	ozone generator	difference	
	33 ± 12	19 ± 1	14 ± 13	47 ± 46

The levels reported in Table 3.6.2, measured directly at the outlet of the devices, can be considered an upper level for values measured in the environmental chamber where additional losses may occur due to deposition to indoor surfaces and gas phase reactions. These levels can be put into perspective by comparing with levels of H_2O_2 and OH radicals reported in indoor and outdoor air:

- **Peroxides:** Hydrogen peroxide concentrations between 0.5 and 3.5 ppb have been reported in urban air, mainly in the gas phase (Hasson and Paulson, 2003). Similar levels of up to 5 ppb have been reported in non-urban tropospheric measurements (Balasubramanian and Husain, 1997). Considering indoor

environments, Li et al (2002) measured gas phase peroxides in the range 0.6 – 1.5 ppb, generated from reaction of ozone with d-limonene in an office with a strong ozone source. These reported indoor and outdoor levels are of the same magnitude as those measured in this study for PAC4. Unfortunately the high background levels prevented us to measure ROS emissions from PAC3. In that case, it is likely that peroxide emissions occurring simultaneously with ozone emissions were of similar magnitude or higher than levels measured from ozone-terpene chemistry.

- **Hydroxyl radicals:** typical daytime outdoor levels are $\sim 10^6 \text{ cm}^{-3}$ ($\sim 10^{-1}$ ppt), and peak above $\sim 10^7 \text{ cm}^{-3}$ (~ 1 ppt) in polluted urban atmospheres (Dusanter et al, 2009). Indoor levels are often in the range of 10^5 cm^{-3} (Weschler and Shields, 1997; Singer et al, 2006), but recent studies reported higher levels that approach those measured outdoors (Gligorovski and Weschler, 2013). In chamber studies with high ozone and terpene concentrations, OH radical concentrations of up to $\sim 10^7 \text{ cm}^{-3}$ (~ 1 ppt) were measured (Destailats et al, 2006). In our study, assuming that the radical species reacting with TPA were exclusively OH radicals, values measured directly at the outlet of the plasma generator (PAC4) were between one and two orders of magnitude higher than OH levels recorded in outdoor air. It is expected that these concentrations will be reduced rapidly in indoor environments due to OH-OH recombination processes in the gas phase, reactions with VOCs and with indoor surfaces. However, breathing air in the proximity of the device will likely lead to exposure to elevated levels of OH radicals.

3.7. Preliminary Tests

A sub-set of the air cleaners were subjected to preliminary experiments to optimize the chamber conditions prior to systematic evaluation of pollutant emissions by each of the units. In particular, PAC2 was used to setup the general chamber conditions, including temperature, relative humidity, air exchange rate, VOC and aldehyde injection rates and pollutant stability under steady-state conditions. These preliminary tests allowed us to evaluate the precision of determinations of VOC and aldehyde chamber concentrations, as well as ozone and aerosol particle levels, when present. In these preliminary experiments, we evaluated:

- (1) chamber background levels with the device turned off;
- (2) the concentration of each pollutant and stability over time of the challenge pollutant mixture by collecting various samples over time;
- (3) the variations of pollutant mixture composition and relative concentrations, and
- (4) the stability of the chamber's air exchange rate.


In each of these experiments, we determined:

- a) VOC concentrations in the chamber by collecting sorbent tubes during steady-state periods with the air cleaner turned off and on;
- b) volatile carbonyl concentrations by collecting DNPH samples, which were subsequently extracted and analyzed by HPLC. These samples were collected at similar periods as VOC samples;
- c) a continuous reading of chamber ozone concentrations using the photometric ozone monitor.
- d) a continuous reading of chamber aerosol particle concentration using the water-based condensation particle counter (W-CPC).

The chamber's air exchange rate was stable, with a fluctuation not larger than $\pm 10\%$ of the reported value over a week-long period. Typically, the duration of a single experiment was equal or less than one week. Over longer periods we observed changes within the range $0.3 - 0.5 \text{ h}^{-1}$, likely due to changes in the performance of the fan used in the chamber's inlet system and/or changes in the pressure drop at the air cleaning system used in the chamber's inlet. In any case, the values corresponding to air exchange rate for each experiment were recorded, and the relevant measured air exchange rates were used in all calculations corresponding to emission rates from each device.

Preliminary tests for ROS emissions were performed with the PAC3 and PAC4 air cleaners, and have been described in Section 3.6.4, above.

Once chamber operation, sampling protocols and analytical methods were optimized, we proceeded to systematically study each of the air cleaners, as described in the next section (Section 4).



**RESULTS
AND
DISCUSSION**

4. EXPERIMENTAL CHARACTERIZATION OF EMISSIONS FROM AIR CLEANERS

4.1. PAC1: PCO Air Cleaner

4.1.1. Summary of observations

This PCO air cleaner is a simple device provided with a single ON/OFF button, and which runs on a single setting. Its operation can be easily verified visually by checking on the fan and viewing the UV lamp (Table 2.1.1). The main observations have been the following:

- No ozone was emitted in Phase 1 nor Phase 2 (Figures 4.1.1 – 4.1.3)
- We observed a partial reduction in the concentrations of most VOCs (Figures 4.1.4 – 4.1.5)
- We observed the formation of a small amount of formaldehyde as a secondary byproduct, with a concentration increase of ~5%. While these concentration changes are not very large, they are still measurable (Figure 4.1.5)
- We did not observe the formation of ultrafine particles (UFP, >5 nm) (Figures 4.1.6 – 4.1.8)
- Results from ROS measurements are reported for all air cleaners in Section 4.7.

The experimental conditions for tests with PAC1 are summarized in Table 4.1.1. Results are presented graphically in Sections 4.1.2 – 4.1.4, and the corresponding pollutant concentrations are presented in Table A.2.1 (Appendix 2).

Table 4.1.1. Experimental conditions used in experiments with PAC1

	Phase 1		Phase 2	
	OFF	ON	OFF	ON
Temperature (°C)	29 ± 1	26 ± 2	25 ± 1	25 ± 0
Relative humidity (%)	31 ± 1	45 ± 7	30 ± 3	33 ± 4
Air exchange rate (h ⁻¹)	0.57 ± 0.01	0.54 ± 0.04	0.44 ± 0.07	0.48 ± 0.11

4.1.2. Ozone

The experimental curves recorded by the ozone monitor during Phase 1 and Phase 2 are shown in Figure 4.1.1 and Figure 4.1.2, respectively. We represent in blue the times at which the air cleaner was turned off, and in red those in which the air cleaner was

turned on. The integrated averages for periods in which the air cleaner was turned on and off for each phase are shown in Figure 4.1.3.

Figure 4.1.1: Ozone concentration profiles for PAC1 – Phase 1

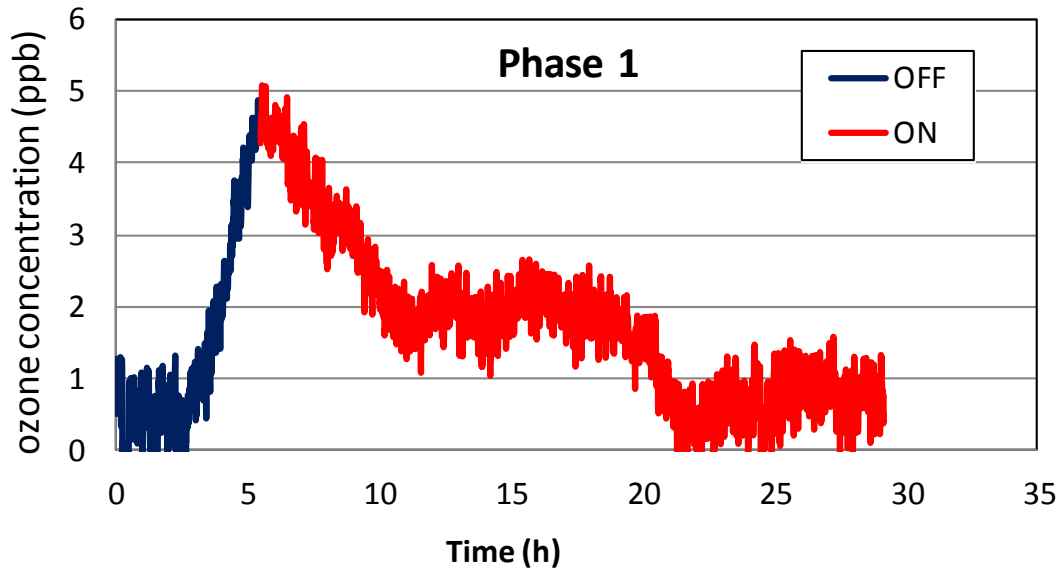


Figure 4.1.2: Ozone concentration profiles for PAC1 – Phase 2

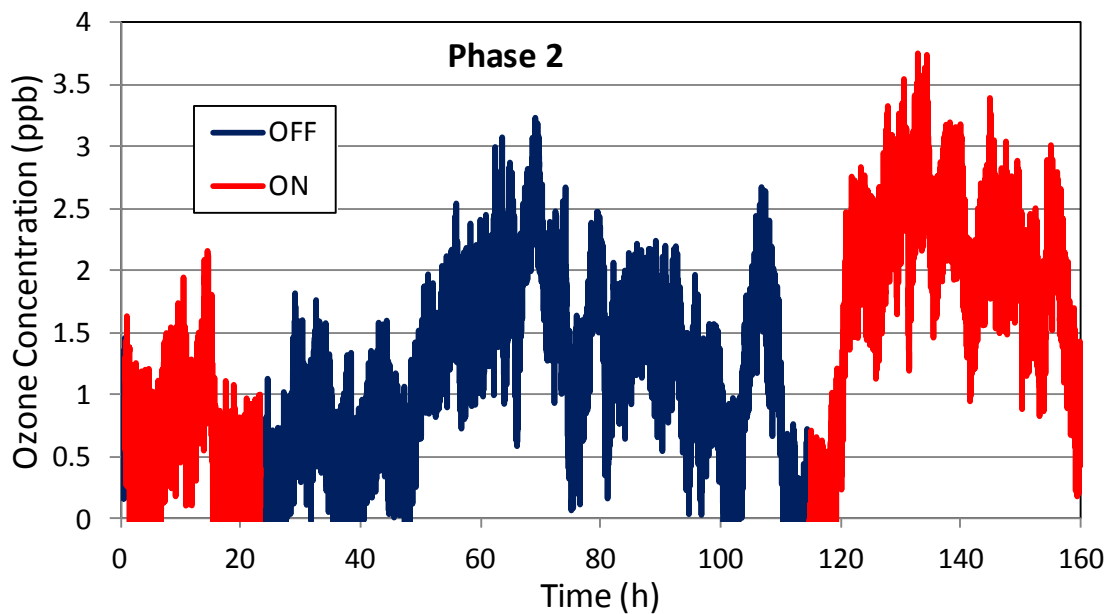
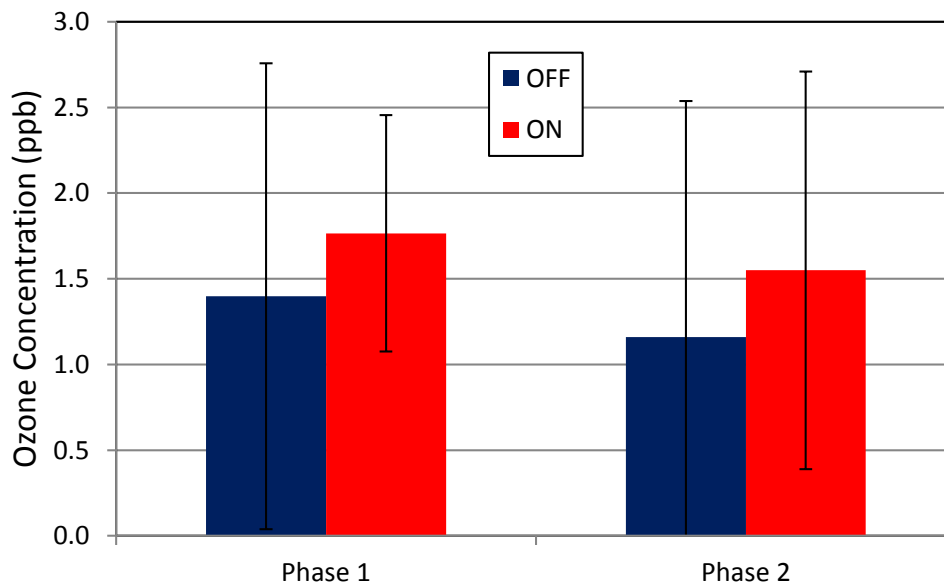


Figure 4.1.3: Average ozone chamber concentrations during periods with air cleaner off and on for PAC1 – Phase 1 and Phase 2



4.1.3. VOCs

Individual VOC concentrations were determined for each phase during OFF and ON periods, and are reported in Figure 4.1.4 (Phase 1) and Figure 4.1.5 (Phase 2). In each case, we include results for the 11 compounds comprising the challenge mixture as well as two byproducts identified in our analysis and which were not included in the challenge mixture: acetaldehyde and acetone. Both compounds were also present in chamber background at ~1 ppb and ~3 ppb, respectively. Very low levels of VOCs were detected in the chamber background, originating either from outdoor air (which cannot be 100% removed at the chamber inlet) or desorption from chamber surfaces.

Each value reported in Figures 4.1.4 and 4.1.5 corresponds to the average of two samples collected simultaneously. The error bars illustrate the absolute difference for each duplicate determination. We performed one set of duplicate determinations for each Phase 1 condition (ON and OFF), and two sets of duplicates for each Phase 2 condition. Repeating Phase 2 determinations twice provided further evidence that it was not necessary to carry out more than one set of duplicate measurements for each condition for other air cleaners.

Figure 4.1.4: Individual VOC & aldehyde concentrations measured for PAC1 – Phase 1. Acetaldehyde and acetone were not part of the challenge mixture.

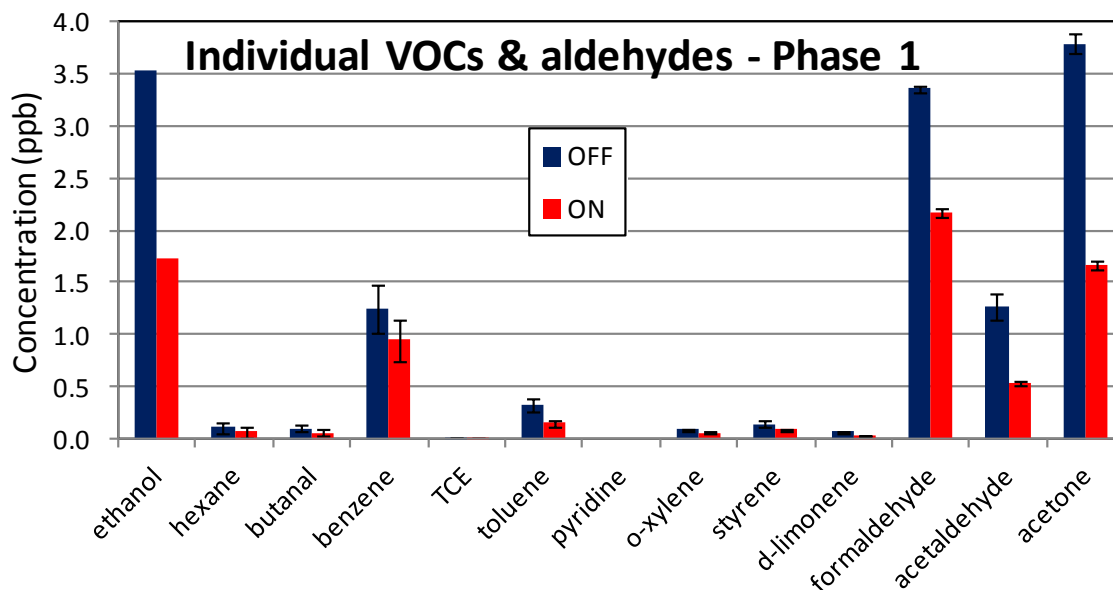
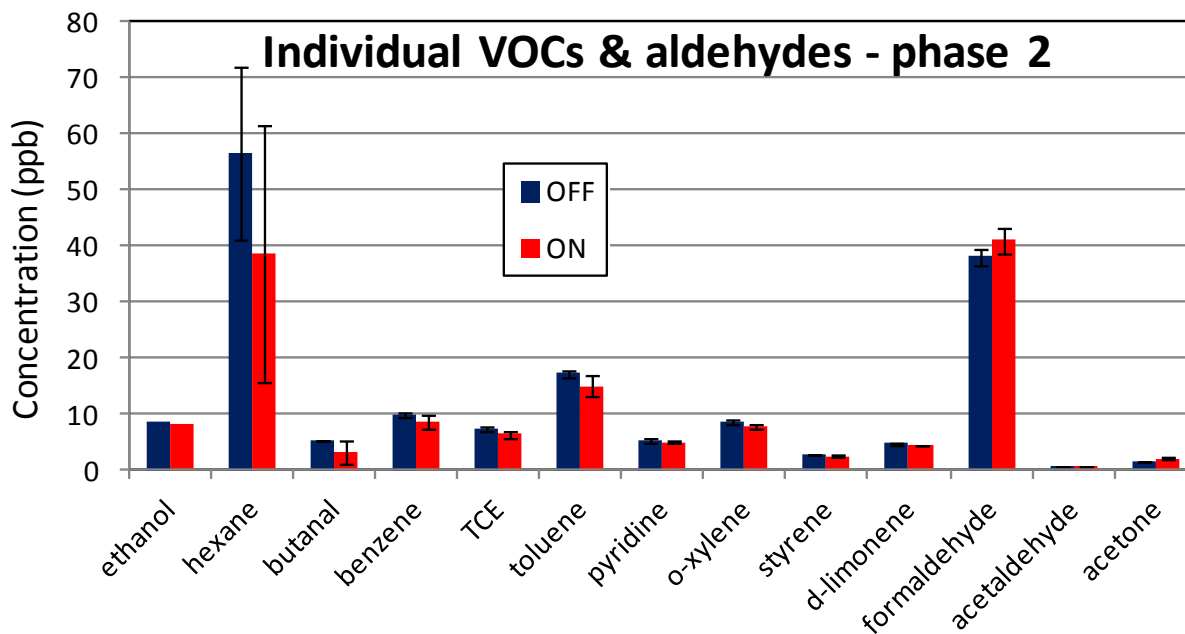


Figure 4.1.5: Individual VOC & aldehyde concentrations measured for PAC1 – Phase 2. Acetaldehyde and acetone were not part of the challenge mixture.



4.1.4. Ultrafine particles

The experimental curves recorded by the W-CPC during Phase 1 and Phase 2 are shown in Figure 4.1.6 and Figure 4.1.7, respectively. We represent in blue the times at which the air cleaner was turned off, and in red those in which the air cleaner was turned on. The integrated averages for periods in which the air cleaner was turned on and off for each phase are shown in Figure 4.1.8. Daily spikes are observed in the morning when the building ventilation is turned on, and constitute the background of our measurements. In most cases, runs were initiated during mid-morning. The data are not background-subtracted; instead, we indicate in each case the range of values corresponding to chamber background levels.

Figure 4.1.6: Ultrafine particle (UFP, >5 nm) concentration profiles for PAC1 – Phase 1

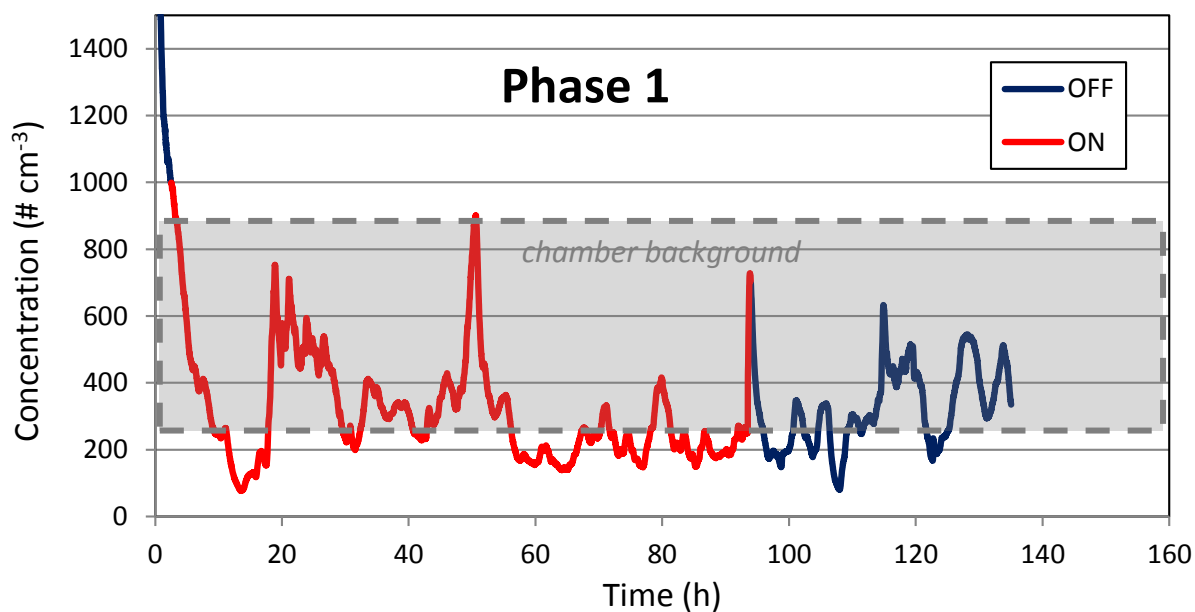


Figure 4.1.7: Ultrafine particle (UFP, >5 nm) concentration profiles for PAC1 – Phase 2

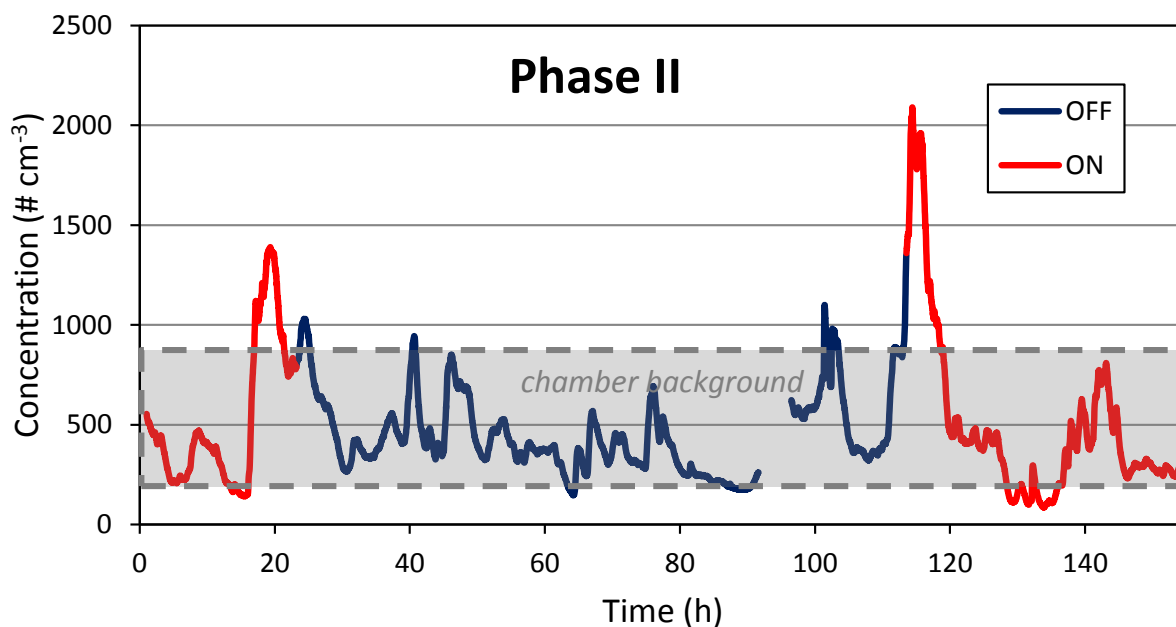
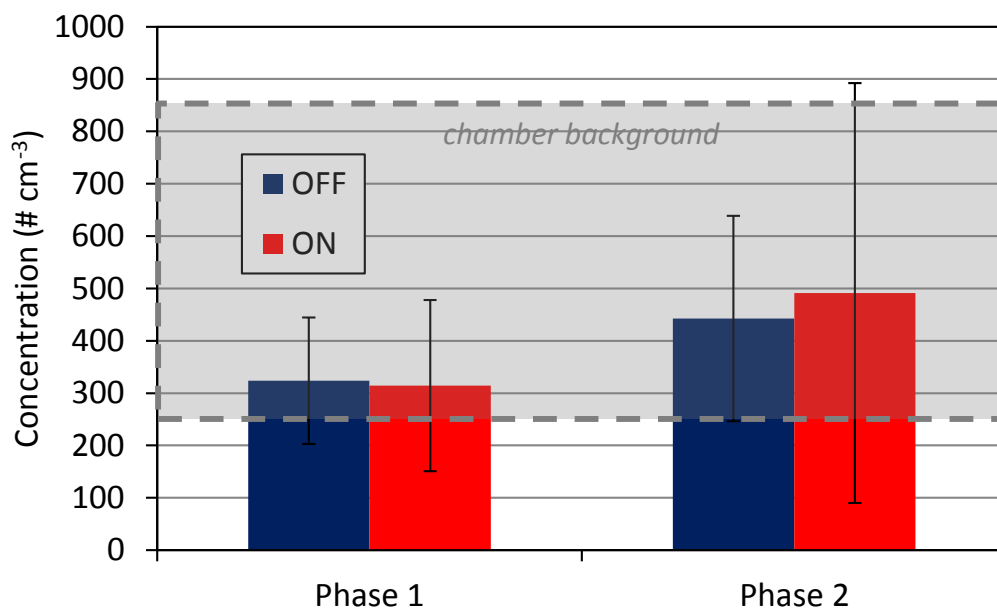


Figure 4.1.8: Average ultrafine particle (UFP, >5 nm) concentration during periods with air cleaner off and on for PAC1



4.2. PAC2: Air Cleaner Combining HEPA / PCO / Catalyst

4.2.1. Summary of observations

This device is a fairly typical “tower” type of air cleaner, it can be operated at three different air flow velocities. All the tests were performed in the middle setting. Its operation can be verified visually by checking on a LED on the top of the device. The main observations have been the following:

- No ozone emissions were observed in Phase 1 nor Phase 2 (Figures 4.2.1 – 4.2.3)
- We did not observe a partial reduction in VOC concentrations, but rather some weak emissions of some VOCs, most notably toluene (Figures 4.2.4 – 4.2.5)
- This device is provided with a HEPA filter, which enables for high filtration efficiency, as evidenced by the significant reduction in particulate matter present at background levels in the chamber (Figures 4.2.6 – 4.2.8)
- No formation of ultrafine particles (UFP, >5 nm) was evident (Figures 4.2.6 – 4.2.8)
- Results from ROS measurements are presented for all air cleaners in Section 4.7.

The experimental conditions for tests carried out with PAC2 are summarized in Table 4.2.1. Results are presented graphically in Sections 4.2.2 – 4.2.4, and the corresponding pollutant concentrations are presented in Table A.2.2 (Appendix 2).

Table 4.2.1: Experimental conditions used in experiments with PAC2

	Phase 1		Phase 2	
	OFF	ON	OFF	ON
Temperature (°C)	24 ± 1	26 ± 1	24 ± 1	25 ± 1
Relative humidity (%)	34 ± 1	30 ± 2	39 ± 1	32 ± 2
Air exchange rate (h ⁻¹)	0.53 ± 0.02	0.56 ± 0.02	0.58 ± 0.01	0.58 ± 0.01

4.2.2. Ozone

The experimental curves recorded by the ozone monitor during Phase 1 and Phase 2 are shown in Figure 4.2.1 and Figure 4.2.2, respectively. We represent in blue the times at which the air cleaner was turned off, and in red those in which the air cleaner was

turned on. The integrated averages for periods in which the air cleaner was turned on and off during each phase are shown in Figure 4.2.3.

Figure 4.2.1: Ozone concentration profiles for PAC2 – Phase 1

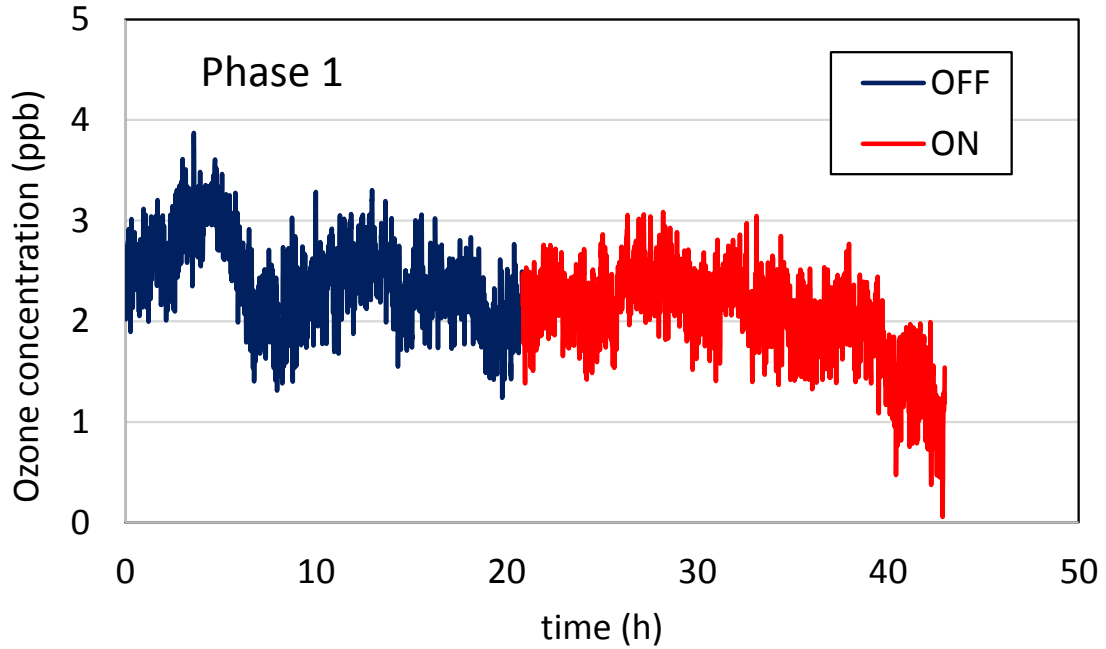


Figure 4.2.2: Ozone concentration profiles for PAC2 – Phase 2

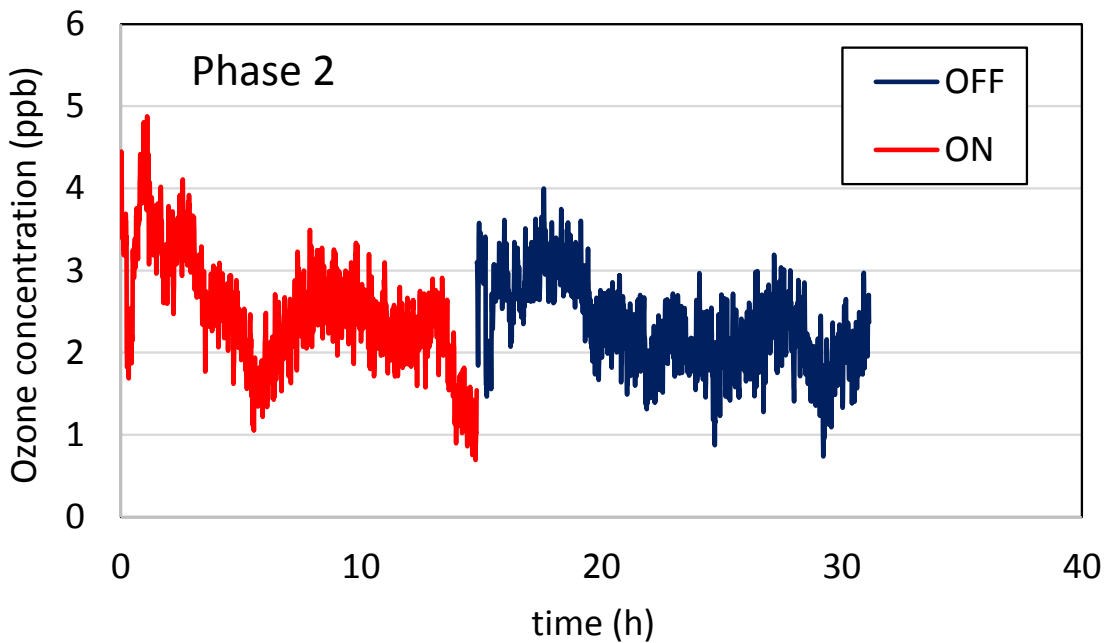
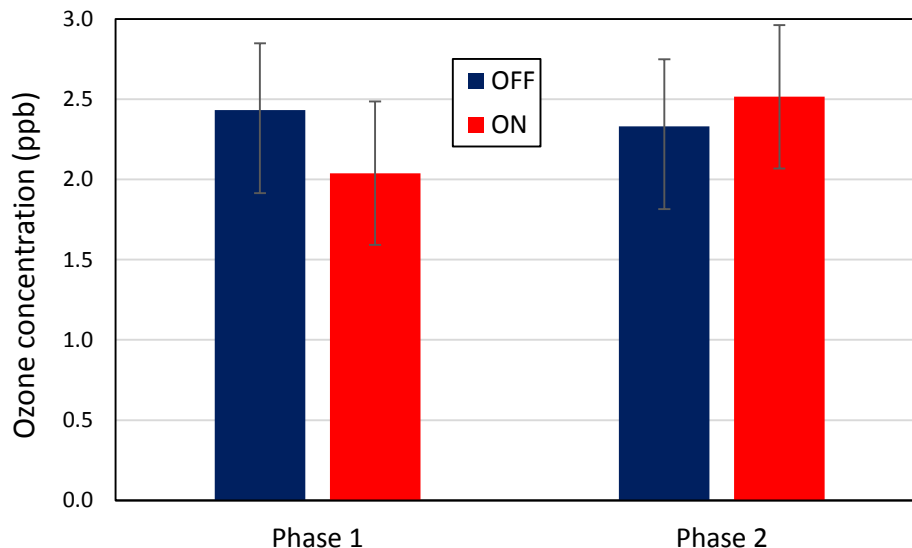


Figure 4.2.3: Average ozone chamber concentrations during periods with air cleaner off and on for PAC2 – Phase 1 and Phase 2



4.2.3. VOCs

Individual VOC concentrations were determined for each phase during OFF and ON periods, and are reported in Figure 4.2.4 (Phase 1) and Figure 4.2.5 (Phase 2). In each case, we include results for the 11 compounds comprising the challenge mixture as well as two byproducts identified in our analysis and which were not included in the challenge mixture: acetaldehyde and acetone. Both compounds were also present in chamber background at ~0.5 ppb and ~1 ppb, respectively.

Each value reported in Figures 4.2.4 and 4.2.5 corresponds to the average of two samples collected simultaneously. The error bars illustrate the absolute difference for each duplicate determination. We performed one set of duplicate determinations for each Phase 1 condition (ON and OFF), and one set of duplicates for each Phase 2 condition.

Figure 4.2.4: Individual VOC & aldehyde concentrations measured for PAC2 – Phase 1 experiments. Acetaldehyde and acetone were not part of the challenge mixture.

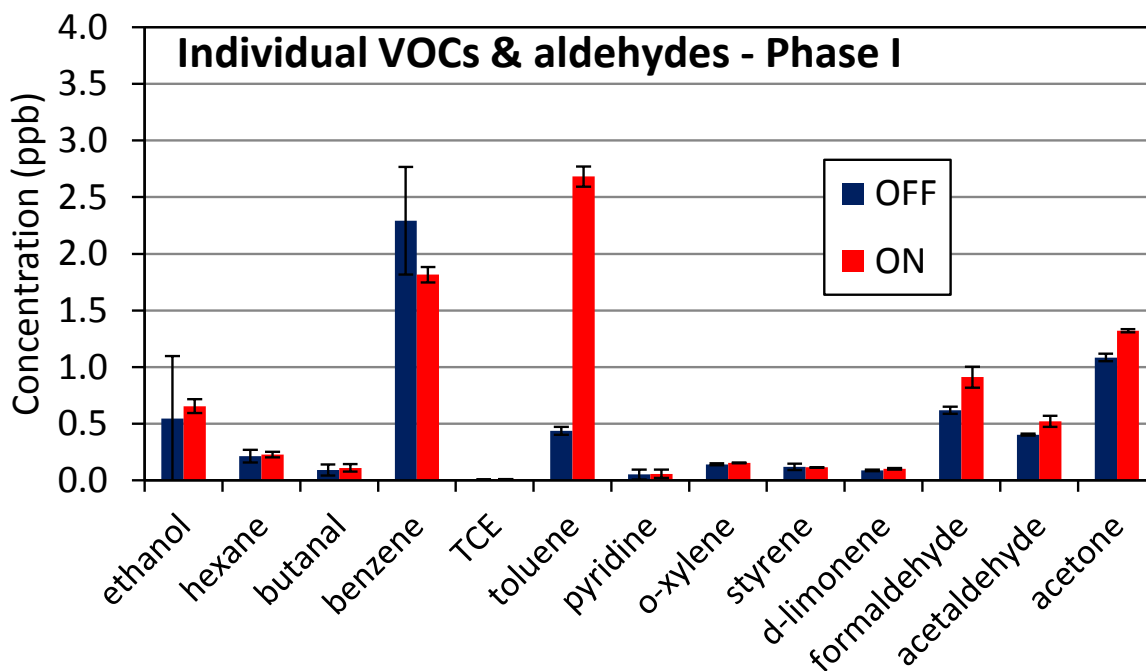
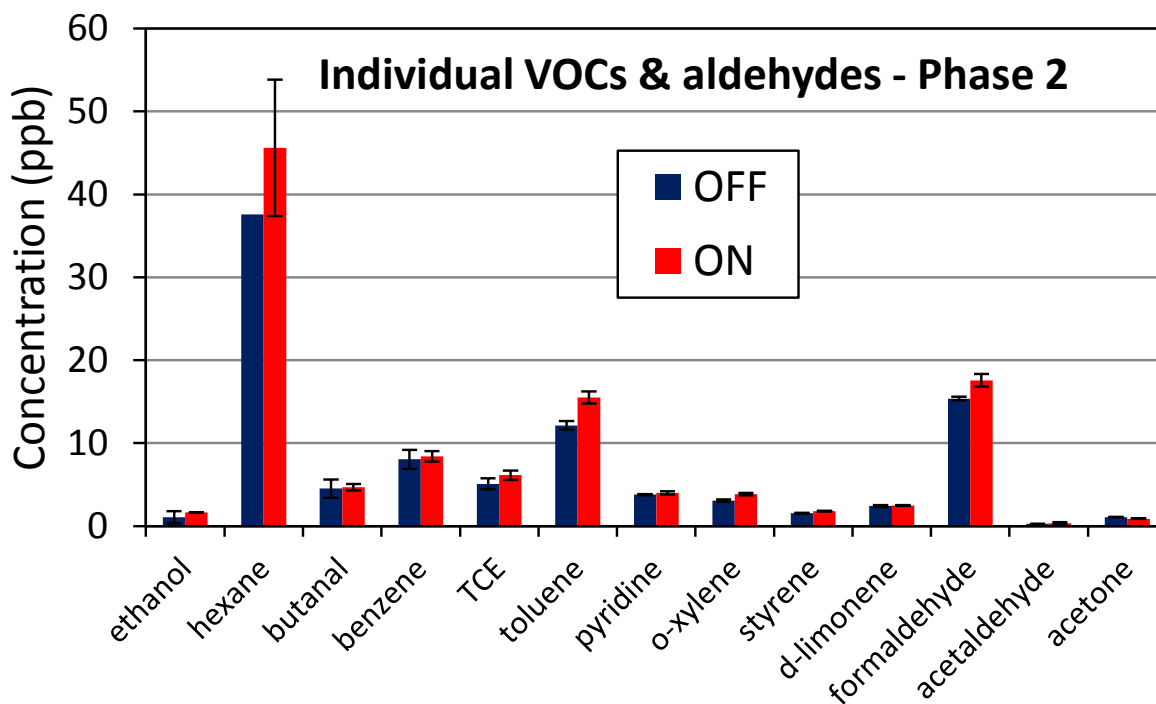


Figure 4.2.5: Individual VOC & aldehyde concentrations measured for PAC2 – Phase 2 experiments. Acetaldehyde and acetone were not part of the challenge mixture.



4.2.4. Ultrafine particles

The experimental curves recorded by the W-CPC during Phase 1 and Phase 2 are shown in Figure 4.2.6 and Figure 4.2.7, respectively. We represent in blue the times at which the air cleaner was turned off, and in red those in which the air cleaner was turned on. The integrated averages for periods in which the air cleaner was turned on and off for each phase are shown in Figure 4.2.8. Daily spikes are observed in the morning when the building ventilation is turned on, and constitute the background of our measurements. The data are not background-subtracted; instead, we indicate in each case the range of values corresponding to chamber background levels.

Figure 4.2.6: Ultrafine particle (UFP, >5 nm) concentration profiles for PAC2 – Phase 1

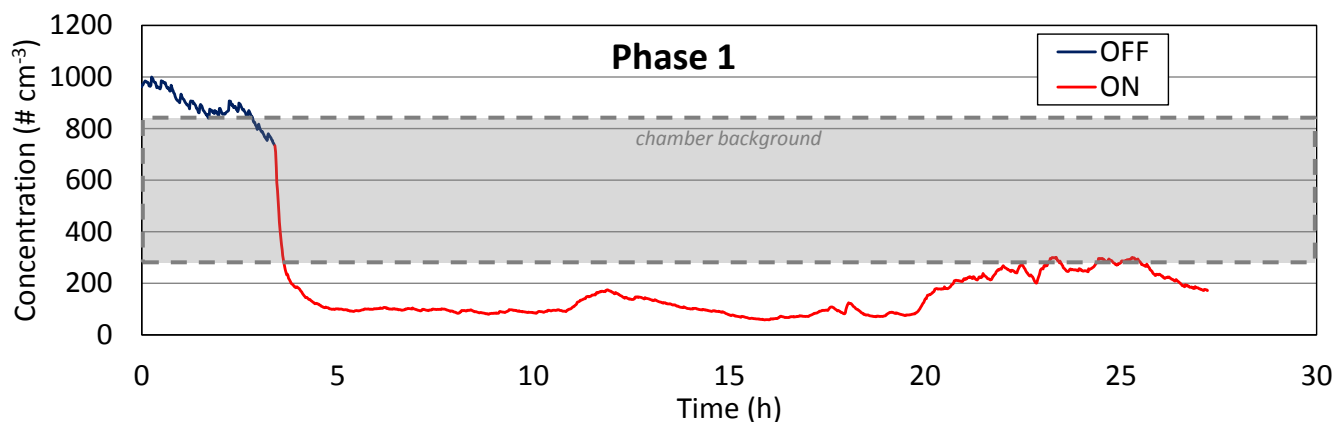


Figure 4.2.7: Ultrafine particle (UFP, >5 nm) concentration profiles for PAC2 – Phase 2

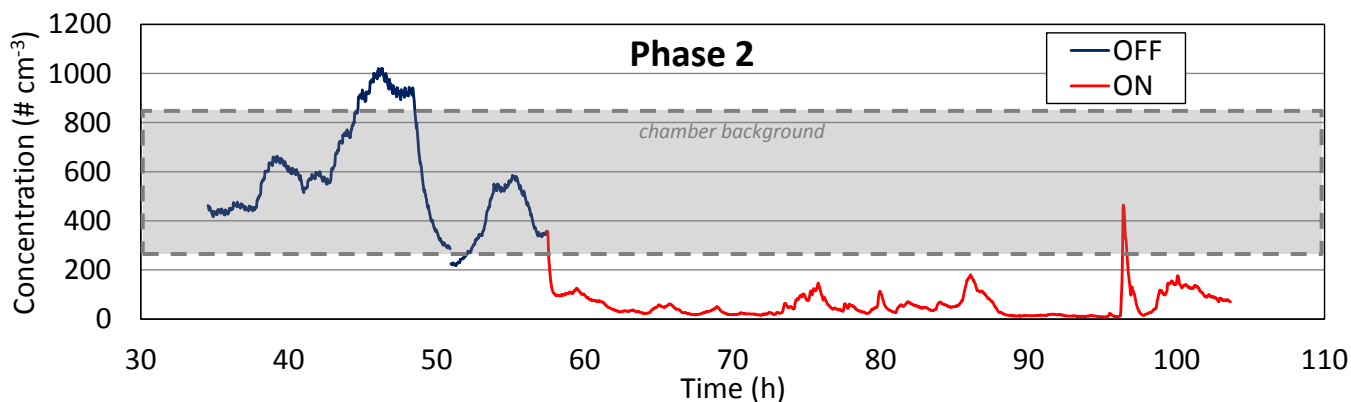
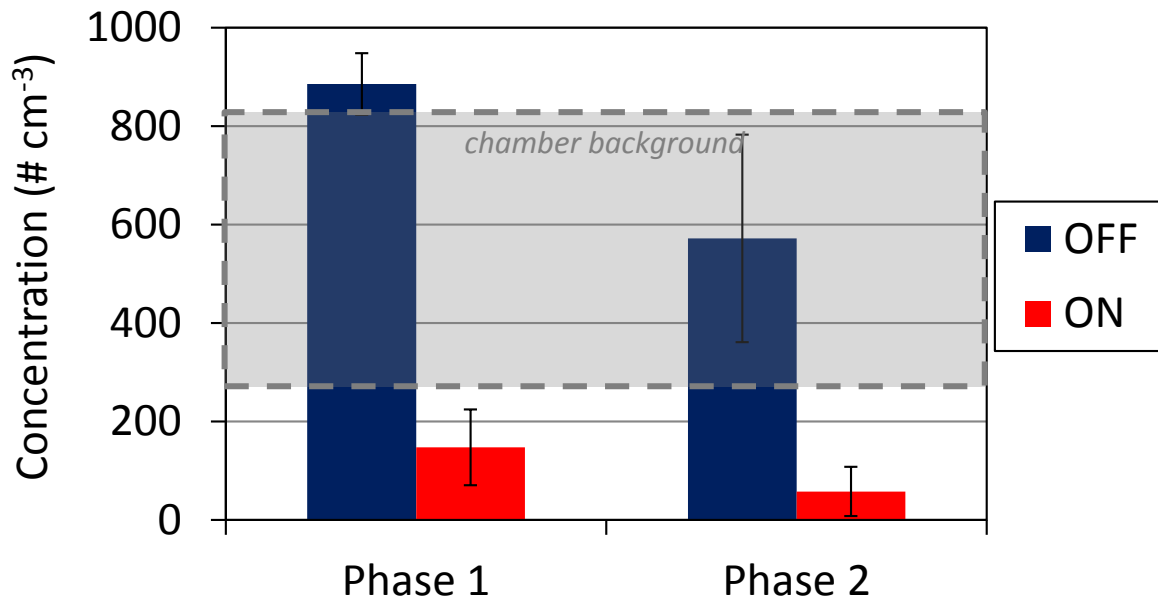


Figure 4.2.8: Average concentration of ultrafine particles (UFP, >5 nm), measured during periods with air cleaner off and on for PAC2



4.3. PAC3: PCO Air Cleaner with Ozone Generation

4.3.1. Summary of observations

This device is a “tower” type of air cleaner with an ON/OFF button and that operates in a single setting. Its operation can be verified visually by viewing blue light emitted by the UV lamp. The main observations have been the following:

- Extremely high ozone emissions were observed in Phase 1 and Phase 2 (~160 ppb), significantly higher than those claimed by manufacturer (90 ppb) (Figures 4.3.1 – 4.3.3)
- A partial reduction in VOC concentrations was observed in Phase 2, with moderate reduction of most VOCs but almost complete depletion of the two alkenes (limonene and styrene), which are very reactive with ozone (Figures 4.3.4 – 4.3.5)
- Formation of ultrafine particles during Phase 2, ~6 times higher than background levels, likely due to reaction of ozone with alkenes (Figures 4.3.6 – 4.3.8)
- Results from ROS measurements are presented for all air cleaners in Section 4.7.

The experimental conditions for tests with PAC3 are summarized in Table 4.3.1. Results are presented graphically in Sections 4.3.2 – 4.3.4, and the corresponding pollutant concentrations are presented in Table A.2.3 (Appendix 2).

Table 4.3.1: Experimental conditions used in experiments with PAC3

	Phase 1		Phase 2	
	OFF	ON	OFF	ON
Temperature (°C)	29 ± 3	24 ± 1	27 ± 1	27 ± 2
Relative humidity (%)	34 ± 9	49 ± 3	36 ± 3	34 ± 2
Air exchange rate (h ⁻¹)	0.48 ± 0.03	0.33 ± 0.04	0.28 ± 0.03	0.30 ± 0.02

4.3.2. Ozone

The experimental curves recorded by the ozone monitor during Phase 1 and Phase 2 are shown in Figure 4.3.1 and Figure 4.3.2, respectively. We represent in blue the times at which the air cleaner was turned off, and in red those in which the air cleaner was turned on. The integrated averages for periods in which the air cleaner was turned on and off during each phase are shown in Figure 4.3.3. It should be noted that maximum (steady-state) ozone levels were reached in Phase 1 after ~2 hours of turning on the

device, while it took more than 10 hours to reach steady-state conditions in Phase 2. This difference reflects the fact that ozone in Phase 2 reacted with VOCs over the transient period.

Figure 4.3.1: Ozone concentration profiles for PAC3 – Phase 1

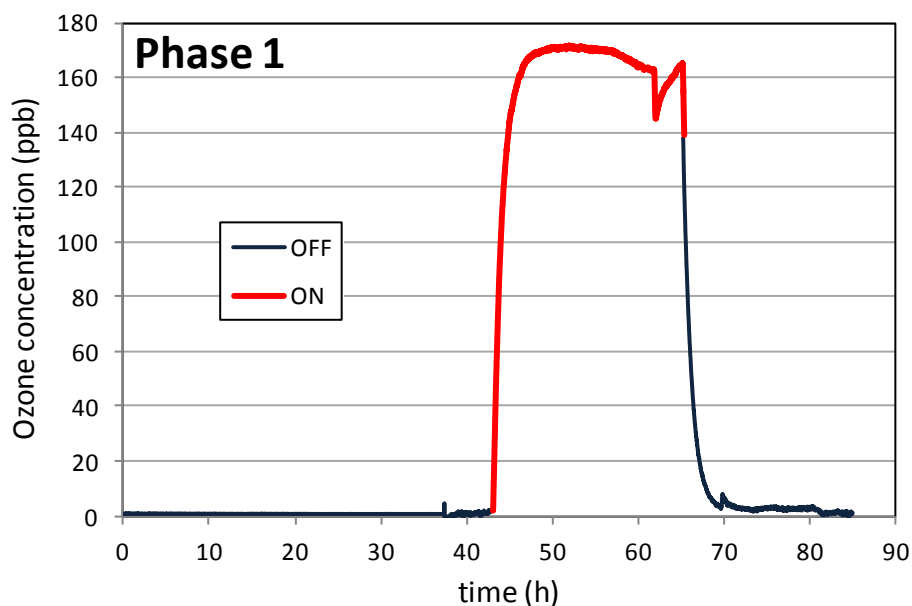


Figure 4.3.2: Ozone concentration profiles for PAC3 – Phase 2

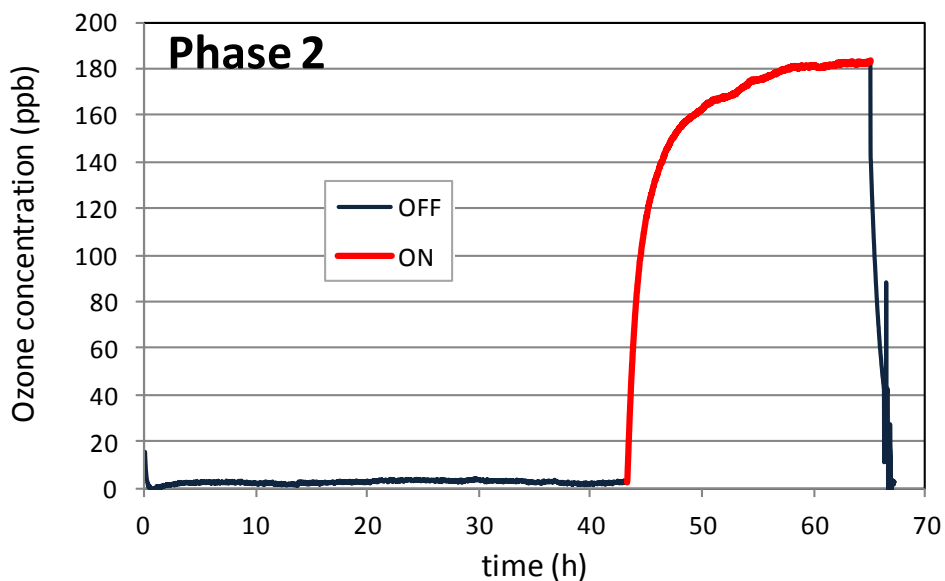
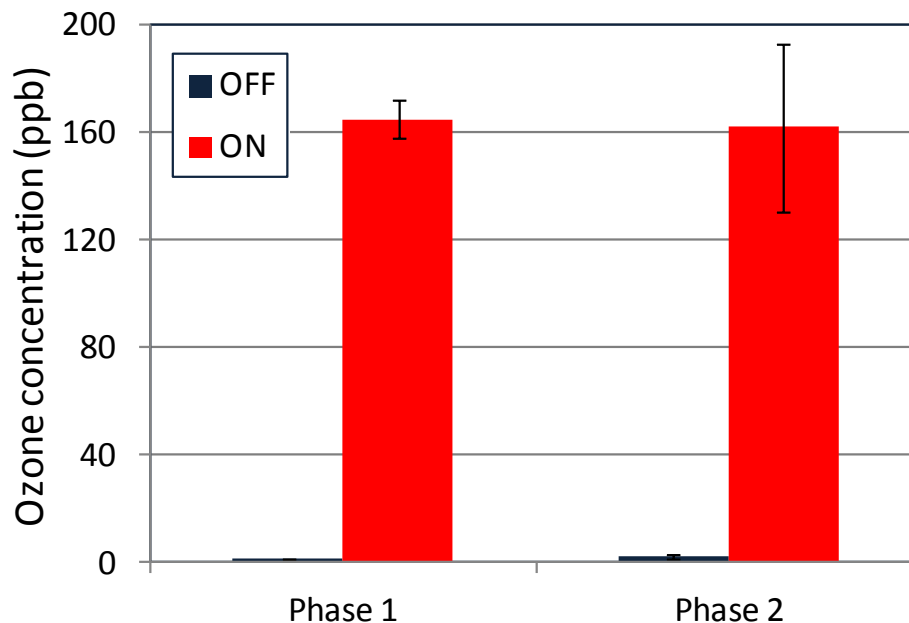


Figure 4.3.3: Average ozone chamber concentrations during periods with air cleaner off and on for PAC3 – Phase 1 and Phase 2



4.3.3. VOCs

Individual VOC concentrations were determined for each phase during OFF and ON periods, and are reported in Figure 4.3.4 (Phase 1) and Figure 4.3.5 (Phase 2). In each case, we include results for the 11 compounds comprising the challenge mixture as well as two byproducts identified in our analysis and which were not included in the challenge mixture: acetaldehyde and acetone. Both compounds were also present in chamber background at ~0.5 ppb and ~1 ppb, respectively. We also include another VOC, benzaldehyde, which is emitted by the device in both Phase 1 and Phase 2.

Each value reported in Figures 4.3.4 and 4.3.5 corresponds to the average of two samples collected simultaneously. The error bars illustrate the absolute difference for each duplicate determination. We performed two sets of duplicate determinations for each Phase 1 condition (ON and OFF), and three set of duplicates for each Phase 2 condition.

Figure 4.3.4: Individual VOC & aldehyde concentrations measured for PAC3 – Phase 1 experiments. Acetaldehyde, acetone and benzaldehyde were not part of the challenge mixture.

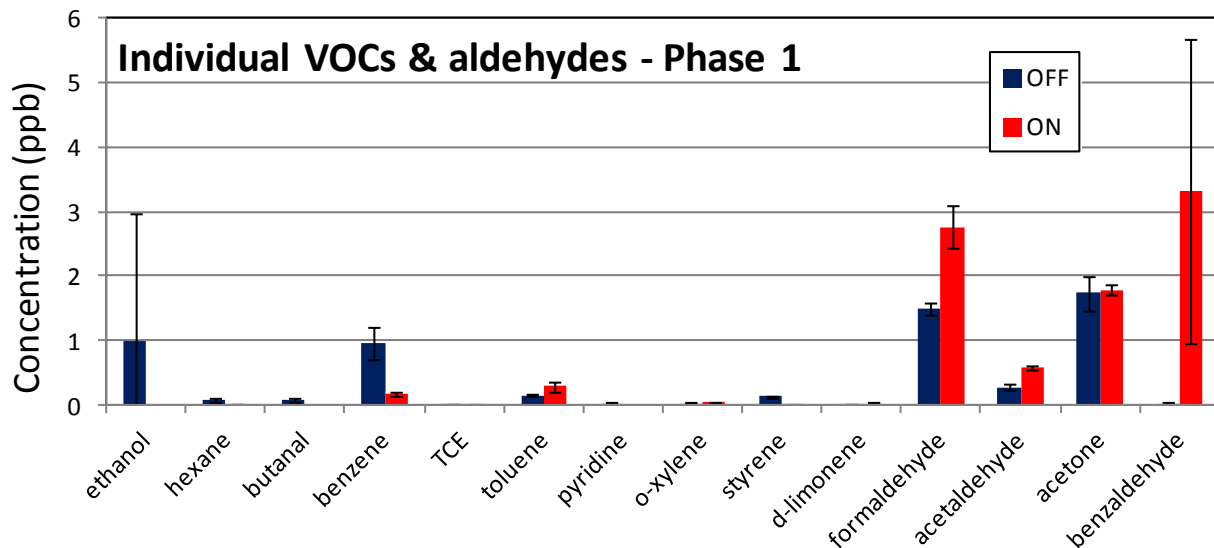
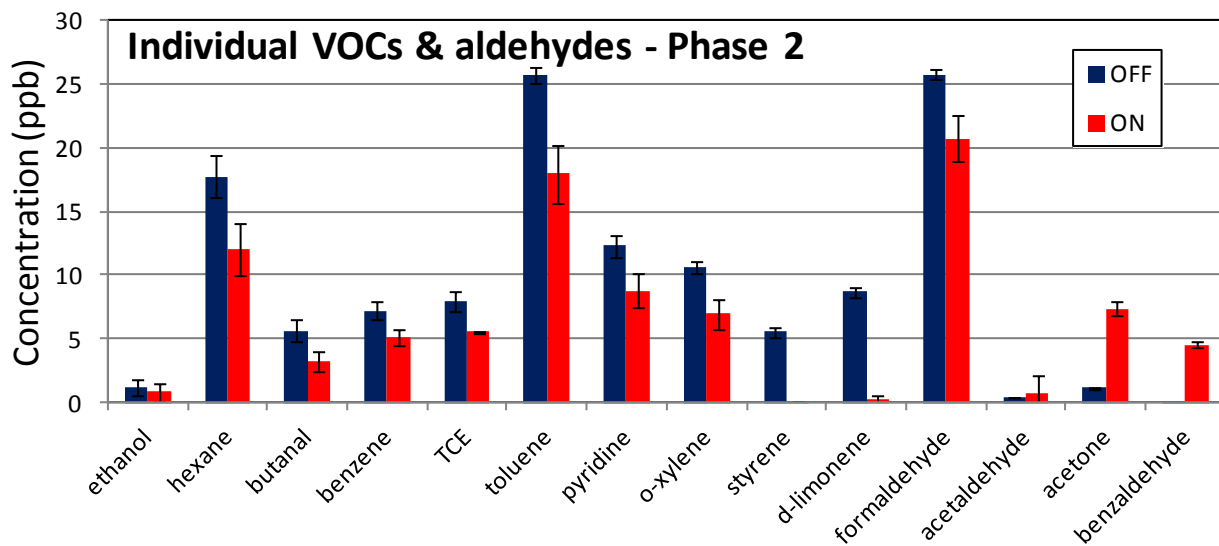


Figure 4.3.5: Individual VOC & aldehyde concentrations measured for PAC3 – Phase 2 experiments. Acetaldehyde, acetone and benzaldehyde were not part of the challenge mixture.



4.3.4. Ultrafine particles

The experimental curves recorded by the W-CPC during Phase 1 and Phase 2 are shown in Figure 4.3.6 and Figure 4.3.7, respectively. We represent in blue the times at which the air cleaner was turned off, and in red those in which the air cleaner was turned on. The integrated averages for periods in which the air cleaner was turned on and off for each phase are shown in Figure 4.3.8. Daily spikes are observed in the morning when the building ventilation is turned on, and constitute the background of our measurements. The data are not background-subtracted; instead, we indicate in each case the range of values corresponding to chamber background levels. Figure 4.3.7 shows clearly particle bursts in the two moments when the air cleaner was turned on on two consecutive days, at times $t = 46$ h and $t = 73$ h.

Figure 4.3.6: Ultrafine particle (UFP, >5 nm) concentration profiles for PAC3 – Phase 1

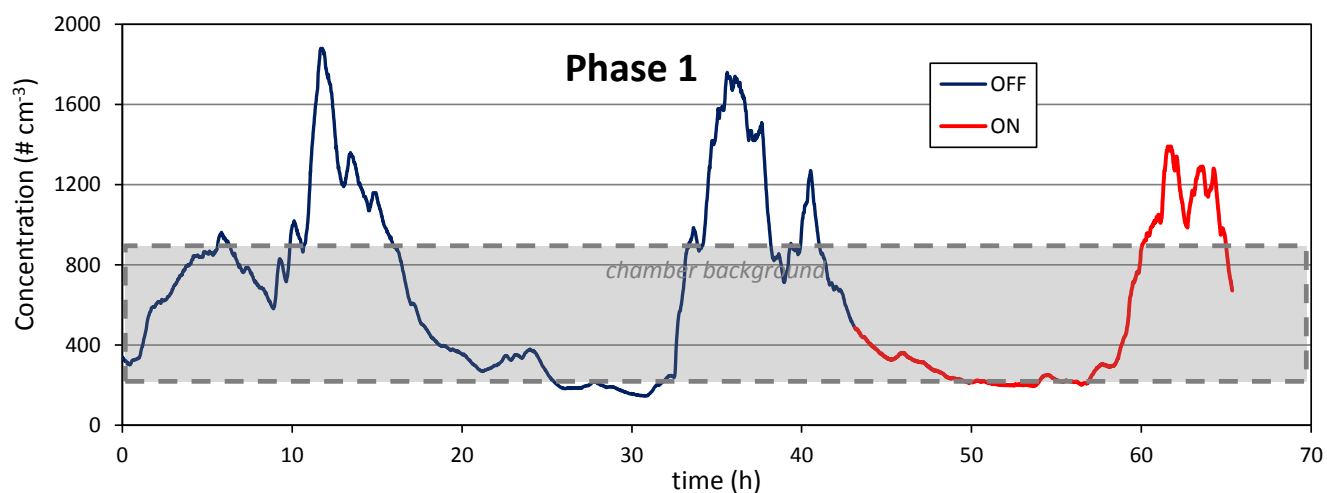


Figure 4.3.7: Ultrafine particle (UFP, >5 nm) concentration profiles for PAC3 – Phase 2

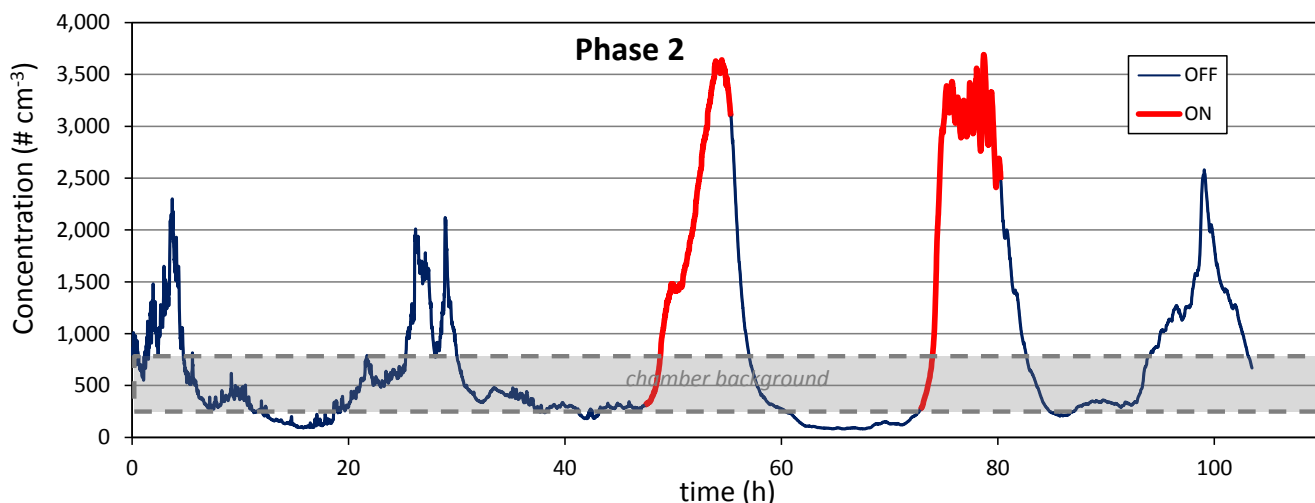
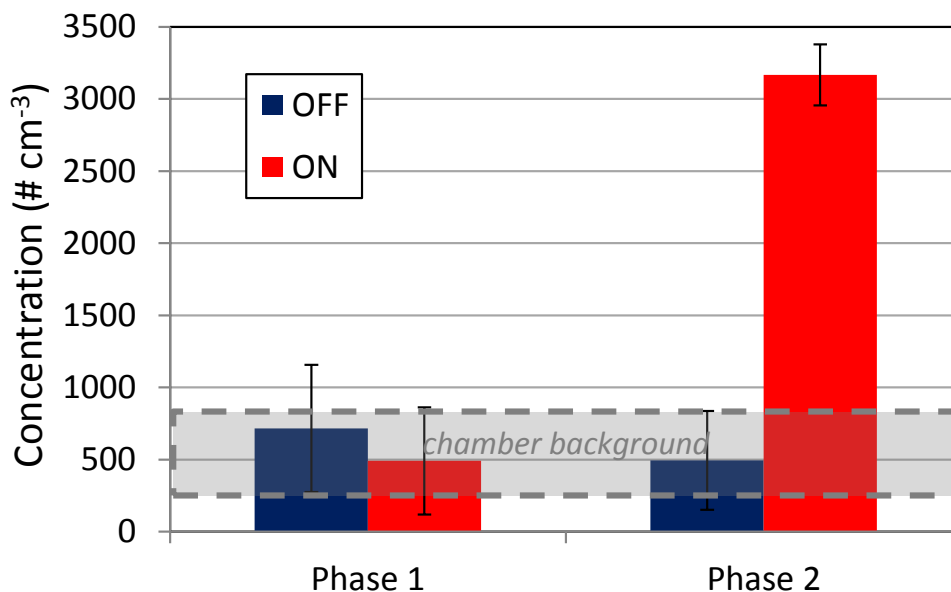


Figure 4.3.8: Average concentration of ultrafine particles (UFP, >5 nm), measured during periods with air cleaner off and on for PAC3
 The data presented are not background-subtracted



4.4. PAC4: Plasma Air Cleaner

4.4.1. Summary of observations

This is the smallest device tested, it is provided with an ON/OFF button and two air velocity settings. We operated it in the “high” setting. Its operation can be verified visually by viewing a LED next to the button which changed colors for the low and high settings. The main observations have been the following:

- Low-level ozone emissions in both Phase 1 and Phase 2 (Figures 4.4.1 – 4.4.3)
- A partial reduction in VOC concentrations was observed in Phase 2, with moderate reduction of most VOCs (Figures 4.4.4 – 4.4.5)
- Formation of formaldehyde as a secondary byproduct, with a concentration increase of the order of 20%. While this is a relatively small increment, it still reflects a measurable change in concentrations (Figures 4.4.4 – 4.4.5)
- We did not observe formation of ultrafine particles (UFP, >5 nm) (Figures 4.4.6 – 4.4.8)
- Results from ROS measurements are presented for all air cleaners in Section 4.7.

The experimental conditions for tests carried out with PAC4 are summarized in Table 4.4.1. Results are presented graphically in Sections 4.4.2 – 4.4.4, and the corresponding pollutant concentrations are presented in Table A.2.4 (Appendix 2).

Table 4.4.1: Experimental conditions used in experiments with PAC4

	Phase 1		Phase 2	
	OFF	ON	OFF	ON
Temperature (°C)	26 ± 1	26 ± 1	27 ± 1	27 ± 1
Relative humidity (%)	43 ± 2	39 ± 7	40 ± 1	39 ± 1
Air exchange rate (h ⁻¹)	0.31 ± 0.03	0.37 ± 0.05	0.54 ± 0.02	0.58 ± 0.02

4.4.2. Ozone

The experimental curves recorded by the ozone monitor during Phase 1 and Phase 2 are shown in Figure 4.4.1 and Figure 4.4.2, respectively. We represent in blue the times at which the air cleaner was turned off, and in red those in which the air cleaner was

turned on. The integrated averages for periods in which the air cleaner was turned on and off during each phase are shown in Figure 4.4.3.

Figure 4.4.1: Ozone concentration profiles for PAC4 – Phase 1

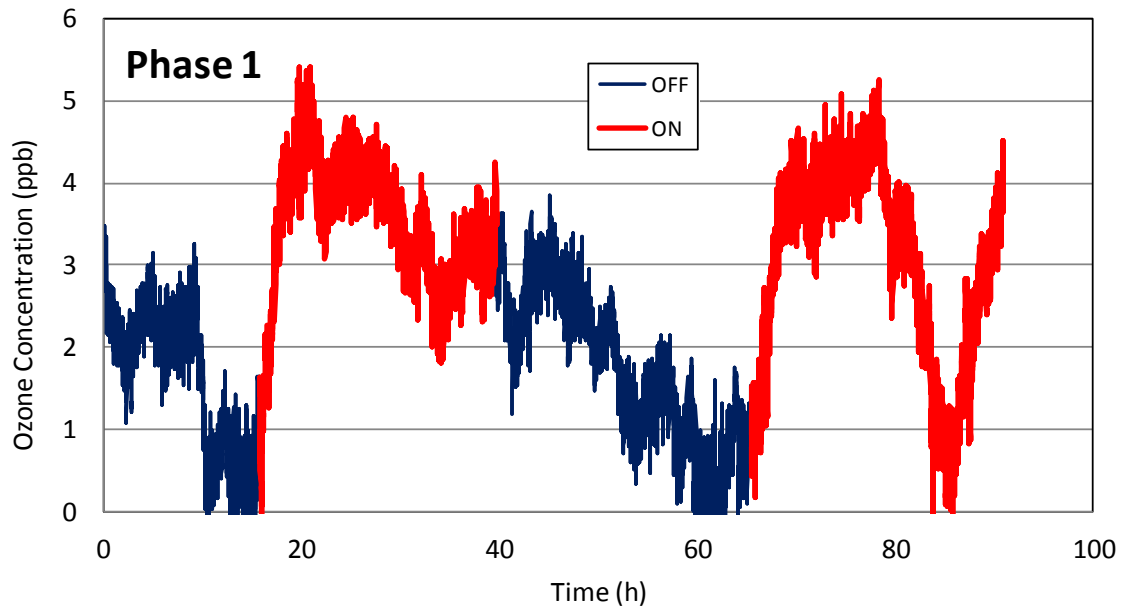


Figure 4.4.2: Ozone concentration profiles for PAC4 – Phase 2

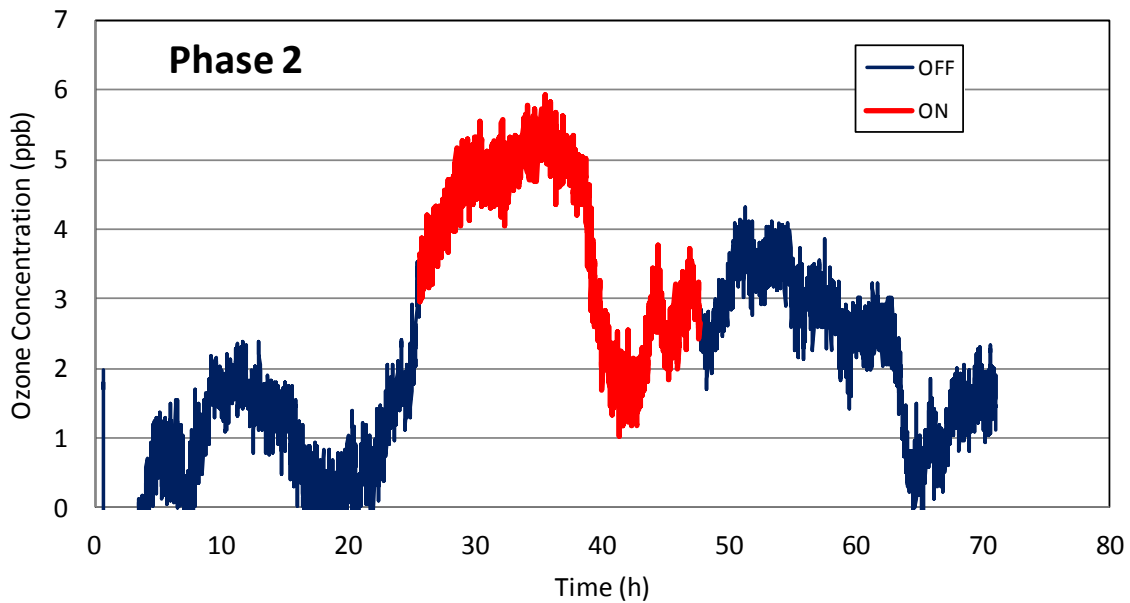
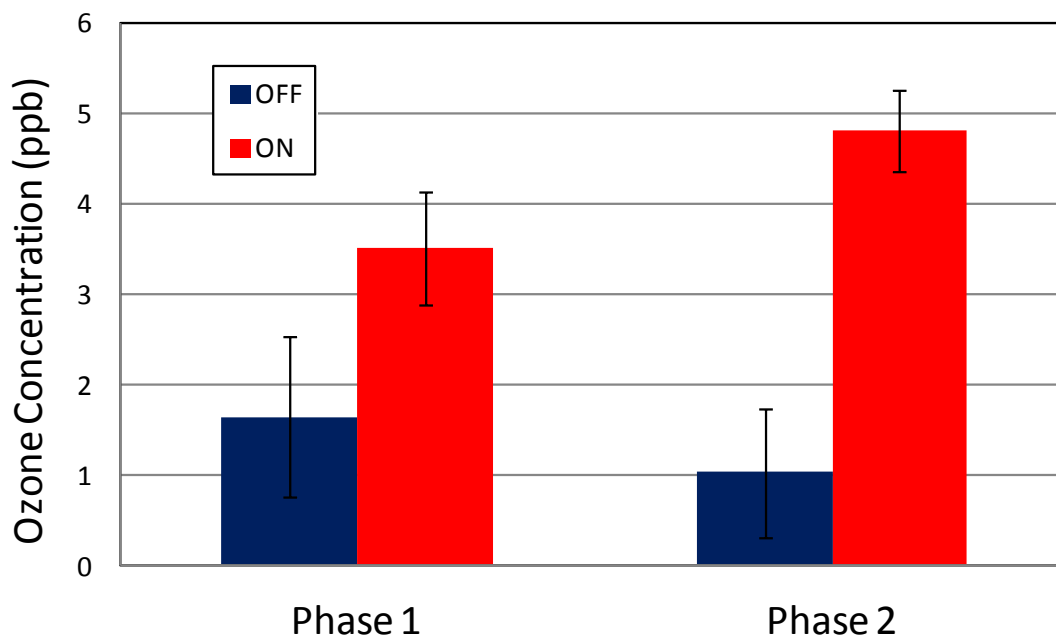


Figure 4.4.3: Average ozone chamber concentrations during periods with air cleaner off and on for PAC4 – Phase 1 and Phase 2



4.4.3. VOCs

Individual VOC concentrations were determined for each phase during OFF and ON periods, and are reported in Figure 4.4.4 (Phase 1) and Figure 4.4.5 (Phase 2). In each case, we include results for the 11 compounds comprising the challenge mixture as well as two byproducts identified in our analysis and which were not included in the challenge mixture: acetaldehyde and acetone. Both compounds were also present in chamber background at ~0.25 ppb and ~1 ppb, respectively.

Each value reported in Figures 4.4.4 and 4.4.5 corresponds to the average of two samples collected simultaneously. The error bars illustrate the absolute difference for each duplicate determination. We performed two sets of duplicate determinations for each Phase 1 condition (ON and OFF), and one set of duplicates for each Phase 2 condition.

Figure 4.4.4: Individual VOC & aldehyde concentrations measured for PAC4 – Phase 1 experiments. Acetaldehyde and acetone were not part of the challenge mixture

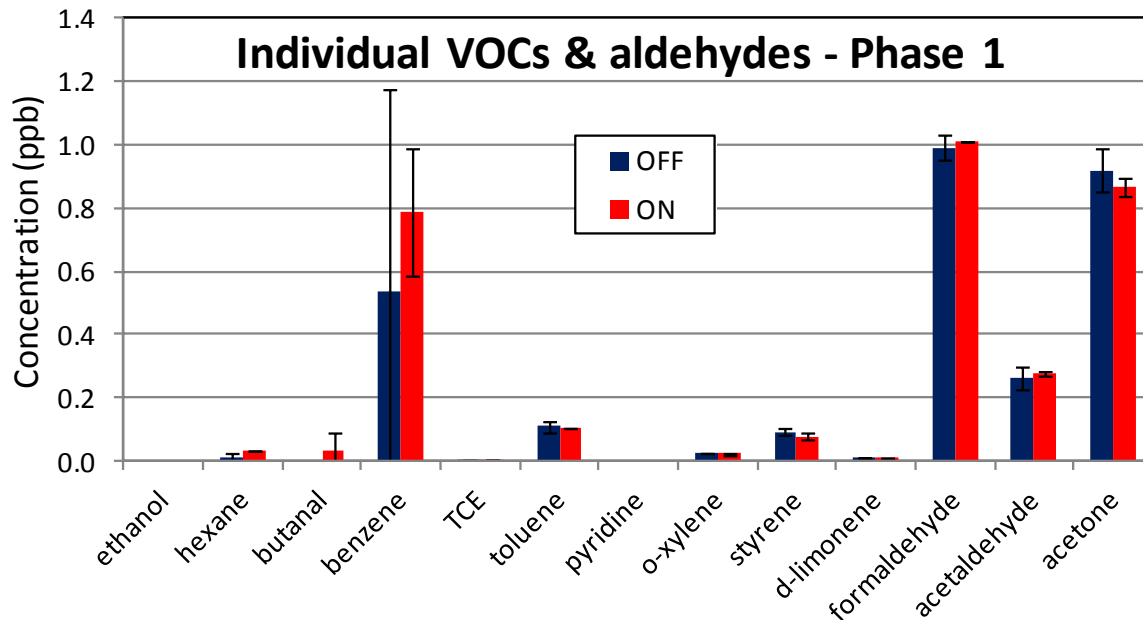
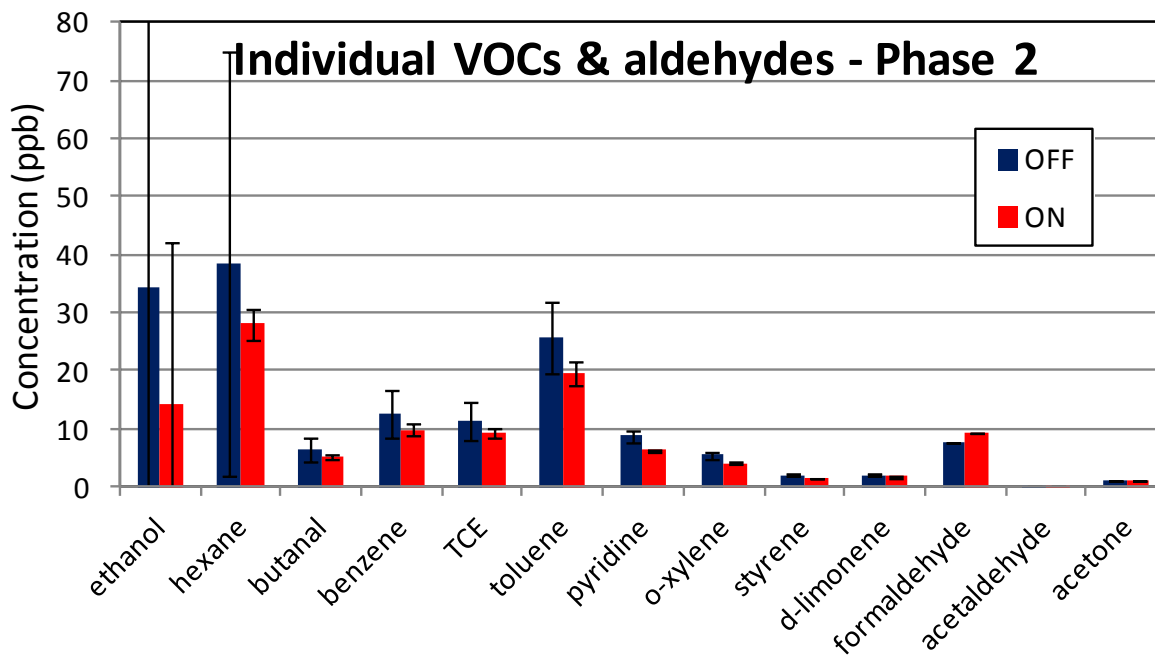


Figure 4.4.5: Individual VOC & aldehyde concentrations measured for PAC4 – Phase 2 experiments. Acetaldehyde and acetone were not part of the challenge mixture.



4.4.4. Ultrafine particles

The experimental curves recorded by the W-CPC during Phase 1 and Phase 2 are shown in Figure 4.4.6 and Figure 4.4.7, respectively. We represent in blue the times at which the air cleaner was turned off, and in red those in which the air cleaner was turned on. The integrated averages for periods in which the air cleaner was turned on and off for each phase are shown in Figure 4.4.8. Daily spikes are observed in the morning when the building ventilation is turned on, and constitute the background of our measurements. The data are not background-subtracted; instead, we indicate in each case the range of values corresponding to chamber background levels.

In Figure 4.4.6 and, most noticeable, in Figure 4.4.7, initial spikes can be observed in some cases when the air cleaner is turned on or off, because it was necessary to open the chamber door to operate the air cleaner manually (as opposed to plugging in and out outside the chamber, the method used for all the other air cleaners). Infiltration of laboratory air, which has a much higher level of particles, is the reason for those spikes. Despite care taken in opening the chamber as little as possible, some infiltration of laboratory air was impossible to avoid.

Figure 4.4.6: Ultrafine particle (UFP, >5 nm) concentration profiles for PAC4 – Phase 1

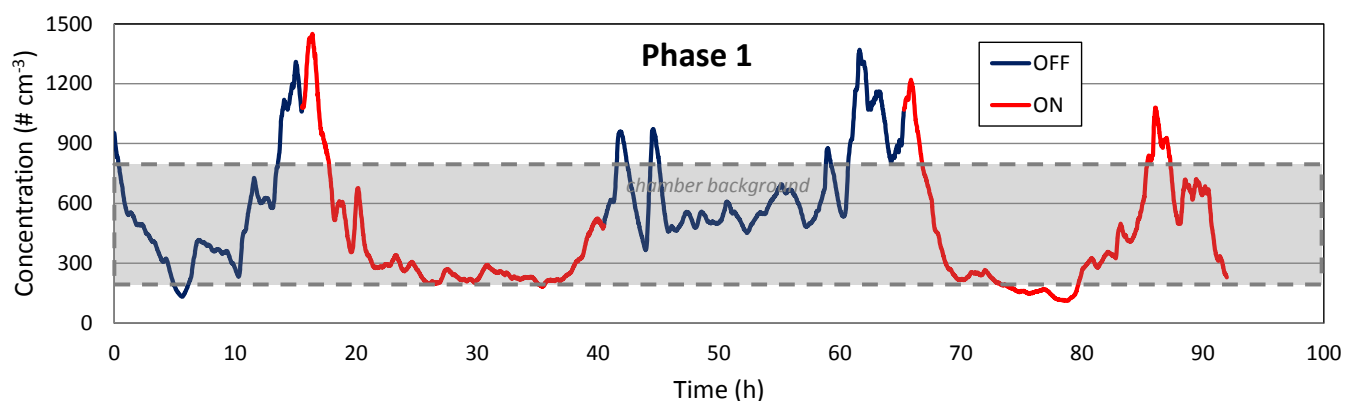


Figure 4.4.7: Ultrafine particle (UFP, >5 nm) concentration profiles for PAC4 – Phase 2

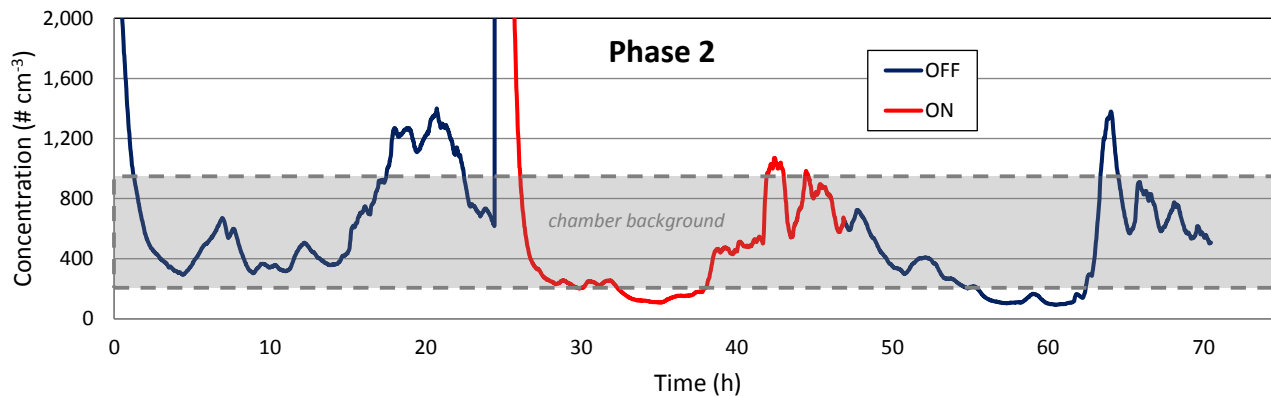
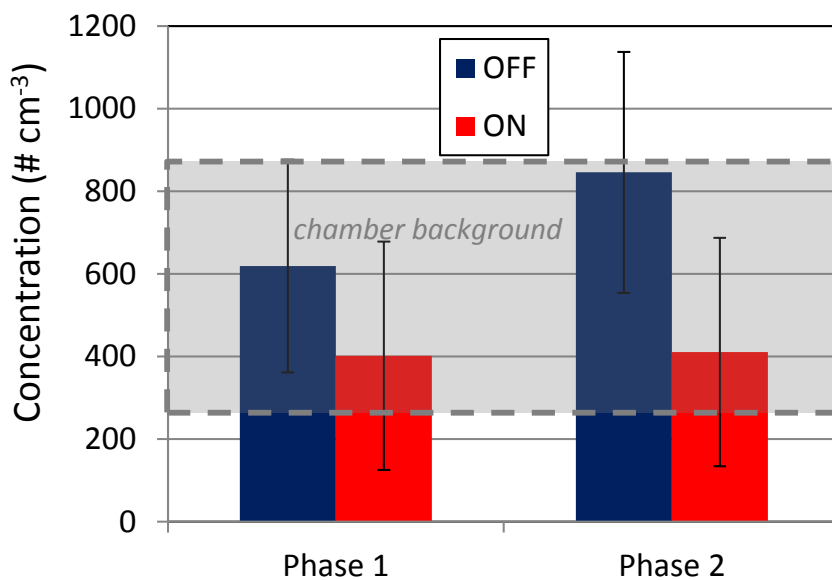


Figure 4.4.8: Average concentration of ultrafine particles (UFP, >5 nm), measured during periods with air cleaner off and on for PAC4



4.5. PAC5: Ceramic Heater with Ionizer

4.5.1. Summary of observations

This device is another typical “tower” air cleaner, it can be operated either as a ionizer (without heating) or as a combined heater/ionizer. We performed tests in both conditions. Its operation can be verified visually by checking on a LED on the top of the device. The main observations have been the following:

- Temperature increased rapidly when the air cleaner/heater was turned on. The device thermostat does not allow for increases above 45 °C (Figure 4.5.1).
- Relative humidity decreased rapidly when the air cleaner/heater was turned on (Figure 4.5.2).
- The ozone monitor was affected by rapid changes in relative humidity and could not be used while the device was heating. Ozone was measured separately, with the device operating only the ionizer function (no heating). No ozone emissions were observed (Fig. 4.5.3 – 4.5.5)
- No reduction of VOC concentrations, but rather weak emissions of VOCs were observed both with the system operating as a ionizer only, and as a heater/ionizer, which may be in part due to desorption from chamber walls upon heating (Figures 4.5.6 – 4.5.7)
- Formaldehyde levels were partially reduced (Figures 4.5.6 – 4.5.7)
- Average concentrations of ultrafine particles (UFP, >5 nm) did not exceed chamber background levels. However, an increase in UFP concentration was observed during heating periods (Figures 4.2.8 – 4.2.10).
- Results from ROS measurements are presented for all air cleaners in Section 4.7.

The experimental conditions for tests carried out with PAC5 are summarized in Table 4.5.1. Results are presented graphically in Sections 4.5.2 – 4.5.4, and the corresponding pollutant concentrations are presented in Tables A.2.5 and A.2.6 (Appendix 2).

Table 4.5.1: Experimental conditions used in experiments with PAC5

	Phase 1		Phase 2	
	OFF	ON	OFF	ON
Temperature (°C)	26 ± 1	33 ± 4	31 ± 1	35 ± 3
Relative humidity (%)	33 ± 3	25 ± 5	22 ± 5	17 ± 5
Air exchange rate (h ⁻¹)	0.66 ± 0.02	0.66 ± 0.02	0.61 ± 0.01	0.62 ± 0.01

Figure 4.5.1: Chamber temperature measured for the operation of PAC5 as a heater/ionizer during Phase 1 and Phase 2

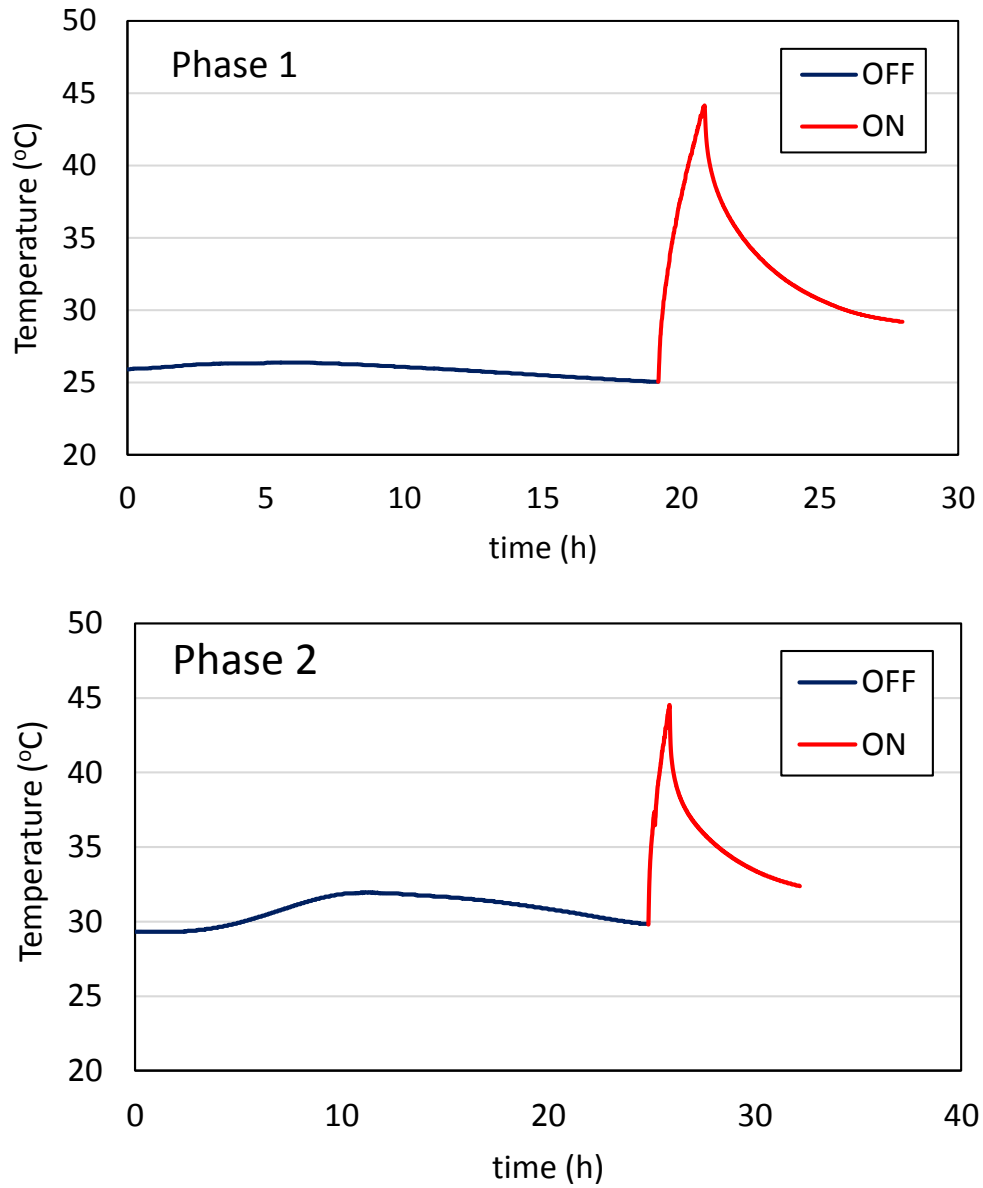
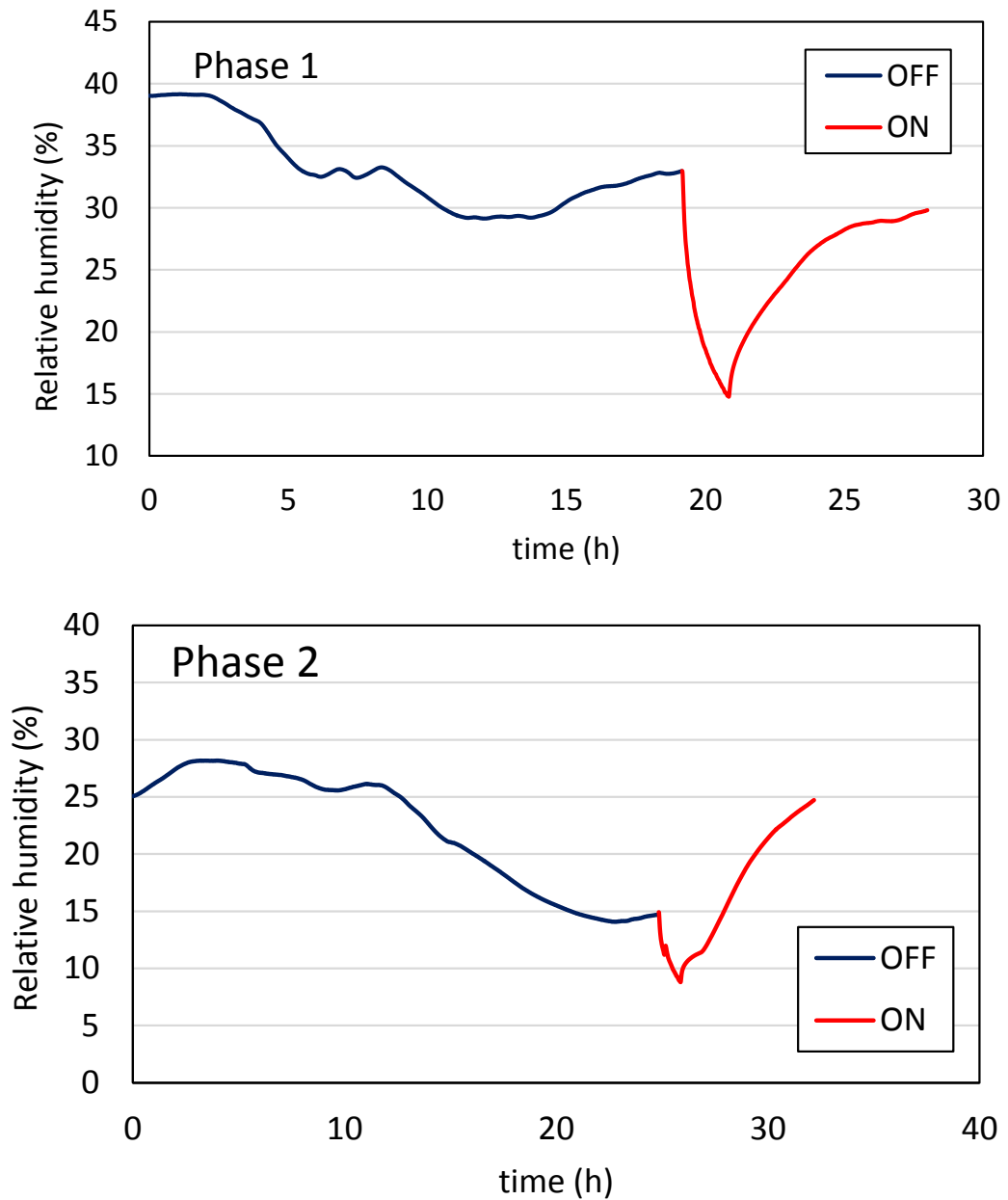


Figure 4.5.2: Chamber relative humidity measured for the operation of PAC5 as a heater/ionizer during Phase 1 and Phase 2



4.5.2. Ozone

The experimental curves recorded by the ozone monitor during Phase 1 and Phase 2 are shown in Figure 4.5.3 and Figure 4.5.4, respectively. We represent in blue the times at which the air cleaner was turned off, and in red those in which the air cleaner was turned on. The integrated averages for periods in which the air cleaner was turned on and off during each phase are shown in Figure 4.5.5.

Ozone could not be measured with the air cleaner operating as a heater because the ozone monitor was affected by the rapid changes in relative humidity shown in Figure 4.5.2 during most of the “ON” period. For that reason, we report only measurements of ozone carried out with the instrument operating as a ionizer only.

Spikes shown in both tests, and most particularly in Phase 2, are not related with the air cleaner. The ozone monitor was probably affected over short periods of time by interferences such as particles inside the sensor.

Figure 4.5.3: Ozone concentration profiles for PAC5 – Phase 1 (ionizer only)

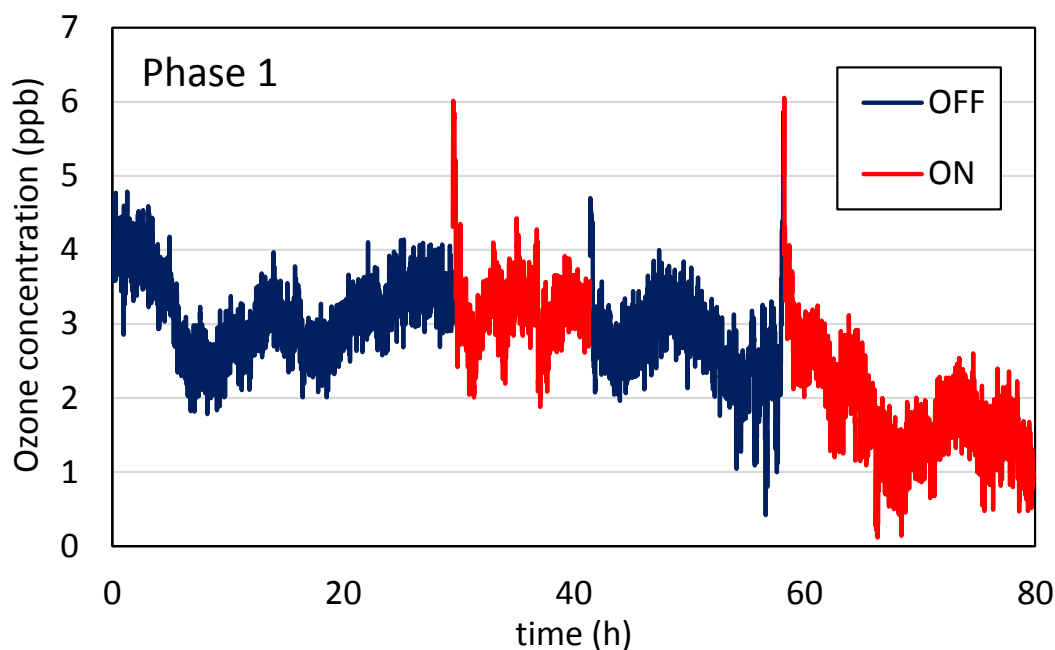


Figure 4.5.4: Ozone concentration profiles for PAC5 – Phase 2 (ionizer only)

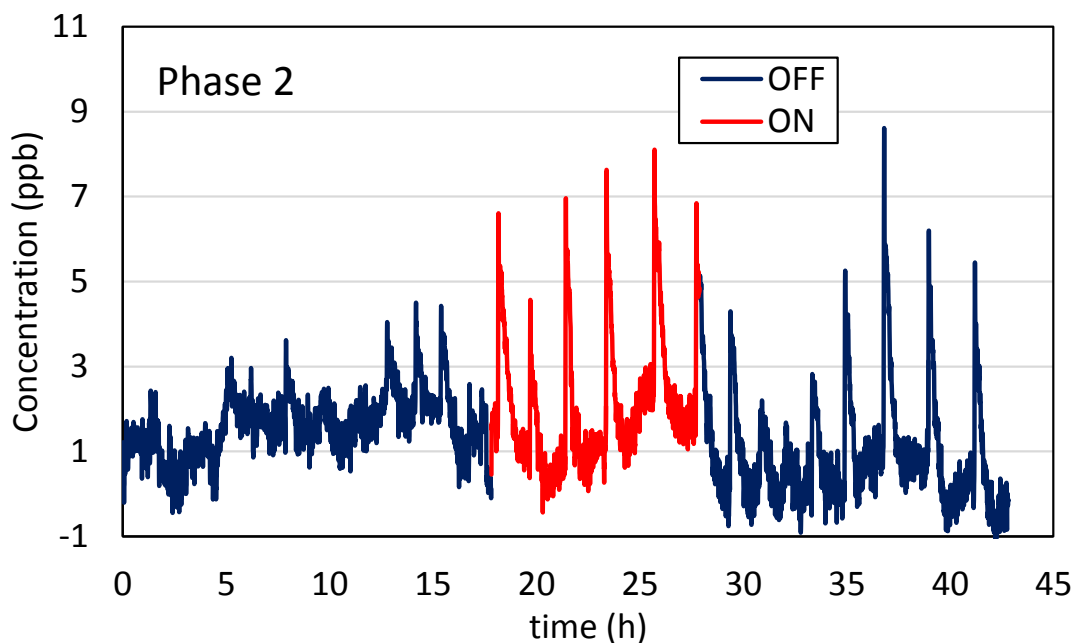
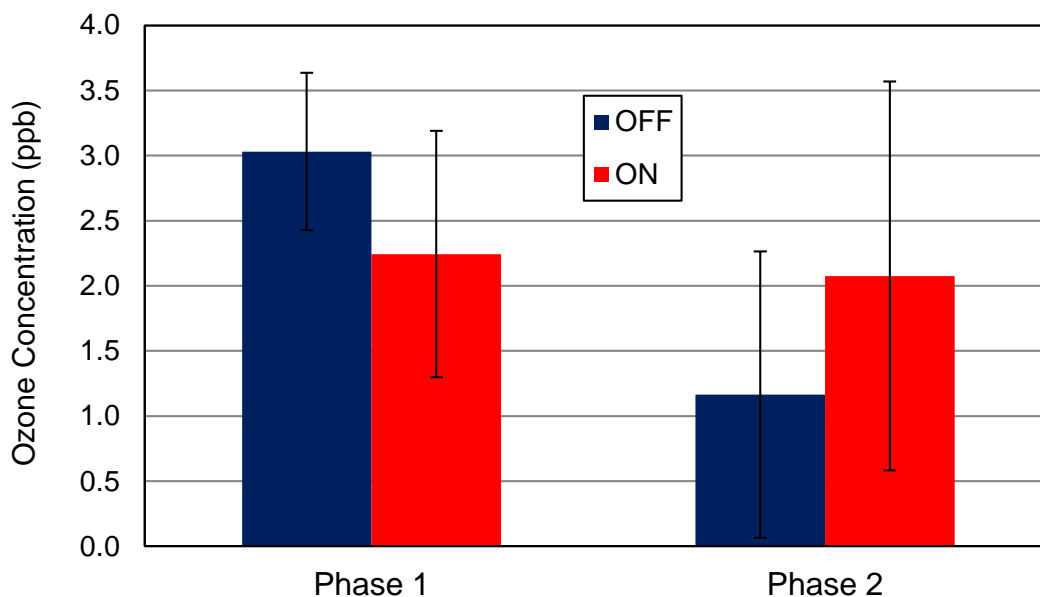


Figure 4.5.5: Average ozone chamber concentrations during periods with air cleaner off and on in Phase 1 and Phase 2 for PAC5 – (ionizer only)



4.5.3. VOCs

Individual VOC concentrations were determined for the instrument operating as a ionizer and as a heater/ionizer for each phase during OFF and ON periods, as reported in Figure 4.5.6 (Phase 1) and Figure 4.5.7 (Phase 2). Samples were collected at the end of the heating period, when temperatures were below 35 °C, to avoid artifacts associated with higher temperatures. In each case, we include results for the 11 compounds comprising the challenge mixture as well as two byproducts identified in our analysis and which were not included in the challenge mixture: acetaldehyde and acetone. Both compounds were also present in chamber background at ~0.25 ppb and ~1 ppb, respectively.

Each value reported in Figures 4.5.6 and 4.5.7 corresponds to the average of two samples collected simultaneously. The error bars illustrate the absolute difference for each duplicate determination. We performed two sets of duplicate determinations for each Phase 1 condition (ON and OFF), and one set of duplicates for each Phase 2 condition.

Figure 4.5.6: Individual VOC & aldehyde concentrations measured for PAC5 – Phase 1 experiments. Acetaldehyde and acetone were not part of the challenge mixture.

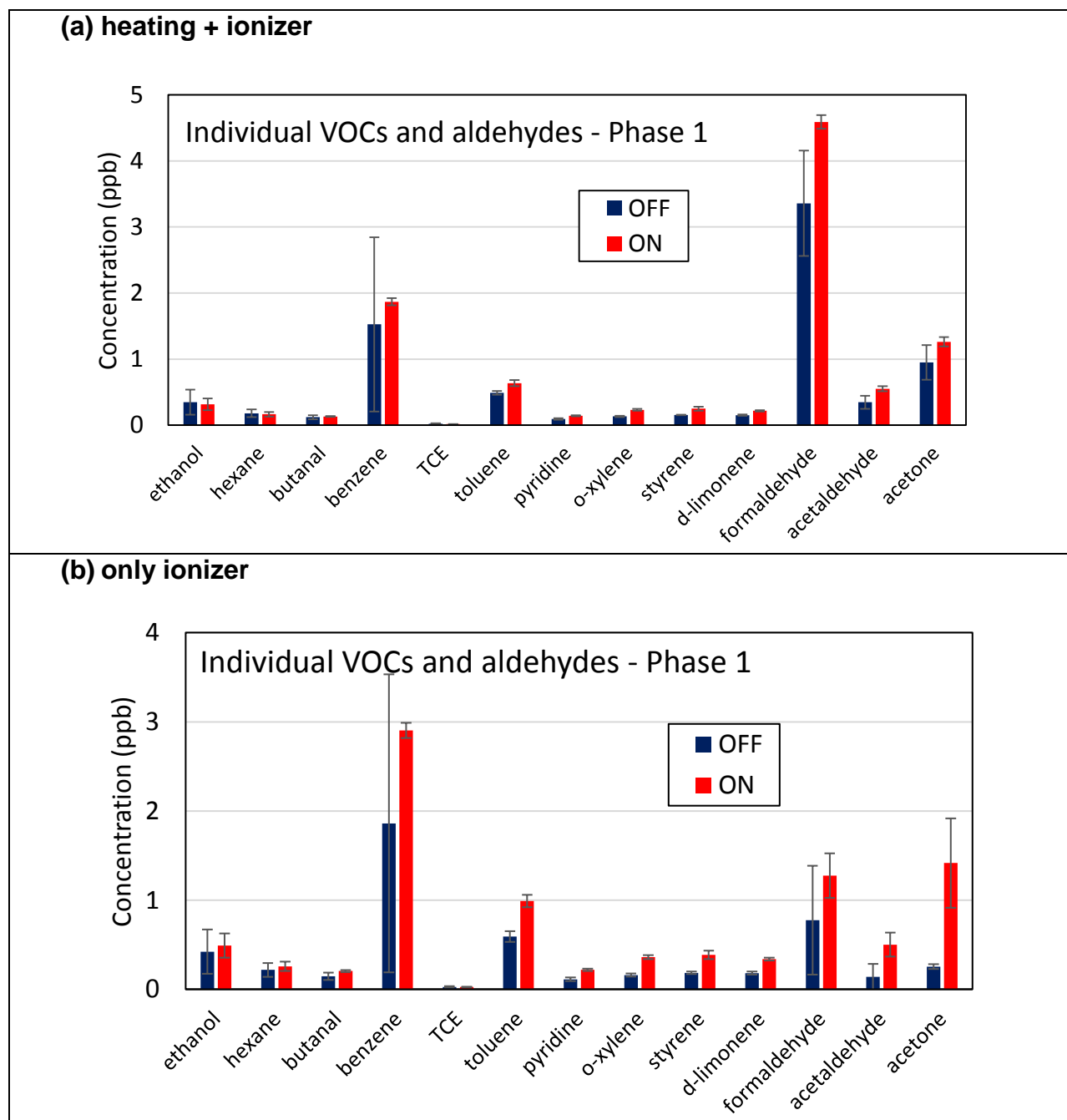
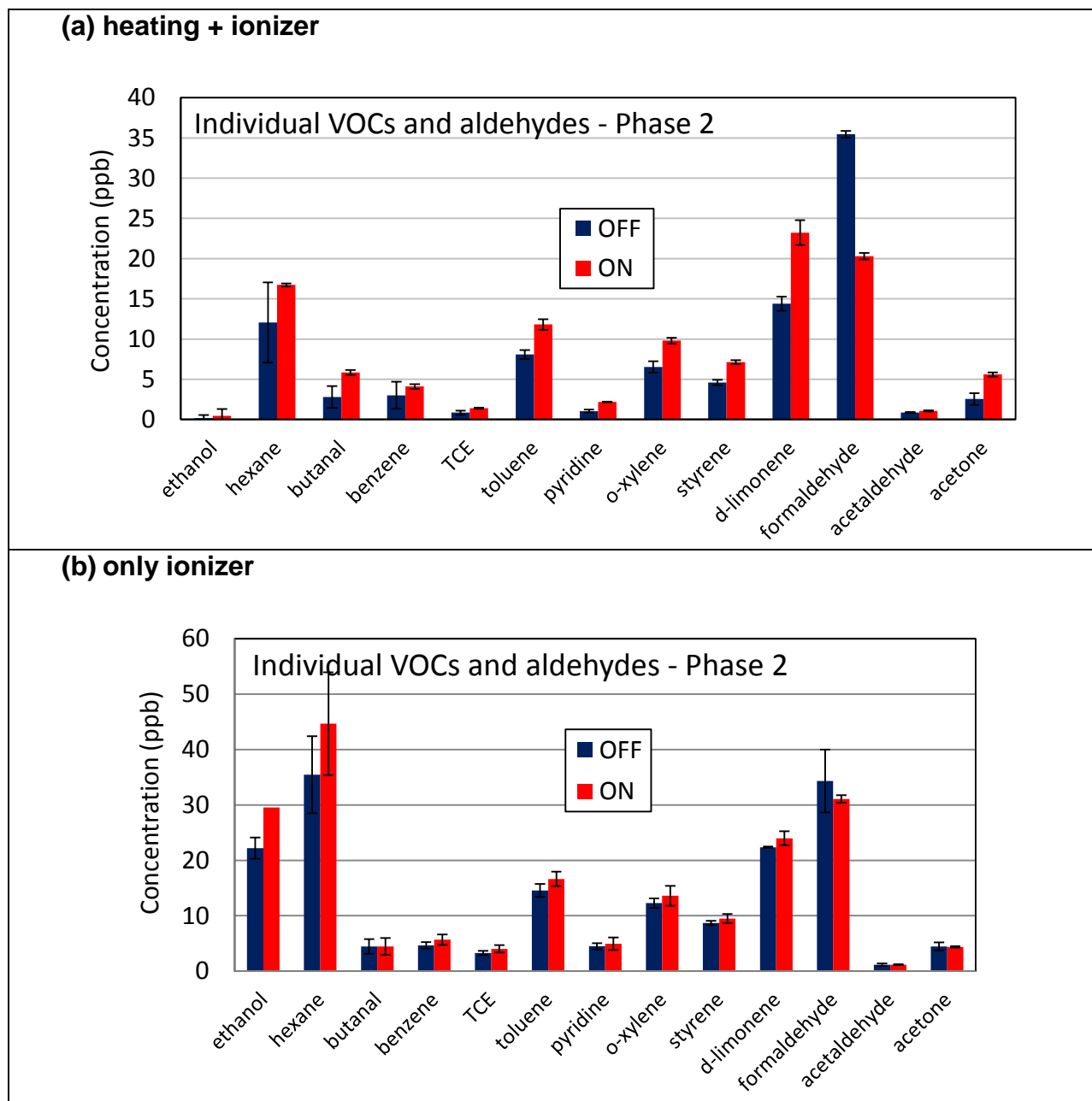


Figure 4.5.7: Individual VOC & aldehyde concentrations measured for PAC5 – Phase 2 experiments. Acetaldehyde and acetone were not part of the challenge mixture.



4.5.4. Ultrafine particles

The experimental curves recorded by the W-CPC during Phase 1 and Phase 2 are shown in Figure 4.5.8 and Figure 4.5.9, respectively. We represent in blue the times at which the air cleaner was turned off, and in red those in which the air cleaner was turned on. The integrated averages for periods in which the air cleaner was turned on and off for each phase are shown in Figure 4.5.10. Daily spikes are observed in the morning when the building ventilation is turned on, and constitute the background of our measurements. The data are not background-subtracted; instead, we indicate in each case the range of values corresponding to chamber background levels. We observed, particularly in Phase 1, a low level particle emission at the moment at which the air cleaner was turned on. However, the increase in UFP measured was not significantly larger than the chamber background.

Figure 4.5.8: Ultrafine particle (UFP, >5 nm) concentration profiles for PAC5 – Phase 1 (heating + ionizer)

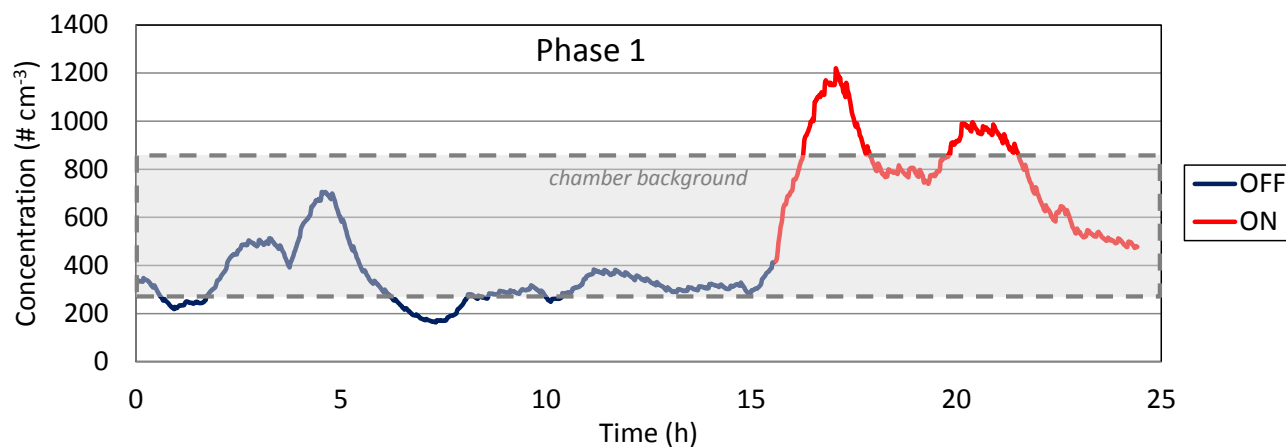


Figure 4.5.9: Ultrafine particle (UFP, >5 nm) concentration profiles for PAC5 – Phase 2 (heating + ionizer)

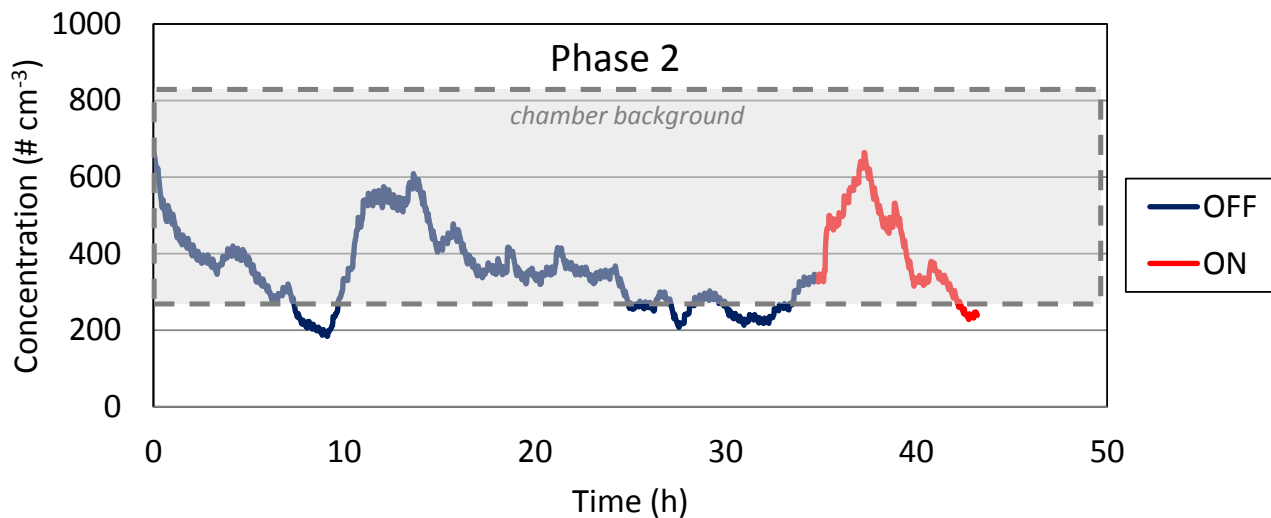
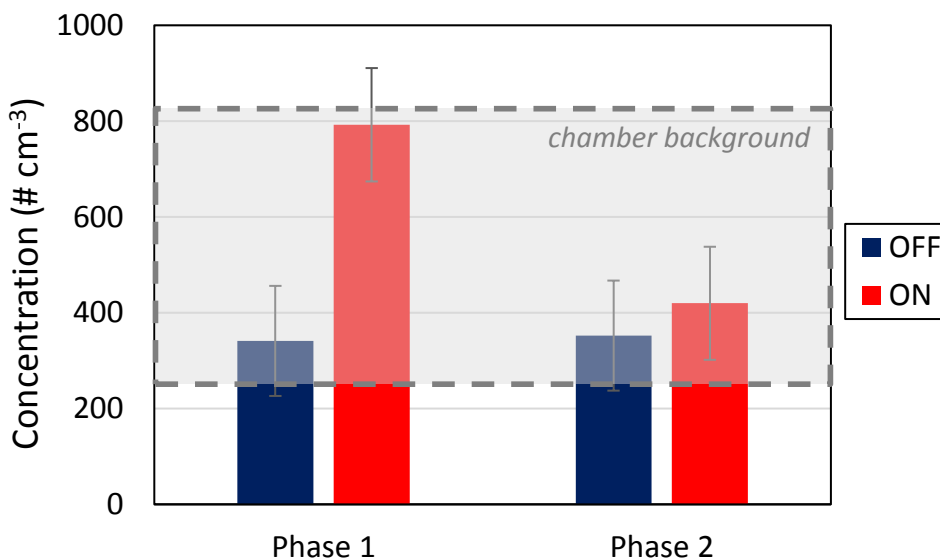


Figure 4.5.10: Average concentration of ultrafine particles (UFP, >5 nm), measured during periods with air cleaner off and on (heating + ionizer) for PAC5



4.6. PAC6: Heating Air Purifier

4.6.1. Summary of observations

This device is provided with an ON/OFF button and a single air velocity setting. Its operation can be verified visually by viewing a blue light on the upper side of the device. The main observations have been the following:

- a. No ozone emissions in both Phase 1 and Phase 2 (Figures 4.6.1 – 4.6.3)
- b. A small reduction in VOC concentrations was observed in Phase 2 (Figures 4.6.4 – 4.4.5)
- c. No formation of secondary byproducts (Figures 4.6.4 – 4.6.5)
- d. We did not observe formation of ultrafine particles (UFP, >5 nm) (Figures 4.6.6 – 4.6.8)
- e. Results from ROS measurements are presented for all air cleaners in Section 4.7.

The experimental conditions for tests carried out with PAC6 are summarized in Table 4.6.1. Results are presented graphically in Sections 4.6.2 – 4.6.4, and the corresponding pollutant concentrations are presented in Table A.2.7 (Appendix 2).

Table 4.6.1: Experimental conditions used in experiments with PAC6

	Phase 1		Phase 2	
	OFF	ON	OFF	ON
Temperature (°C)	25 ± 1	26 ± 2	25 ± 1	26 ± 1
Relative humidity (%)	28 ± 3	22 ± 1	31 ± 2	30 ± 2
Air exchange rate (h ⁻¹)	0.48 ± 0.02	0.47 ± 0.02	0.54 ± 0.04	0.54 ± 0.04

4.6.2. Ozone

The experimental curves recorded by the ozone monitor during Phase 1 and Phase 2 are shown in Figure 4.6.1 and Figure 4.6.2, respectively. We represent in blue the times at which the air cleaner was turned off, and in red those in which the air cleaner was turned on. The integrated averages for periods in which the air cleaner was turned on and off during each phase are shown in Figure 4.6.3.

Figure 4.6.1: Ozone concentration profiles for PAC6 – Phase 1

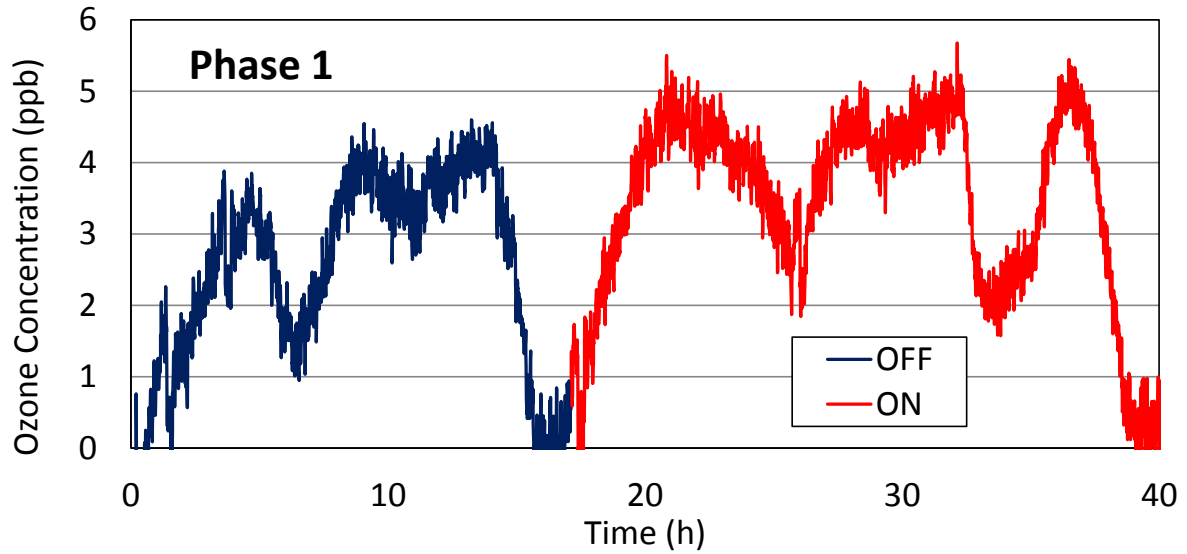


Figure 4.6.2: Ozone concentration profiles for PAC6 – Phase 2

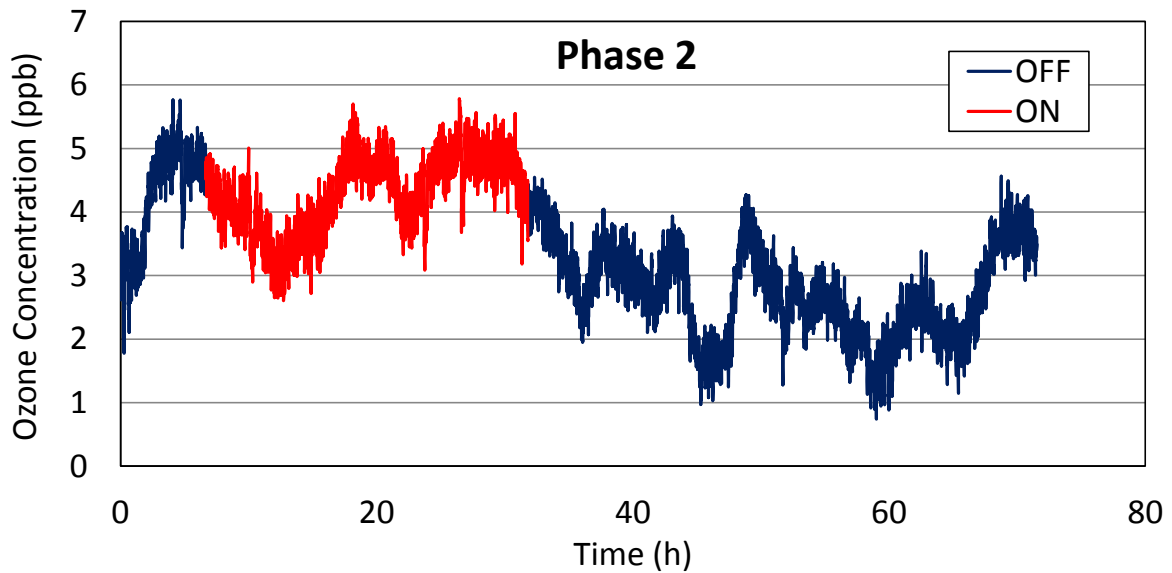
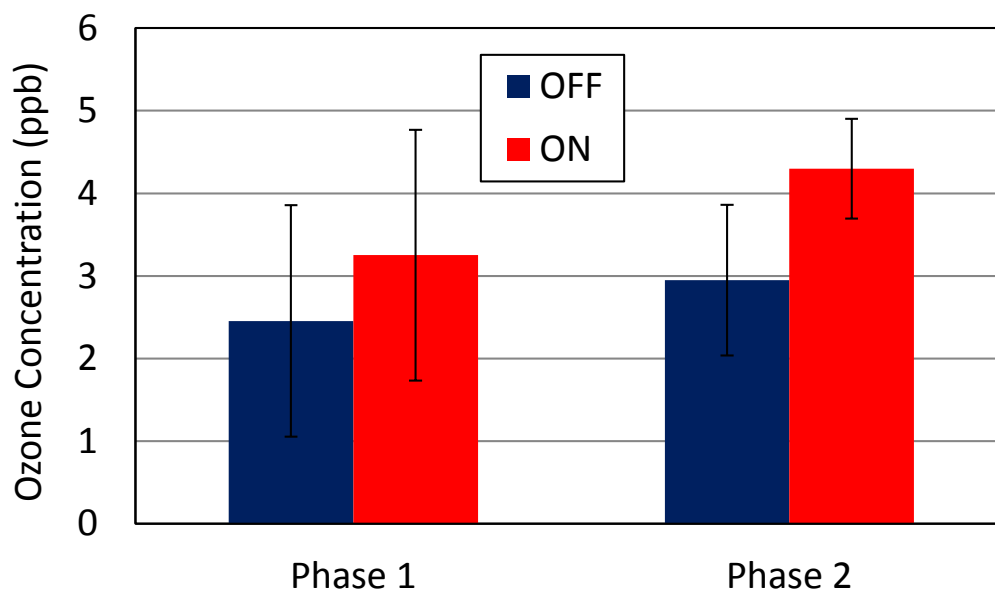


Figure 4.6.3: Average ozone chamber concentrations during periods with air cleaner off and on during Phase 1 and Phase 2 for PAC6



4.6.3. VOCs

Individual VOC concentrations were determined for each phase during OFF and ON periods, and are reported in Figure 4.6.4 (Phase 1) and Figure 4.6.5 (Phase 2). In each case, we include results for the 11 compounds comprising the challenge mixture as well as two byproducts identified in our analysis and which were not included in the challenge mixture: acetaldehyde and acetone. Both compounds were also present in chamber background at ~0.25 ppb and ~1 ppb, respectively.

Each value reported in Figures 4.6.4 and 4.6.5 corresponds to the average of two samples collected simultaneously. The error bars illustrate the absolute difference for each duplicate determination. We performed one set of duplicate determinations for each Phase 1 condition (ON and OFF), and one set of duplicates for each Phase 2 condition.

Figure 4.6.4: Individual VOC & aldehyde concentrations measured for PAC6 – Phase 1 experiments. Acetaldehyde and acetone were not part of the challenge mixture.

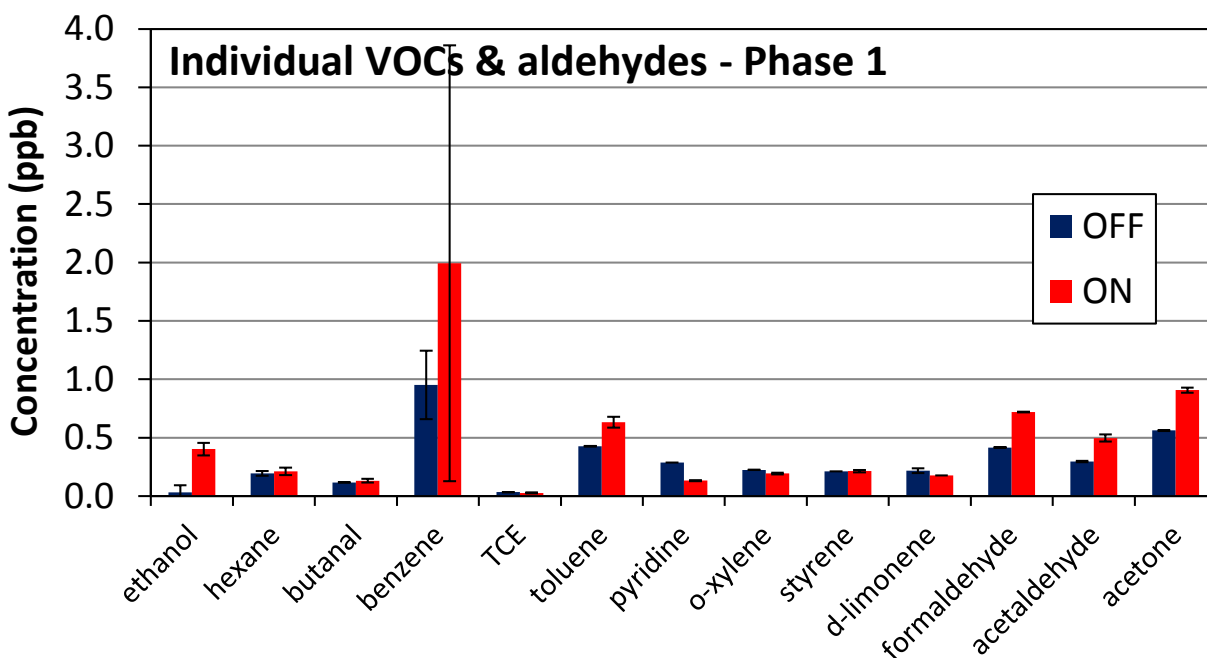
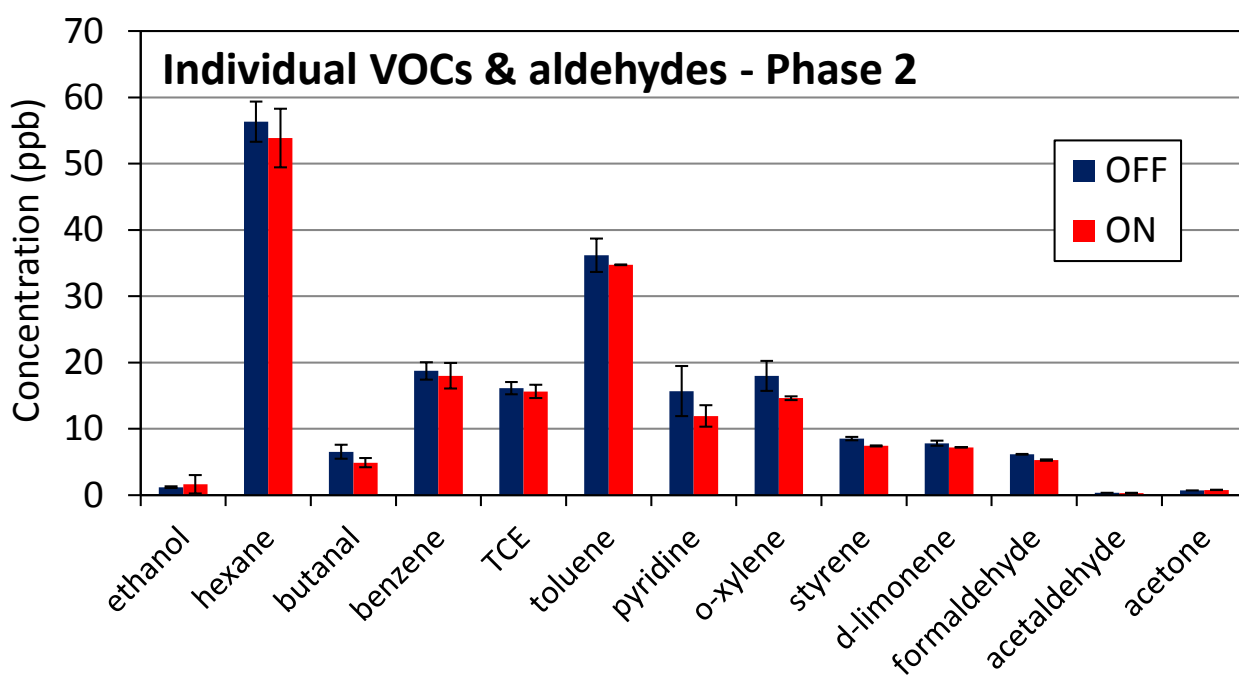


Figure 4.6.5: Individual VOC & aldehyde concentrations measured for PAC6 – Phase 2 experiments. Acetaldehyde and acetone were not part of the challenge mixture.



4.6.4. Ultrafine particles

The experimental curves recorded by the W-CPC during Phase 1 and Phase 2 are shown in Figure 4.6.6 and Figure 4.6.7, respectively. We represent in blue the times at which the air cleaner was turned off, and in red those in which the air cleaner was turned on. The integrated averages for periods in which the air cleaner was turned on and off for each phase are shown in Figure 4.6.8. Daily spikes are observed in the morning when the building ventilation is turned on, and constitute the background of our measurements. The data are not background-subtracted; instead, we indicate in each case the range of values corresponding to chamber background levels.

Figure 4.6.6: Ultrafine particle (UFP, >5 nm) concentration profiles for PAC6 – Phase 1

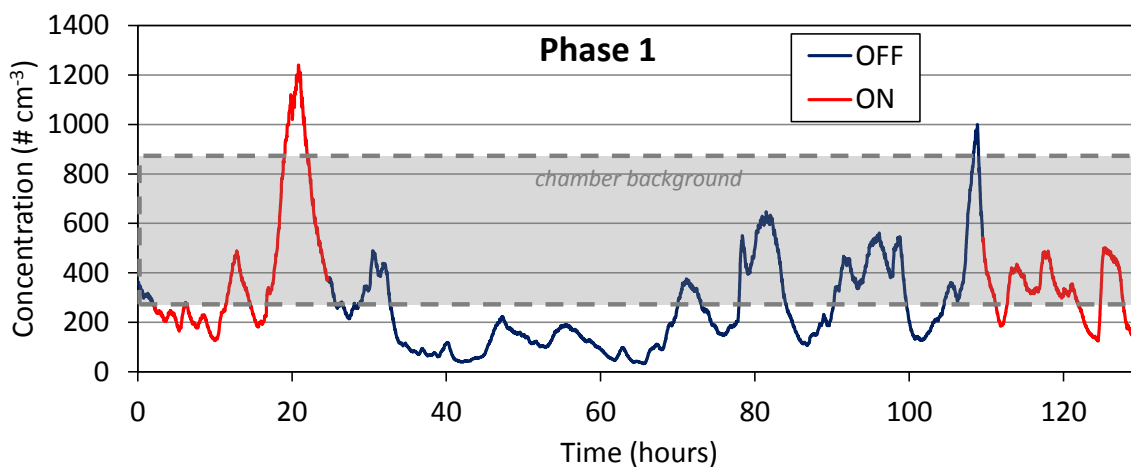


Figure 4.6.7: Ultrafine particle (UFP, >5 nm) concentration profiles for PAC6 – Phase 2

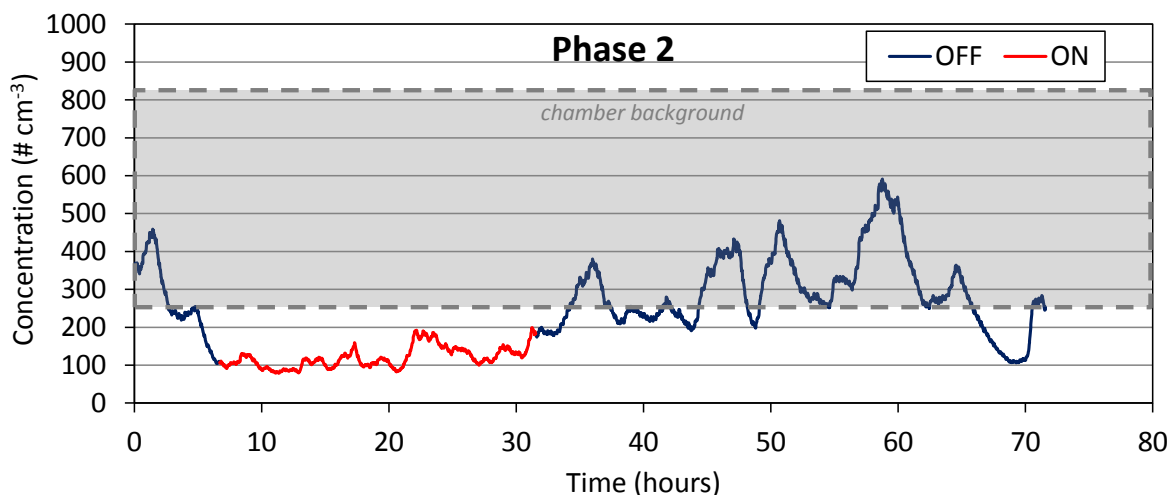
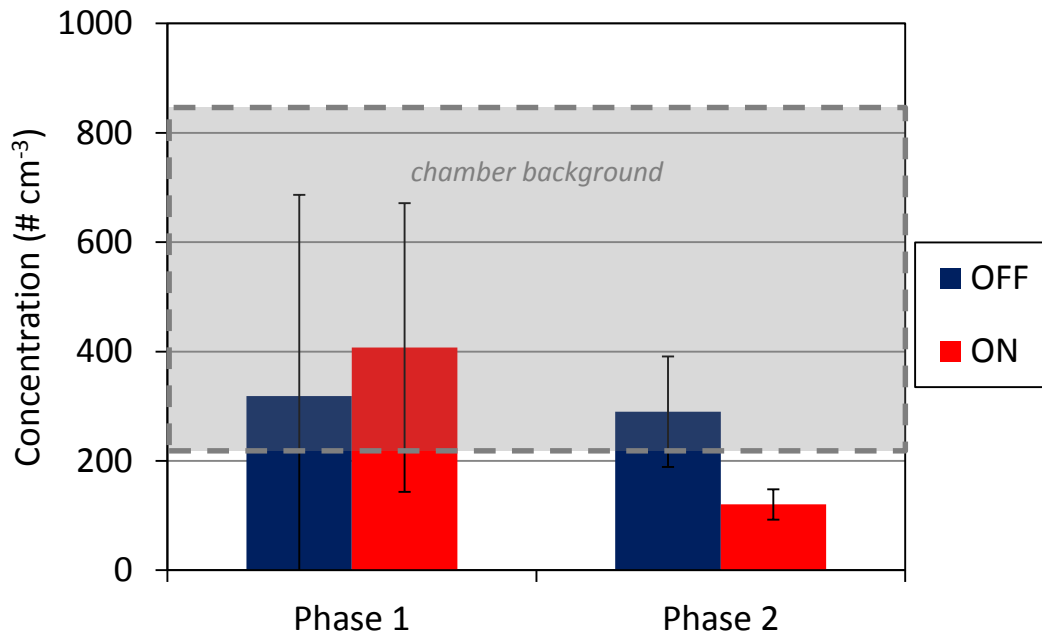


Figure 4.6.8: Average concentration of ultrafine particles (UFP, >5 nm), measured during periods with air cleaner off and on for PAC6



4.7. ROS measurements

Samples were collected from chamber air during OFF and ON periods, simultaneously with the VOC and aldehyde samples. The method described in Section 3.6 was applied to those samples immediately after collection. Results for all six air cleaners are reported in Figures 4.7.1 (DCFH), 4.7.2 (AuR) and 4.7.3 (TPA).

In most cases, ROS concentrations were within the chamber blank values, which are listed in Table 4.7.1, indicating that there was no increase in ROS levels when the air cleaners were operating. The chamber background (blank) levels were calculated as an average of all Phase 1 and all Phase 2 determinations with the air cleaner OFF.

Only for PAC3 the measured ROS levels were systematically higher than chamber blank. As was shown in Sections 3.6.3 and 3.6.4, these ROS levels correspond to the decomposition of dissolved ozone in the buffers used to collect the sample, and not to gas phase peroxide or radicals which cannot be accounted for separately. It should be noted that the ROS concentrations measured for PAC3 with DCFH and TPA were between two and three times higher in Phase 2 than in Phase 1, suggesting that the reaction of ozone with VOCs leads to the formation of measurable levels of additional ROS. Also, the fact that the same effect was not observed with AuR suggests that those additional ROS are not peroxides but rather radical species.

Table 4.7.1: Blank levels determined during OFF periods in the determination of ROS concentrations

Probe	Phase 1 chamber background (ppb)	Phase 2 chamber background (ppb)
DCFH	0.19 ± 0.31	0.20 ± 0.19
AuR	0.09 ± 0.12	0.09 ± 0.06
TPA	0.27 ± 0.26	0.19 ± 0.16

Figure 4.7.1: ROS concentrations determined in the chamber using DCFH

The blue line indicates the average of all OFF samples, and the blue box corresponds to \pm one standard deviation. This area is considered the chamber blank. Samples below the detection limit are marked as n.d. (not detected).

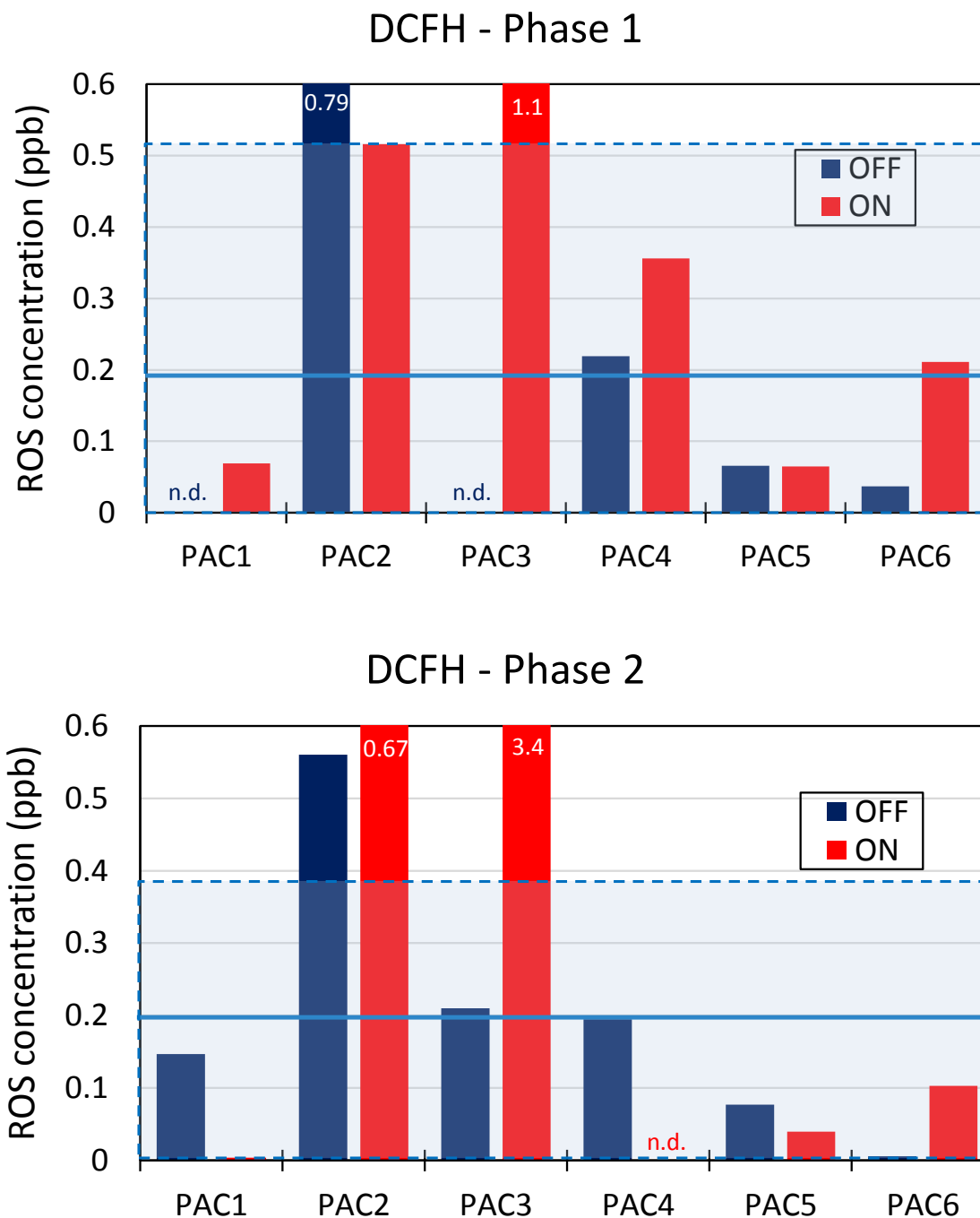


Figure 4.7.2: ROS concentrations determined in the chamber using AuR

The blue line indicates the average of all OFF samples, and the shaded box corresponds to \pm one standard deviation. This area is considered the chamber blank. Samples below the detection limit are marked as n.d. (not detected).

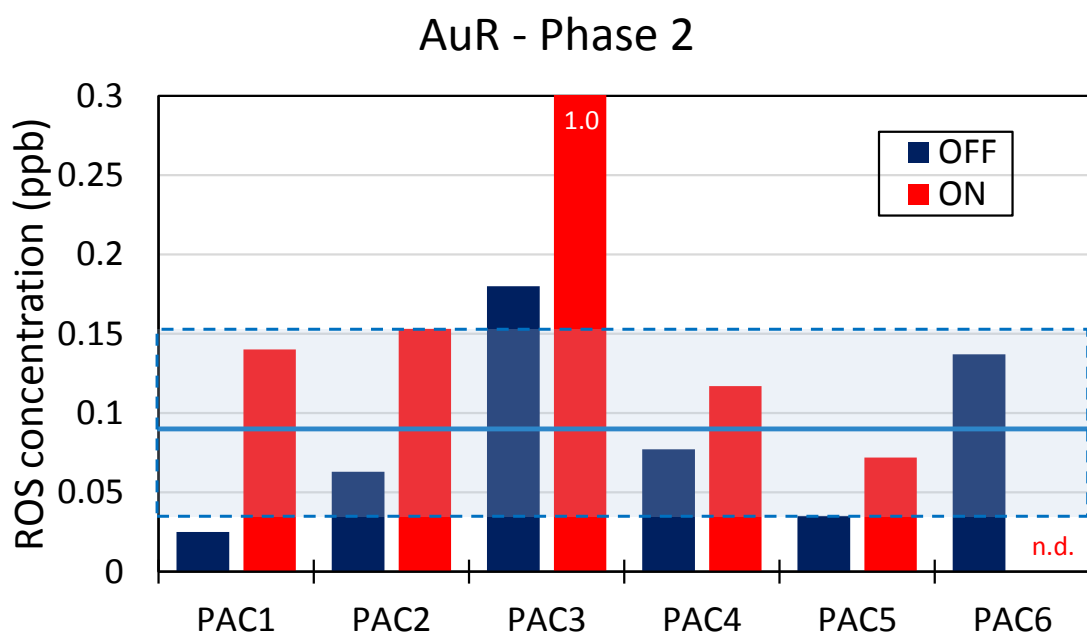
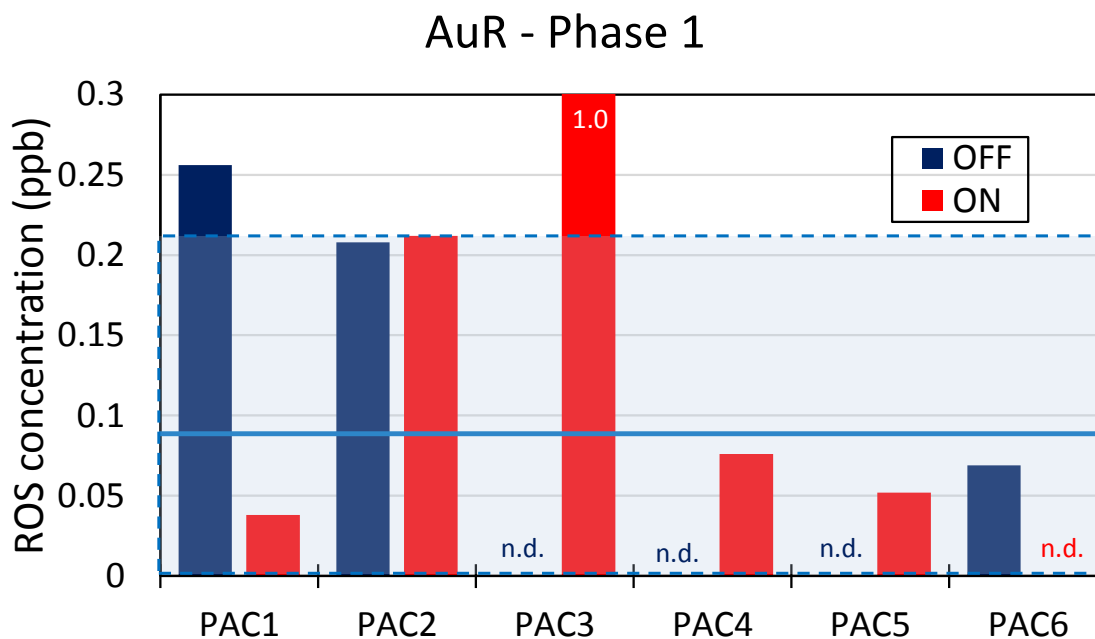
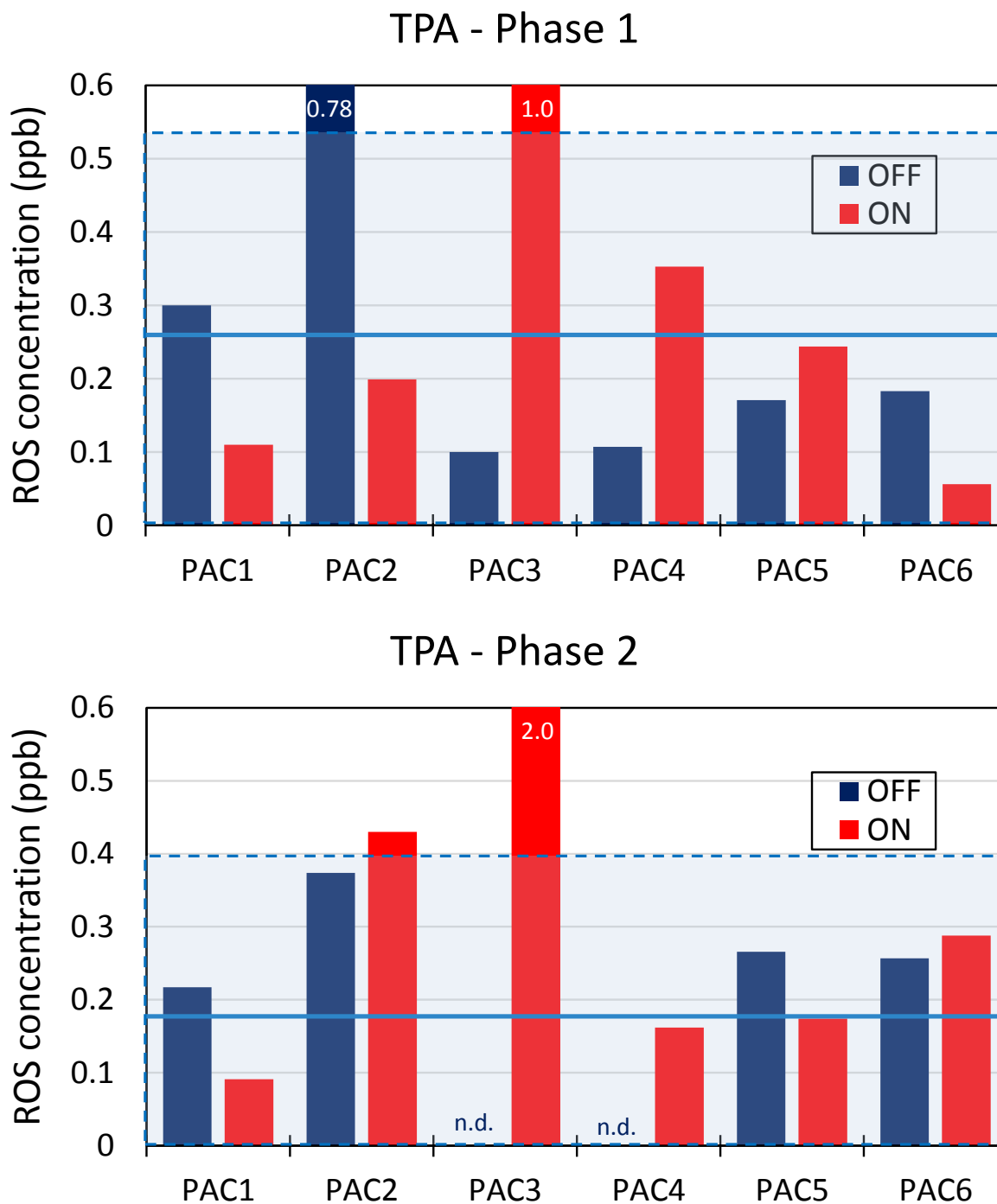


Figure 4.7.3: ROS concentrations determined in the chamber using TPA

The blue line indicates the average of all OFF samples, and the shaded box corresponds to \pm one standard deviation. This area is considered the chamber blank. Samples below the detection limit are marked as n.d. (not detected).



5. EVALUATION OF THE IMPACTS OF AIR CLEANERS ON INDOOR AIR QUALITY

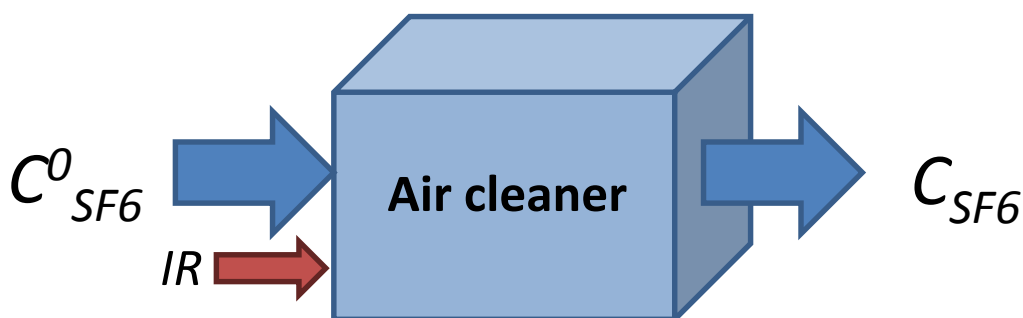
5.1. Determination of air flow in each device

Airflow through the air cleaners was measured by calculating the dilution of a tracer gas injected at the inlet. Sulfur hexafluoride (SF_6) was injected using a peristaltic pump at $5.55 \text{ cm}^3/\text{min}$. A B&K Multigas Monitor Type 1302 was used to measure the SF_6 concentration at the air cleaner outlet. All sampling was carried out in a well-ventilated laboratory in order to minimize recirculation of SF_6 through the device. The B&K monitor was run for a minimum of 10 minutes before sampling from each air cleaner in order to obtain a background level of SF_6 . Between three and five representative locations were chosen at the outlet of each air cleaner, and 4-5 measurements were taken at each location.

A calibration of the B&K monitor and adjustment of the inlet concentration was carried out by sampling air in Tedlar bags, diluting and determining SF_6 concentration by gas chromatography with electron capture device (GC/ECD), a standard quantitation method for SF_6 . Measured SF_6 concentrations were averaged and used to calculate flow rates through the air cleaners as indicated in Figure 5.11. The air flow rate through the device F_{AC} (in $\text{m}^3 \text{ h}^{-1}$) is calculated as a function of the SF_6 injection rate IR (in $\text{m}^3 \text{ h}^{-1}$) and $C^0_{\text{SF}_6}$ and C_{SF_6} , the inlet and outlet SF_6 concentration, respectively (both in ppm) as shown in equation 5.1. Table 5.1.1 reports the results of these measurements.

$$F_{AC} = \frac{IR}{C_{\text{SF}_6} - C^0_{\text{SF}_6}} \quad (5.1)$$

Figure 5.1.1: Determination of air flow rate through devices



An alternative method was used to verify values corresponding to three of the six air cleaners with air flows below 6 cfm. The method consisted on measuring air velocities using a hotwire anemometer (TSI VelociCalc Plus 8360) at the center of concentric rings of a circular cross section of ductwork connected at the outlet of the air cleaner. Low-air flows could be corroborated with this alternative technique. This method is not suitable for higher air flows because it under-predicts the results due to friction losses in the ductwork.

Table 5.1.1: Air flow through each air cleaner determined by SF₆ dilution

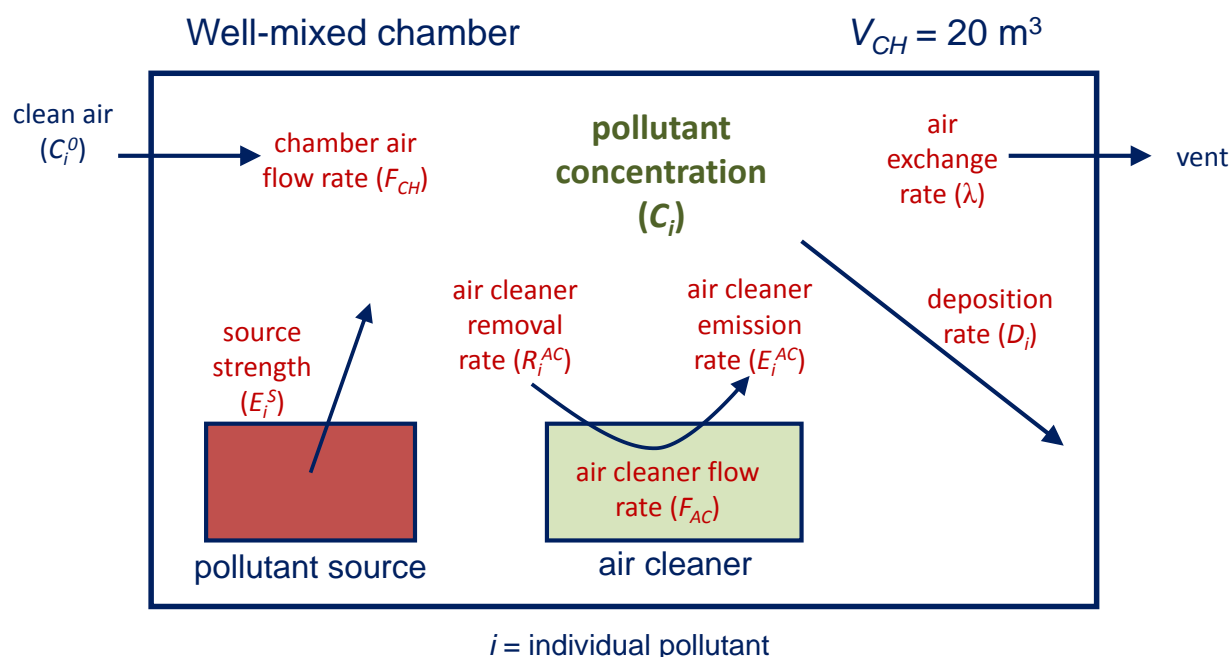
Air Cleaner	Type	Setting	Flow through device, F_{AC}	
			(cfm)	(m ³ h ⁻¹)
PAC1	PCO	Single	82 ± 7	139 ± 12
PAC2	PCO/HEPA/catalyst	Low Mid High	118 ± 10 124 ± 11 279 ± 22	200 ± 17 211 ± 19 474 ± 37
PAC3	PCO w/ ozone generation	Single	5.9 ± 0.2	10.0 ± 0.3
PAC4	Plasma	Low High	3.0 ± 0.2 4.7 ± 0.3	5.1 ± 0.3 8.0 ± 0.5
PAC5	Ceramic heater	Single	86 ± 4	146 ± 7
PAC6	Heater	Single	2.4 ± 0.4	4.1 ± 0.7

These F_{AC} air cleaner flow values have been used to determine emission rates and for modeling various scenarios.

5.2. Net Direct (Primary) Pollutant Emissions (Phase 1)

Figure 5.2.1 illustrates the chamber setup and includes the main parameters used for the analysis presented in this report.

Figure 5.2.1: Parameters used in this study



In this schematic representation, V_{CH} is the chamber volume (expressed in m^3); C_i is the pollutant concentration in the chamber (in $\mu\text{g m}^{-3}$); λ is the air exchange rate (in h^{-1}); F_{CH} is the chamber air flow rate (in $\text{m}^3 \text{ h}^{-1}$); C_i^0 is the concentration of pollutant i in air entering the chamber; F_{AC} is the air cleaner flow rate (in $\text{m}^3 \text{ h}^{-1}$); E_i^S is the indoor pollutant source strength for sources other than the air cleaner (in $\mu\text{g h}^{-1}$); D_i is the deposition rate for pollutant i (in h^{-1}); and E_i^{AC} and R_i^{AC} are the air cleaner's pollutant emission and removal rates, respectively (both in $\mu\text{g h}^{-1}$). Background levels are assumed to be zero.

We express the mass balance for pollutant i at times when the air cleaner is turned off as follows:

$$\frac{E_i^S}{V_{CH}} + \frac{F_{CH}}{V_{CH}} \cdot C_i^0 = (\lambda + D_i) \cdot C_i^{OFF} \quad (5.2)$$

where C_i^{OFF} is the chamber pollutant concentration with the air cleaner turned off. When the air cleaner is turned on and the system reached steady-state conditions, the mass balance includes two additional terms, to account for emissions generated at the air cleaner and to the partial elimination of the same pollutant by the air cleaner, as expressed by:

$$\frac{E_i^S}{V_{CH}} + \frac{F_{CH}}{V_{CH}} \cdot C_i^0 + \frac{E_i^{AC}}{V_{CH}} = (\lambda + D_i) \cdot C_i^{ON} + \frac{R_i^{AC}}{V_{CH}} \quad (5.3)$$

where C_i^{ON} is the chamber pollutant concentration with the air cleaner turned on. This equation assumes that the air exchange and deposition rates do not change when the air cleaner is turned on. Substituting equation 5.2 into equation 5.3 yields the following expression for the air cleaner emission rate E_i^{AC} :

$$E_i^{AC} = (\lambda + D_i) \cdot V_{CH} \cdot (C_i^{ON} - C_i^{OFF}) + R_i^{AC} \quad (5.4)$$

When $C_i^{ON} > C_i^{OFF}$, our experimental measurements of those quantities allow for the determination of the net pollutant emission rate accessible experimentally, E_i , given by:

$$E_i = E_i^{AC} - R_i^{AC} = (\lambda + D_i) \cdot V_{CH} \cdot (C_i^{ON} - C_i^{OFF}) \quad (5.5)$$

Similarly, the net pollutant removal rates R_i can be determined in cases where $C_i^{ON} < C_i^{OFF}$, as follows:

$$R_i = R_i^{AC} - E_i^{AC} = (\lambda + D_i) \cdot V_{CH} \cdot (C_i^{OFF} - C_i^{ON}) \quad (5.6)$$

We assume that the deposition rate D_i for VOCs included in this study is negligible with respect to the air exchange rate. However, we cannot neglect D_i for ozone and ROS. The ozone deposition rate was determined experimentally at the beginning and at the end of the study from ozone decay rates at time when chamber ventilation rates were measured, as described in Section 3.4. This yielded $D_{ozone} = 0.64 \pm 0.08 \text{ h}^{-1}$.

Given the lack of similar information for ROS deposition, we will use $D_{ROS} = 0.64 \text{ h}^{-1}$ by adopting the ozone deposition velocity as a surrogate. This is likely a lower-limit estimate of the real value for these very reactive compounds.

Table 5.2.1 summarizes net pollutant emission rates E_i and net pollutant removal rates R_i determined for the studied air cleaners operating under a clean air atmosphere in Phase 1. The results can be summarized as follows:

- a) Ozone: Very high ozone emission rates were observed for PAC3, and much lower values for PAC4, while the other devices did not show measurable ozone emissions.
- b) ROS: Within the sensitivity of the methods relying on all three fluorescent probes, we could not detect an increase in ROS levels during operation of the air cleaners with respect to chamber background levels. Only PAC3 showed higher levels than chamber background both in Phase 1 and Phase 2 determinations; however, those levels corresponded to decomposition of dissolved ozone in the buffers used to collect the sample, and not to gas phase peroxide or radicals which could not be accounted for separately.
- c) PM: Only two devices removed particulate matter in measureable amounts: PAC2 (provided with HEPA filtration) and PAC4 (plasma). Since these measurements are based on chamber background PM, which was not designed as a realistic aerosol challenge, we report these results only to provide a qualitative idea of the air cleaner performance, but these values cannot be translated into quantitative removal efficiencies under typical indoor PM conditions.
- d) VOCs: four out of six devices showed a measurable net emission of volatile organics, one device had virtually no effect on VOC concentrations and only one air cleaner (PAC1) reduced further the initially very low levels present in the chamber during Phase 1 (initial TVOC ~ 3 to 10 ppb) . We report in this table only VOC emission (or removal) rates that were equal or higher in magnitude than $5 \mu\text{g h}^{-1}$, leading to a concentration change in the chamber of at least $\sim 1/3$ ppb.

Putting these results in context, the air cleaner PAC3 stands out as a strong ozone emitter. Having achieved a concentration of almost 200 ppb in the chamber, this device likely exceeds most health-based criteria for ozone under various scenarios and raises serious concerns. This is discussed in more detail in Section 5.4, below.

Other emissions reported in Table 5.2.1 include hazardous VOCs such as formaldehyde, which was emitted by half of the devices, at a maximum rate of $20 \mu\text{g h}^{-1}$. These rates can be compared with those reported for well-known strong sources. For example, 1 m^2 of wood particle board emits formaldehyde typically at rates in the order of hundreds of $\mu\text{g h}^{-1}$ (Salthammer et al, 2010). This suggests that emissions from air cleaners are likely lower than those strong sources, although not necessarily negligible. Air cleaner emission rates are also two to three orders of magnitude lower than formaldehyde whole-house emission rates determined by Offermann (2009), in the range $5,000 - 16,000 \mu\text{g h}^{-1}$.

Other VOCs emitted at high levels by at least one air cleaner include toluene and benzaldehyde. In most cases, low level VOC emissions are likely due to plastic materials used to build the device (including the frame, body and electronic components), and perhaps also oils, solvents or lubricants used in manufacturing. These emissions are comparable to those described by our group in a study of emissions by electronic office equipment (Maddalena et al, 2009; Destailats et al, 2008). The only device with a net removal of VOCs during Phase 1 (PAC1) is built using a metal case and, relative to other air cleaners, has much less plastic.

Table 5.2.1: Net emission rates (E_i , in red and bold font) or removal rates (R_i , in black) determined in Phase 1

	PAC1	PAC2	PAC3	PAC4	PAC5		PAC6
					ionizer	ion + heat	
ozone (mg h ⁻¹)	-	-	6.3	0.07	-	N/A	-
UFPs (# particles h ⁻¹) ⁽¹⁾	-	8.6E+09	-	2.4E+09	-	-	-
VOCs (µg h⁻¹)							
ethanol	47	-	19	-	-	-	6
hexane	-	-	-	-	-	-	-
butanal	-	-	-	-	-	-	-
benzene	10	16	19	5.3	43	14	22
TCE	-	-	-	-	-	-	-
toluene	7.4	92	-	-	20	7.3	5.2
pyridine	-	-	-	-	-	-	-
o-xylene	-	-	-	-	12	5.7	-
styrene	-	-	-	-	11	5.4	-
d-limonene	-	-	-	-	11	5.0	-
formaldehyde	16	-	13	-	8.1	20	-
acetaldehyde ⁽²⁾	15	-	-	-	8.6	5.0	-
acetone ⁽²⁾	56	6.1	-	-	36	9.8	5.6
benzaldehyde ⁽²⁾	-	-	115	-	-	-	-
TOTAL VOCs (µg h ⁻¹)	152	82	90	5.3	150	72	39

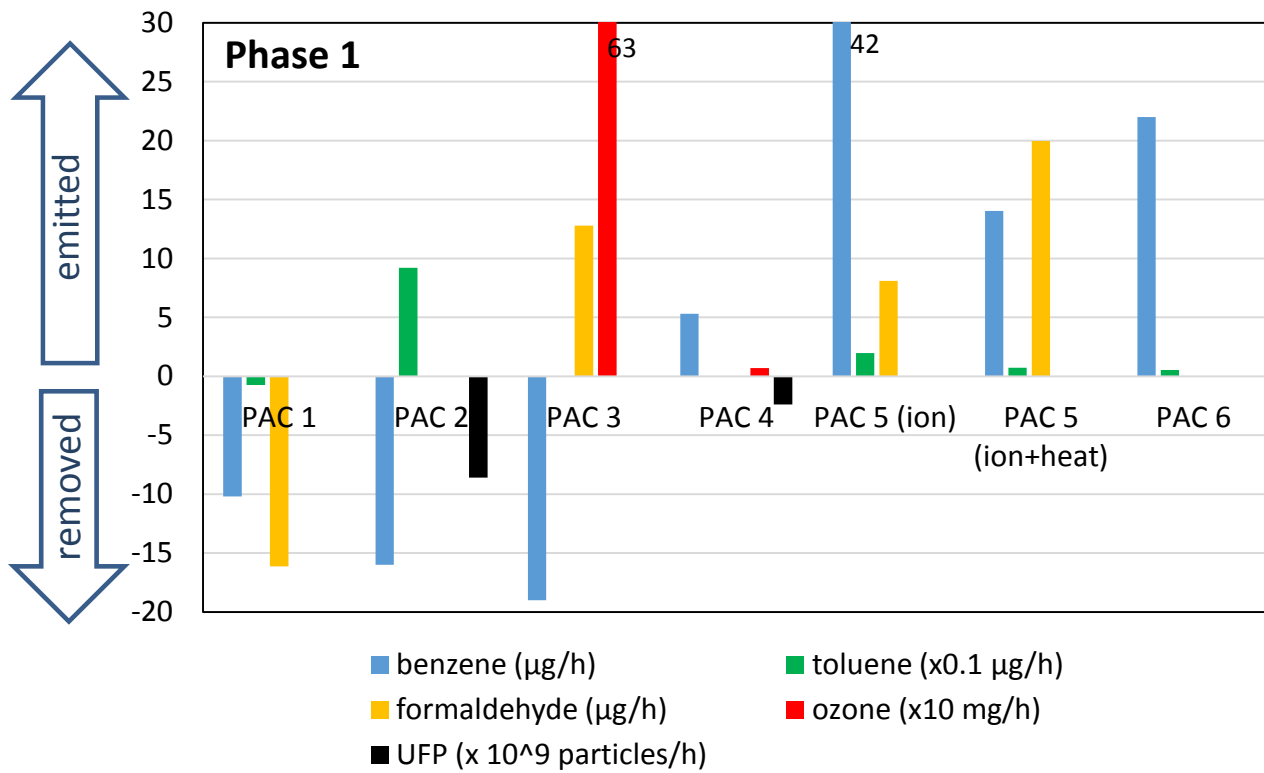
(1) these values are presented as a qualitative indication of the air cleaner performance, but cannot be translated into quantitative removal efficiencies under typical indoor PM conditions.

(2) VOCs not included in challenge mixture

N/A: not measured due to artifacts introduced by fast RH changes on ozone monitor signal.

Figure 5.2.2 compares side-by-side emission and removal rates of key pollutants in Phase 1 for all air cleaners.

Figure 5.2.2: Emission and removal rates of key VOCs, UFP and ozone for each air cleaner in Phase 1. Positive values correspond to emission rates, and negative values correspond to removal rates.



5.3. Net Pollutant Emissions or Removal in the Presence of Challenge Mixture (Phase 2)

5.3.1. Pollutant emission and removal rates in Phase 2

In Phase 2, net pollutant emission rates E_i and removal rates R_i were determined according to equation 5.5 and 5.6, respectively. These rates are expected to be close to those observed in indoor environments because chamber VOC concentrations were typical. Table 5.3.1 summarizes emission rates determined for all air cleaners in the presence of a challenge VOC mixture. Also in this case, we report only those rates that are equal or higher than $5 \mu\text{g h}^{-1}$. The results can be summarized as follows:

- a) Ozone: Similar to results from Phase 1, the same magnitude of very high ozone emission rates were observed for PAC3, and much lower values for PAC4, while the other devices did not present measurable emissions.
- e) ROS: Within the sensitivity of the methods relying on all three fluorescent probes, we could not detect an increase in ROS levels during operation of the air cleaners with respect to chamber background levels. Only PAC3 showed higher levels than chamber background both in Phase 1 and Phase 2 determinations; however, those levels corresponded to decomposition of dissolved ozone in the buffers used to collect the sample, and not to gas phase peroxide or radicals which could not be accounted for separately.
- f) PM removal: Also in this case, only two device removed particulate matter in measureable amounts: PAC2 (provided with HEPA filtration) and PAC4 (plasma). As described above for Phase 1 results, these measurements are based on chamber background PM, which was not designed as a realistic aerosol challenge, and are therefore reported only as a qualitative indication of the air cleaner performance. These values cannot be translated into quantitative removal efficiencies under typical indoor PM conditions.
- b) UFP formation: In the presence of ozone-reacting VOCs such as limonene and styrene, the air cleaner that emits high levels of ozone (PAC3) becomes a source of ultrafine particles due to the nucleation of oxidation byproducts and agglomeration of new particles. This process has been extensively described in the literature (e.g., Singer et al, 2006; Destailats et al, 2006; Coleman et al, 2008; Waring et al, 2011). Initially small particles (a few tenths of nm) grow rapidly to a size of 100-300 nm at rates that compete with ventilation rates. We evaluated the yield of UFPs in Section 5.3.2, below.
- c) VOCs: In the presence of a VOC challenge that reproduced realistic indoor conditions (initial TVOC \sim 100 to 200 ppb) during Phase 2, four out of the six devices were able to remove a measurable amount of volatile organics, while the other two devices showed net VOC emissions. We report in this table only VOC

emission (or removal) rates that were equal or higher in magnitude than $5 \mu\text{g h}^{-1}$ for each compound, leading to a concentration change in the chamber of at least $\sim 1/3$ ppb.

The air cleaner PAC3 stands out as a strong ozone emitter, confirming the findings of Phase 1. In addition of the harmful ozone levels, the presence of ozone-reactive VOCs led to the formation of UFPs, raising additional concerns about the use of this device.

Comparing with Phase 1 results, both VOC emission and removal rates are roughly one order of magnitude higher in Phase 2. In the case of devices that remove VOCs, the fraction of those compounds eliminated from indoor air was between 8 and 29%. Their removal efficiency performance is analyzed in more detail in Section 5.3.3, below. The two devices showing net emission of VOCs are primarily aimed at particulate filtration or electrostatic charging, not VOC removal; in one case (PAC5) there is no technology present to eliminate VOCs, and in the other (PAC2) the PCO component likely does not have enough capacity to process incoming air. These devices are the two largest units tested, and contain large amounts of surface area (including in one case filtration elements) where VOCs can adsorb, accumulate and desorb. In one case (PAC2), emissions are dominated by toluene from its plastic constituents, as described in Phase 1. The other device (PAC5) shows across-the-board emissions of all VOCs present in our challenge mixture, indicating that emissions do not originate in the device itself, but rather in adsorption and subsequent reemission of challenge VOCs.

Considering emissions of individual VOCs, formaldehyde is produced as byproduct of two of the three PCO devices, and also as a byproduct of the plasma air cleaner. The formaldehyde emission rates are between 25 and $33 \mu\text{g h}^{-1}$, slightly higher than those recorded in Phase 1. These are not negligible emissions, although they are significantly lower than strong formaldehyde indoor sources such as particle board, as discussed above. These values are between two and three orders of magnitude lower than the whole-house formaldehyde emission rates of $5,000 - 16,000 \mu\text{g h}^{-1}$ reported by Offermann (2009).

Similar to our observation from Phase 1, other VOCs emitted at high levels by at least one air cleaner in Phase 2 include toluene (PAC2) and benzaldehyde (PAC3), presumably due to emissions from plastic constituents.

Figure 5.3.1 compares side-by-side emission and removal rates of key pollutants in Phase 2 for all air cleaners.

Table 5.3.1: Net emission rates (E_i , in red and bold font) or removal rates (R_i , in black) determined in Phase 2

	PAC1	PAC2	PAC3	PAC4	PAC5		PAC6
					ionizer	ion + heat	
ozone (mg h ⁻¹)	-	-	5.9	0.18	-	N/A	-
UFPs (# particles h ⁻¹) ⁽¹⁾	-	6.0E+09	3.10E+10	4.9E+09	-	-	-
VOCs (µg h⁻¹)							
ethanol	-	16	5.4	539	215	7.4	11
hexane	582	N/A	116	409	398	202	97
butanal	30	-	23	23		62	30
benzene	34	13	38	99	40	42	25
TCE	47	65	74	122	49	37	29
toluene	79	147	171	267	96	173	61
pyridine	10	-	66	90	19	45	136
o-xylene	37	40	91	63	71	176	163
styrene	7.0	12	133	23	41	134	52
d-limonene	8.3	-	273	21	111	605	39
formaldehyde	33	31	36	25	49	229	12
acetaldehyde ⁽²⁾	-	-	-	-			-
acetone ⁽²⁾	9	5.0	86	-		89	-
benzaldehyde ⁽²⁾	-	-	111	-			-
TOTAL VOCs (µg h ⁻¹)	792	319	829	1629	992	1343	634
% chamber VOCs ⁽³⁾	-14 %	+15 %	-28 %	-29 %	+12 %	+19 %	-8 %

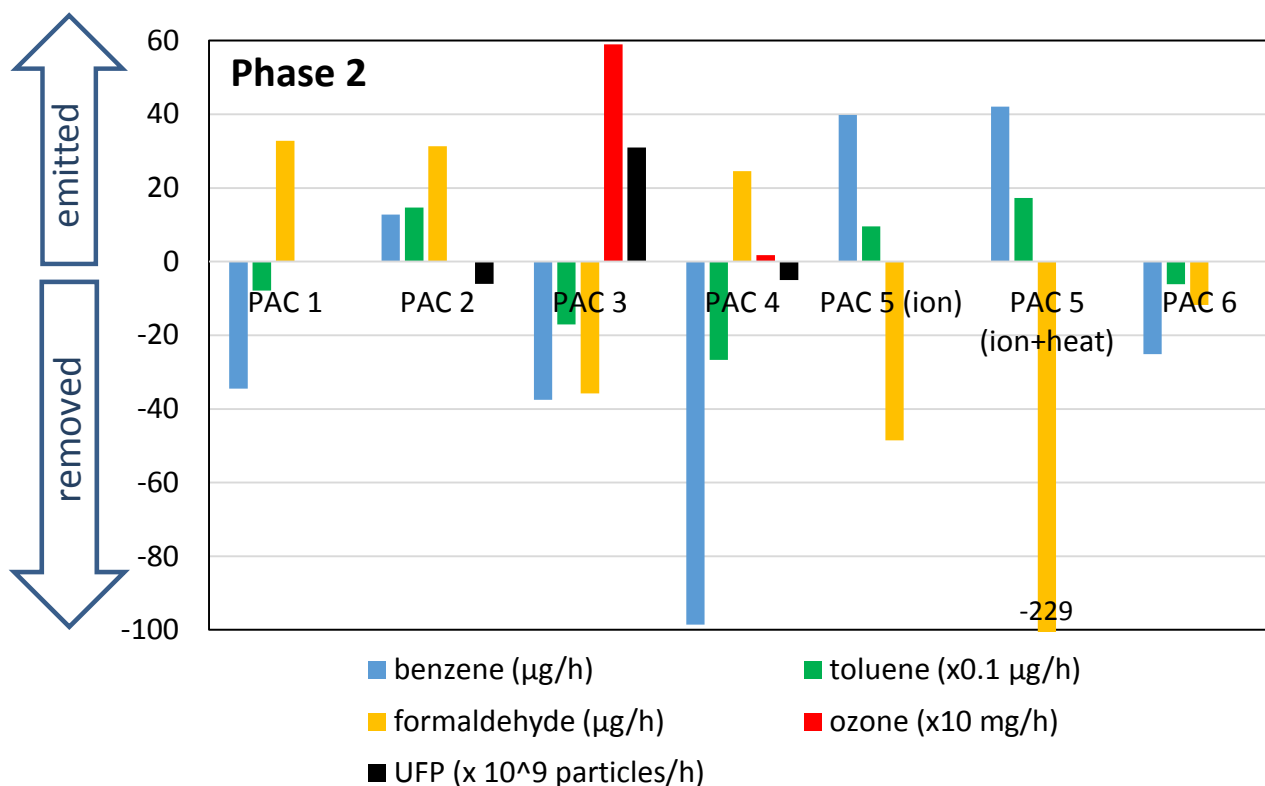
(1) these values are presented as a qualitative indication of the air cleaner performance, but cannot be translated into quantitative removal efficiencies under typical indoor PM conditions.

(2) VOCs not included in challenge mixture

(3) Indicates the fraction of the total VOC concentration removed (black) or incremented (red)

N/A: not measured due to artifacts introduced by fast RH changes on ozone monitor signal or due to inconsistency in the analytical determination.

Figure 5.3.1: Emission and removal rates of key VOCs, UFP and ozone for each air cleaner in Phase 2. Positive values correspond to emission rates, and negative values correspond to removal rates.



5.3.2. Yields of Byproducts Generated in the Air Cleaning Process

Pollutants emitted as a consequence of the operation of the air cleaner, even in the absence of a challenge mixture, include ozone (PAC3, PAC4) and ROS (PAC4). In addition, other pollutants were emitted during Phase 2 as a consequence of chemical reactions with VOCs present in the challenge mixture induced by the air cleaner, including the formation of UFP (PAC3), formaldehyde (PAC1, PAC2, PAC4) and acetone (PAC3). For those cases, we assign one, two or multiple VOCs as the likely precursor, as listed in Table 5.3.2.

In the case of UFPs formed during operation of PAC3, limonene and styrene are the only two VOCs from those present in the challenge mixture that have a fast enough reaction rate with ozone to produce significant UFPs. Also, in both cases the UFP formation in chamber studies has been well established. The procedure to determine aerosol yield determinations was adopted from Waring et al (2011). In our experiments, ozone was present in excess with respect to those precursors, so the mass yield of secondary organic aerosol (SOA), Y_{SOA} , is given by

$$Y_{SOA} = \frac{m_{SOA}}{m_L + m_S} \quad (5.7)$$

where m_{SOA} is the mass of aerosol formed per unit time, and m_L and m_S are the mass of limonene and styrene that reacted in the experiment with the PAC3 air cleaner per unit time, respectively. The latter can be calculated directly from the change in concentrations measured with air cleaner on and off. Since our aerosol measurements include particle number concentration and not mass concentrations, the mass of aerosol formed can be calculated assuming that the density of aerosol particles is $1 \text{ mg } \mu\text{L}^{-1}$ and for a range of values of the aerosol geometrical mean diameter (GMD). The cited study by Waring et al (2011) reported GMD between 64 and 134 nm for ozone reactions with limonene and other terpenes. For this range of particle sizes, we determine $Y_{SOA} = 1$ to 5%. However, if GDM was in the proximity of 200 nm, as reported for several experimental conditions described in our previous work (Coleman et al, 2008), the yield of particles could increase up to $Y_{SOA} = 15 \%$.

An accurate determination of formaldehyde and acetone yields, Y_F and Y_A , is challenging because there are multiple precursors, particularly for formaldehyde, and the fraction of each precursor that leads to byproduct formation is, in most cases, unknown. However, we estimated Y_F for PAC1 (PCO) and PAC4 (plasma), and Y_A for PAC3 (PCO/O₃) based on the total VOC reacted, as follows

$$Y_F = \frac{m_F}{\sum_i m_i} \quad ; \quad Y_A = \frac{m_A}{\sum_i m_i} \quad (5.8)$$

where m_F is the mass of formaldehyde formed, m_A is the mass of acetone formed, and m_i is the mass of each VOC reacted per unit time. Results are presented in Table 5.3.2. Estimation of the yield of formaldehyde by PAC2 was not possible because several other VOCs were also emitted simultaneously.

Table 5.3.2: Yield of byproducts observed in Phase 2

Byproduct observed in Phase 2	Air Cleaner	Likely precursor(s)	Yield (%)
UFP (SOA)	PAC3	limonene, styrene	1 – 5
formaldehyde	PAC1	Multiple VOCs	4
	PAC2		N/A
	PAC4		1.5
acetone	PAC3	Multiple VOCs	8

N/A: not determined because several other VOCs were emitted simultaneously

5.3.3. Evaluation of VOC removal effectiveness

We define ω_i , the chamber concentration reduction factor for pollutant i (in %), as the relative change in average concentrations of OFF and ON periods, as follows:

$$\omega_i = \frac{(C_i^{OFF} - C_i^{ON})}{C_i^{OFF}} \quad (5.9)$$

The chamber concentration reduction factor ω_i depends on two parameters related with the device's effectiveness:

- the recycle ratio (ρ , unitless), represents the number of times chamber air can be processed by the air cleaner. It is directly proportional to the airflow through the air cleaner, and inversely proportional to the air exchange rate. This parameter is defined as

$$\rho = \frac{\text{airflow through air cleaner}}{\text{airflow through chamber}} = \frac{F_{AC}}{F_{CH}} = \frac{F_{AC}}{\lambda \cdot V} \quad (5.10)$$

- b. the single-pass removal efficiency ($\phi_i^{\rho,ss}$) for each compound i under steady-state conditions (ss), which is also a function of the recycle ratio (ρ), defined as:

$$\phi_i^{\rho,ss} = \frac{(C_i^{upstream} - C_i^{downstream})}{C_i^{upstream}} \quad (5.11)$$

These two parameters represent the two main variables responsible for air cleaner efficiency, associated with system throughput and intrinsic efficiency, respectively. In previously published work (Destailats et al, 2012), we developed a model to describe the relationship between the chamber concentration reduction factor ω_i and the single-pass removal efficiency $\phi_i^{\rho,ss}$, which can be expressed as the following simple correlation:

$$\omega_i = 1 - \left(\frac{1}{1 + \rho \cdot \phi_i^{\rho,ss}} \right) \quad (5.12)$$

The recycle ratio for each of the experiments performed in Phase 2 are reported in Table 5.3.3. With these values, we represent in Figure 5.3.1 the dependence of the chamber concentration reduction factor ω_i , with the single-pass removal efficiency ($\phi_i^{\rho,ss}$) as a function of the recycle ratio (ρ), and as described in equation 5.12.

Figure 5.3.2 describes graphically the performance of four of the studied air cleaners, for which we observed net VOC elimination in Phase 2 (PAC1, PAC3, PAC4 and PAC6). The solid lines represent the ideal behavior described by equation 5.12, and the data points overlaid on each curve correspond to each of the VOCs that was partially removed from the chamber. We identify toluene in each of the four data series for illustrative purposes. Overall, the chamber concentration reduction factor for most compounds was in the range $0 < \omega_i < 0.4$, with most data points plotted in the bottom half of the figure. These results clearly illustrate that, regardless of the type of device and choice of technology, the capacity of these air cleaners to remove VOCs from indoor air is from moderate to low. It should be noted that PAC6 is marketed as an anti-microbial technology, and presumably is not designed to maximize VOC removal. However, the other devices claim good VOC elimination.

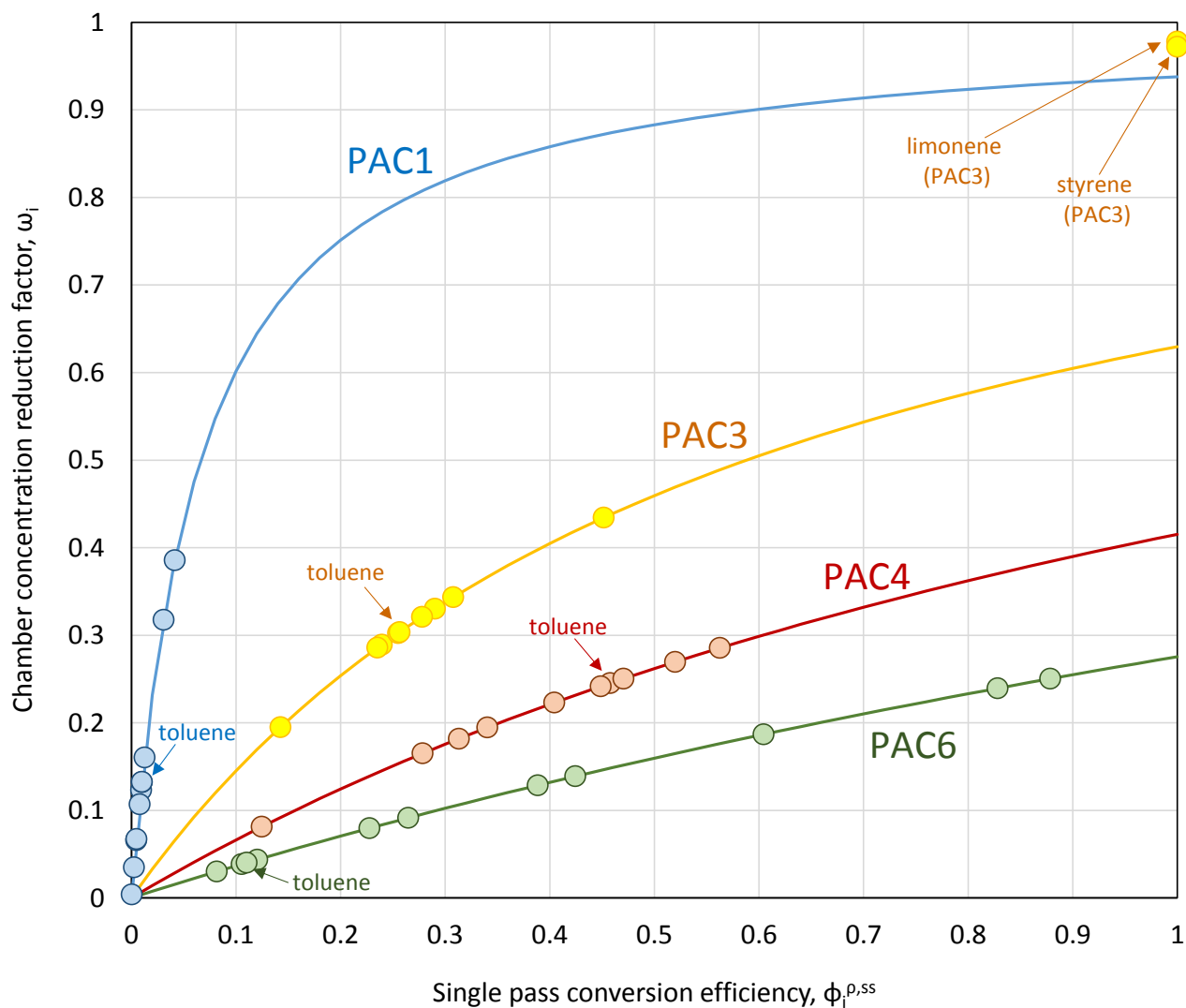
Figure 5.3.2 illustrates clearly that PAC1, with a much higher recycle ratio, is the air cleaner that has the highest potential capacity to remove VOCs, but its intrinsic efficiency is insufficient, as shown by its very low $\phi_i^{\rho,ss}$ values. By contrast, devices with very low throughput, such as PAC4 and PAC6, are those showing the highest intrinsic removal efficiency. Those devices are limited by design, as their optimal hypothetical chamber reduction factor when $\phi_i^{\rho,ss} = 1$ is only 0.41 and 0.27, respectively.

It is important to keep in mind that an important assumption was made in deriving equation 5.12: in this model, all pollutant removal takes place inside the air cleaner (e.g., on the surface of a catalyst). However, we know that two of these devices emit ozone (PAC3 and PAC4), and one of them also emits ROS (PAC4). Those reactive species can react with VOCs in indoor air, further contributing to reducing concentrations. That effect is evident from considering the results for styrene and limonene in the PAC3 experiment: the chamber concentration reduction factor for those compounds was $\omega_{styrene} = 0.97$ and $\omega_{limonene} = 0.98$, both of which were much higher than the optimal hypothetical values predicted by equation 5.12 for an air cleaner operating at the corresponding recycling ratio (0.63). The reason for this remarkable difference is precisely the fact that those two compounds are very reactive with ozone in the gas phase, and it is likely that most of their elimination takes place in the air, rather than inside the air cleaner.

Table 5.3.3: Determination of the recycle ratio for each experiment in Phase 2

Air Cleaner	Type	Air cleaner flow F_{AC} ($m^3 h^{-1}$)		Air Exchange Rate λ (h^{-1})	Chamber Flow F_{CH} ($m^3 h^{-1}$)	Recycle Ratio (ρ)
PAC1	PCO	139 ± 12		0.46	9.2	15.1
PAC2	PCO/HEPA/ catalyst	Low	200 ± 17			
		Mid	211 ± 19	0.58	11.6	18.2
		High	474 ± 37			
PAC3	PCO w/ O ₃ generation	10.0 ± 0.3		0.29	5.8	1.7
PAC4	Plasma	Low	5.1 ± 0.3			
		High	8.0 ± 0.5	0.56	11.2	0.71
PAC5	Ceramic heater	146 ± 7		0.61	12.2	12.0
PAC6	Heater	4.1 ± 0.7		0.54	10.8	0.38

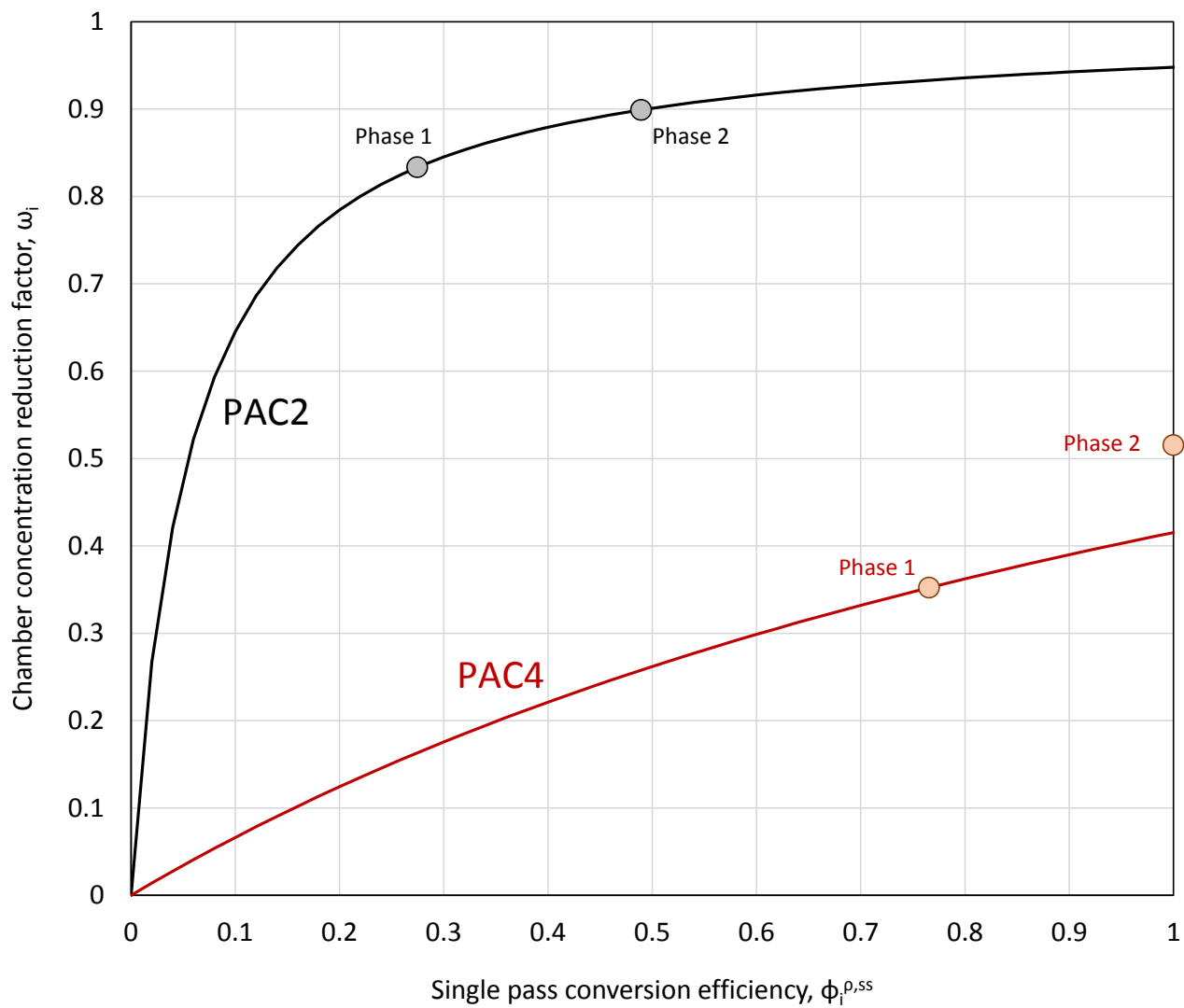
Figure 5.3.2: VOC chamber concentration reduction factor ω_i as a function of the single-pass removal efficiency $\Phi_i^{p,ss}$ predicted using Phase 2 results and equation 5.12 for recycle ratios of 1.51 (blue), 1.7 (yellow), 0.71 (red) and 0.38 (green)



Considering air cleaner's performance with respect to particulate matter, our experiments were not designed to challenge the devices with PM of realistic size distribution and concentrations typical of indoor aerosols. Furthermore, more than half of the devices are not designed to remove particulate matter. Despite these considerations, we found that two devices (PAC2 and PAC4) showed consistently good PM removal capacity. For that reason, we performed the same analysis using equation 5.12 applied to the relative reduction in particle count by each air cleaner, independent of possible changes in size distribution that may have occurred in the process. The results are shown in Figure 5.3.3. We calculated PM removal efficiency for both Phase 1 and Phase 2 determination, since background levels in the chamber were similar in all cases. Results for PAC2 show a high chamber concentration reduction factor, with $\omega_{PM} = 0.83$ in Phase 1 and $\omega_{PM} = 0.90$ in Phase 2. This device combines very high throughput (with the highest recycle ratio of $\rho=18$) with moderate intrinsic particle removal efficiency, with $0.27 < \Phi_{PM}^{\rho,ss} < 0.49$. By contrast PAC4 shows a chamber reduction factor consistent with an almost optimal single-pass removal efficiency, for the relatively low recycle ratio corresponding to that air cleaner. In fact, one of the two determinations exceeded the hypothetical optimal value, suggesting that also in the case of PM elimination, the plasma may operate through processes taking place not just inside the air cleaner but also in indoor air (e.g., charging particles by plasma ions with accelerating deposition to surfaces).

Appendix 3 lists the numeric values plotted in Figures 5.3.2 and 5.3.3.

Figure 5.3.3: PM chamber concentration reduction factor ω_i as a function of the single-pass removal efficiency $\Phi_i^{p,ss}$ predicted using Phase 2 results and equation 5.12 for recycle ratios of 1.8 (black) and 0.71 (red)



5.4. Predicted Impacts on Typical Indoor Scenarios

5.4.1. Indoor Pollutant Levels Predicted through a Material-Balance Model

The emission rates and byproduct yields determined in sections 5.2 and 5.3 were used to predict the expected indoor concentration changes for each pollutant due to operation of each air cleaner under two model scenarios. A first-order material-balance model was applied to establish pollutant levels in each case. Two typical residential scenarios were considered:

- a) Scenario 1: three air cleaners operating simultaneously in different rooms of a 1,500-ft² house ventilated according to ASHRAE 62.2 ventilation rates, and
- b) Scenario 2: a single air cleaner operating in a small furnished bedroom with door closed and minimum ventilation.

Table 5.4.1: Parameters used to model the two indoor scenarios

Scenario	Indoor air volume, V (m ³)	Surface to Volume (S/V) ratio (m ⁻¹)	Air exchange rate, λ (h ⁻¹)	Number of devices (N)
LBNL chamber	20	2.2	0.3 to 0.5	1
Scenario #1: 1,500-ft ² house	1115	2.5	0.12	3
Scenario #2: small furnished room	30	3.5	0.05	1

In some cases, the pollutant emission rates of air cleaners are dependent on the indoor air pollutant concentration, an example is the production of formaldehyde from incomplete decomposition of indoor air pollutants in a PCO air cleaner. In other cases, the pollutant emission rates of air cleaners are not affected by the indoor air pollutant concentration, an example is the emission of toluene from the plastic case of an air cleaner. If the air cleaner also removes an emitted VOC, the pollutant removal rate, and the net pollutant emission rate, will vary with the indoor air concentration of the pollutant. Consequently, the pollutant concentration changes presented in this section

are illustrative examples for a house or room that have indoor VOC concentrations and compositions matching the Phase 2 test conditions.

Scenario 1 was adopted from a model house used by Offermann (2009). The outdoor air ventilation rate prescribed by ASHRAE 62.2-2004 for a home of these characteristics is 52 cfm (88 m³ h⁻¹). The total ventilation was calculated by adding to this value an infiltration rate of 2 cfm for every 100 ft² (30 cfm or 51 m³ h⁻¹, in this case). Based on the total outdoor ventilation rate of 82 cfm (137 m³ h⁻¹) and the indoor air volume of 1115 m³, the air exchange rate in the model home is 0.12 h⁻¹, which is within the range expected for a tight energy-efficient new home (Stephens and Siegel, 2012; Offermann, 2009).

Scenario 2 represents a “worst-case” situation, where indoor air is almost stagnant and pollutants disperse into a relatively small indoor air volume. This is a situation that may be encountered commonly if an air cleaner is used in the bedroom during the night when there is little wind or indoor-to-outdoor temperature difference to drive air infiltration.

In Scenario 1, we use a surface-to-volume ratio of $S/V = 2.5 \text{ m}^{-1}$, which is the middle of the range described for several residential spaces including bedrooms, bathrooms, offices and multipurpose spaces by Singer et al (2007). For Scenario 2, we used $S/V = 3.5 \text{ m}^{-1}$ which is the average of the five bedrooms considered in the same study.

For each scenario and each air cleaner, we calculated the incremental concentration ΔC_i achieved due to use of the device(s), as follows:

$$\Delta C_i = (C_i^{ON} - C_i^{OFF}) = \frac{N \cdot E_i}{(\lambda + D_i) \cdot V} \quad (5.13)$$

or

$$\Delta C_i = (C_i^{ON} - C_i^{OFF}) = -\frac{N \cdot R_i}{(\lambda + D_i) \cdot V} \quad (5.14)$$

for pollutants that were emitted (with emission rate E_i) or removed (with removal rate R_i), respectively. In these equations, N represents the number of air cleaners in operation. It should be noted that ΔC_i values obtained with equation 5.13 are positive (increments to existing levels) while those obtained with equation 5.14 are negative (reduction of existing levels). The values of N , λ and V used in each of the scenarios are reported in Table 5.4.1. For VOCs, we assume that D_i is negligible, consistent with the approach described above for the determination of emission and removal rates. However, ozone and ROS are expected to deposit to indoor surfaces at rates that are equal or higher than those determined for our chamber.

In order to predict a deposition rate for ozone and ROS, it should be considered which surface materials are likely present in each scenario. According to the Singer et al (2007) study, surface material categories in bedrooms include primarily (and with a

relatively similar weight) painted gypsum wallboard/plaster, other hard surfaces (e.g., wood, plastic) and plush materials (such as carpet and bedding). While less relevant for bedrooms, nonporous materials such as glass and tiles were much more predominant in other rooms (e.g., bathrooms). It is important to keep in mind that sorptive capacity and chemical interactions of each material with different pollutants may vary greatly. Hence, the actual surface area may be larger than the measured area and their use may lead to a conservative estimate of deposition rates. It should also be kept in mind that the degree of ozone removal at indoor surfaces is affected not only by the specific reactivity of each material and its surface area exposed, but also by the fluid mechanics of the room, which determines the thickness of the adjacent boundary layer (Kunkel et al, 2010). Ozone deposition rates can be calculated as follows:

$$D_{\text{ozone}} = \frac{\sum_{\alpha} v_{\text{ozone}}^{\alpha} S_{\text{ozone}}^{\alpha}}{V} \quad (5.15)$$

where $v_{\text{ozone}}^{\alpha}$ is the ozone deposition velocity for surface material α (in m h^{-1}), $S_{\text{ozone}}^{\alpha}$ is the surface area of material α exposed to ozone (in m^2), and V is the space volume (in m^3). Table 5.4.2 lists literature values reported for deposition velocities corresponding to ozone on various indoor surfaces.

Table 5.4.2: Values reported in the literature for ozone deposition velocities, v_i^{α}

Material (α)	$v_{\text{ozone}}^{\alpha}$ (m h^{-1})
Stainless steel	0.30 – 0.54 ^(a)
Carpet	6.1 ^(c) 0.58 – 2.30 ^(d)
Cotton muslin	0.54 – 3.9 ^(a)
Plywood	0.18 – 1.1 ^(a)
Glass	0.96 – 1.74 ^(a)
Gypsum wallboard	unpainted 2.4 ^(b) painted 0.32 ^(c) painted 0.42 ^(f)
Perlite ceiling tile	2.3 ^(c)
Activated carbon (for passive air cleaning)	5.3 ^(b)
<i>Average typical indoor conditions, integrating all surfaces</i>	<i>0.54 – 2.70 ^(e)</i>

(a) Cano-Ruiz et al, 1993

(b) Kunkel et al, 2010

(c) Gall et al, 2013

(d) Morrison and Nazaroff, 2002

(e) Nazaroff et al, 1993

(f) Poppendieck et al, 2007

For the purpose of predicting ozone deposition to indoor surfaces in our two model scenarios, we will use a range of deposition velocities of $0.30 < v_{ozone}^{\alpha} < 2.70$, in order to estimate an upper and lower limit of ozone concentrations. This range comprises almost all the values included in Table 5.4.2, except for the upper and lower extremes.

The data shown in Table 5.4.2 allows evaluation in more detail the nature of ozone deposition in the LBNL chamber. Assuming that the only material exposed is stainless steel ($\alpha = st.steel$), equation 5.15 can be simplified to the following expression:

$$D_{ozone} = \frac{v_{ozone}^{st.steel} S_{ozone}^{st.steel}}{V_{CH}} \quad (5.16)$$

Considering the narrow range of values reported for stainless steel ($0.30 \text{ m h}^{-1} < v_{ozone}^{st.steel} < 0.54 \text{ m h}^{-1}$), the exposed chamber surface area ($S_{ozone}^{st.steel} = 43.5 \text{ m}^2$) and the chamber volume ($V_{CH} = 20 \text{ m}^3$), the predicted ozone deposition rate in the chamber is $D_{ozone}^{st.steel} = 0.65 \text{ to } 1.17 \text{ h}^{-1}$. Our experimentally determined value, $D_{ozone} = 0.64 \pm 0.08 \text{ h}^{-1}$, is at the lower end of this prediction.

Tables 5.4.3 and 5.4.4 present the predicted house pollutant concentration changes ΔC_i for Scenario 1 and Scenario 2, respectively. In both cases, these predictions are based on experimental results from Phase 2.

In Scenario 1 (full house), we observe that predicted ozone concentration increments are significant (up to $19 \mu\text{g m}^{-3}$, equivalent to 10 ppb) when PAC3 is used, but ozone increases predicted for PAC4 are negligible. Predicted VOC concentration changes in Scenario 1 are small, with a maximum of $\Delta C_i = -36 \mu\text{g m}^{-3}$ total VOC reduction for PAC4 and $\Delta C_i = 30 \mu\text{g m}^{-3}$ increase of total VOC levels for PAC5. Those amounts (equivalent to $\sim \pm 10$ ppb of total VOC) constitute small but measureable changes in total VOC levels. For most air cleaners, formaldehyde levels are predicted to change by equal or less than $1 \mu\text{g m}^{-3}$, except for PAC5 which is predicted to remove up to $5 \mu\text{g m}^{-3}$ (3 ppb). These predicted changes in formaldehyde concentrations are minor compared with typical indoor levels.

In Scenario 2 (small room), the predicted increments in ozone levels are very high (up to $191 \mu\text{g m}^{-3}$, equivalent to 96 ppb) when PAC3 is used. Ozone is also predicted to increase when PAC4 is used, but only by a maximum of $5.5 \mu\text{g m}^{-3}$ (3 ppb). Predicted VOC concentration changes in Scenario 2 are substantial, with a maximum of $\Delta C_i = -1086 \mu\text{g m}^{-3}$ reduction for PAC4 and $\Delta C_i = 895 \mu\text{g m}^{-3}$ increase of total VOC levels for PAC5. Those amounts, equivalent to several hundreds of ppb, constitute a major impact (positive or negative) on total VOC levels. Formaldehyde levels are predicted to drop between 8 and $153 \mu\text{g m}^{-3}$ (7 and 125 ppb) with PAC3, PAC5 and PAC6, and to increase between 17 and $22 \mu\text{g m}^{-3}$ (14 and 18 ppb) with PAC1, PAC2 and PAC4. All those changes in formaldehyde concentration constitute a major impact on indoor levels for this pollutant.

Table 5.4.3: Pollutant concentration change ΔC_i ($\mu\text{g m}^{-3}$) in Scenario 1 based on results from Phase 2. Negative changes (concentration reductions) are shown in black, and positive changes (increases in concentration) are shown in **red and bold font**

	PAC1	PAC2	PAC3	PAC4	PAC5		PAC6
					ionizer	ion + heat	
ozone	-	-	2 - 19	0.1 - 0.6	-	-	-
SOA	-		0.3 - 3.8		-	-	-
VOCs							
ethanol		0.36	-0.12	-12	4.8	0.17	0.25
hexane	-13		-2.6	-9.1	8.9	4.5	-2.2
butanal	-0.7		-0.52	-0.5		1.4	-0.67
benzene	-0.76	0.29	-0.85	-2.2	0.90	0.94	-0.56
TCE	-1.0	1.5	-1.7	-2.7	1.1	0.83	-0.65
toluene	-1.7	3.3	-3.8	-5.9	2.1	3.9	-1.4
pyridine	-0.22		-1.5	-2.0	0.43	1.0	-3.0
o-xylene	-0.83	0.90	-2.0	-1.4	1.6	3.9	-3.6
styrene	-0.16	0.27	-2.9	-0.52	0.92	3.0	-1.2
d-limonene	-0.19		-6.1	-0.47	2.5	13	-0.8
formaldehyde	0.74	0.70	-0.81	0.56	-1.10	-5.1	-0.3
<i>acetaldehyde</i>							
<i>acetone</i>	-0.20	-0.11	1.9			-2.0	
<i>benzaldehyde</i>			2.5				
TOTAL VOCs	-18	7.2	-19	-36	22	30	-14

The compounds listed in italics were not present in the challenge mixture.

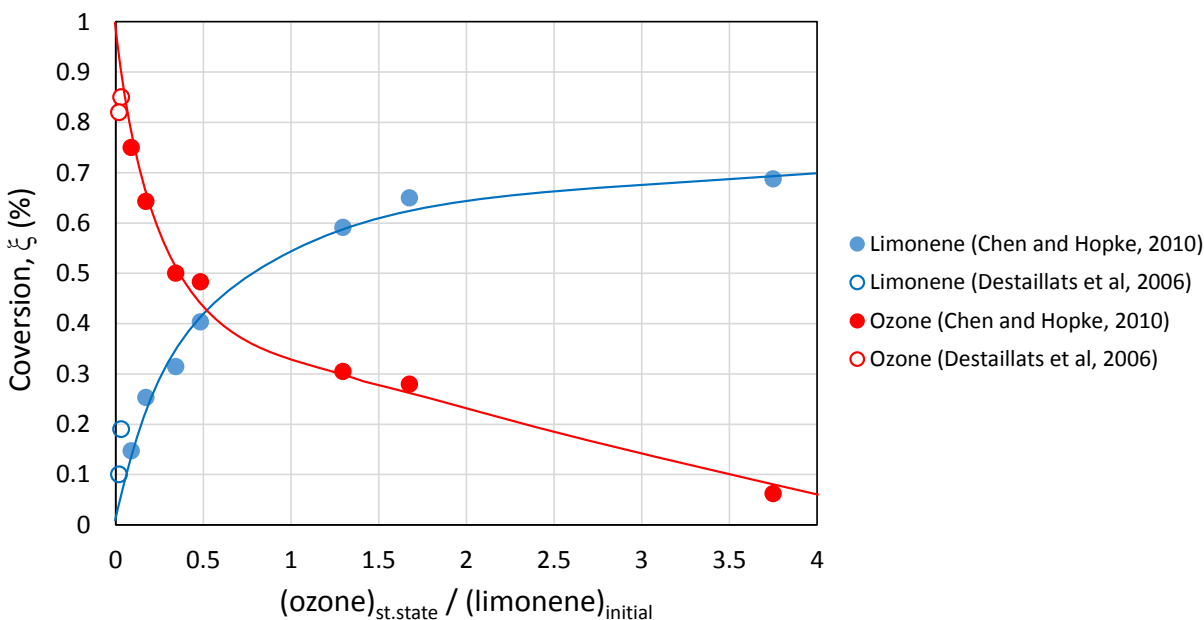
Table 5.4.4: Pollutant concentration change ΔC_i ($\mu\text{g m}^{-3}$) in Scenario 2 based on results from Phase 2. Negative changes (concentration reductions) are shown in black, and positive changes (increases in concentration) are shown in **red and bold font**

	PAC1	PAC2	PAC3	PAC4	PAC5		PAC6
					ionizer	ion + heat	
ozone	-	-	22 - 191	0.6 - 5.5	-	-	-
SOA	-		0.4 - 6.7		-	-	-
VOCs							
ethanol		11	-3.6	-359	143	4.9	7.3
hexane	-388		-77	-272	265	134	-64
butanal	-20		-15	-15		41	-20
benzene	-23	8.7	-25	-66	27	28	-16
TCE	-31	43	-49	-81	33	24	-19
toluene	-53	98	-114	-178	64	115	-40
pyridine	-6.7		-44	-60	13	30	-90
o-xylene	-25	27	-61	-42	47	117	-108
styrene	-4.7	8.0	-89	-15	27	89	-34
d-limonene	-5.5		-182	-14	74	403	-26
formaldehyde	22	20	-24	17	-33	-152	-8.0
<i>acetaldehyde</i>							
<i>acetone</i>	-6.0	-3.3	57			-59	
<i>benzaldehyde</i>			74				
TOTAL VOCs	-528	213	-553	-1086	661	895	-422

The compounds listed in italics were not present in the challenge mixture.

We estimated steady-state SOA concentrations when PAC3 is operating in the presence of ozone-reacting VOCs using the yield range determined in Section 5.3.2 ($Y_{SOA} = 1 - 15\%$). The predicted ozone concentration varied by one order of magnitude between Scenario 1 (3 – 13 ppb) and Scenario 2 (23 – 120 ppb). The upper limit of ozone concentrations for Scenario 2 was comparable to those determined in the LBNL chamber (~160 ppb). At those high ozone levels, it is reasonable to assume that ozone-reacting VOCs were practically depleted, as observed in our experiments. However, for lower ozone concentrations, the conversion of those SOA precursors is likely only partial, and was estimated using results from experimental determinations reported in the literature. In Figure 5.4.1 we plot the ozone and limonene conversion ξ determined in two different chamber studies for a broad range of reactant concentrations (Chen and Hopke, 2010; Destailats et al, 2006). Conversion of each reactant is shown as a function of the ratio between ozone measured at chamber steady-state conditions and initial limonene concentrations before ozone was admitted to the chamber.

Figure 5.4.1: Reported conversion of limonene and ozone in chamber studies



For the purpose of our model prediction, we assume that the only ozone-reactive VOC present is limonene, which is among the most reactive terpenes and has one of the highest SOA formation potential. We will also assume an initial limonene concentration of 10 ppb ($56 \mu\text{g}/\text{m}^3$) before operating the air cleaner. This level is representative of common limonene levels found indoors (Offermann, 2009). For those conditions, in

Scenario 1 the $(\text{ozone})_{\text{st.state}}/(\text{limonene})_{\text{initial}}$ concentration ratio is between 0.3 and 1.3, and according with the data shown in Figure 5.4.1, the conversion of limonene in that range is between 0.3 and 0.6 (we use in our estimation a mid-range value of 0.45). For Scenario 2, the ozone/limonene concentration ratio is between 2.3 and 12, and the corresponding limonene conversion spans from 0.65 up to ~ 1 (we use a mid-range value of 0.80). The SOA steady-state concentration, $(\text{SOA})_{\text{st.state}}$, is estimated as the product of limonene concentration, its conversion ζ_{limonene} and the SOA yield Y_{SOA} , as follows:

$$(\text{SOA})_{\text{st.state}} = (\text{limonene})_{\text{initial}} \cdot \zeta_{\text{limonene}} \cdot Y_{\text{SOA}} \quad (5.17)$$

For Scenario 1, we predict a SOA concentration at steady state $(\text{SOA})_{\text{st.state}} = 0.3$ to $3.8 \mu\text{g}/\text{m}^3$, and for Scenario 2 we estimate $(\text{SOA})_{\text{st.state}} = 0.4$ to $6.7 \mu\text{g}/\text{m}^3$. These values are reported in Table 5.4.3 and 5.4.4, respectively.

It should be kept in mind that these predictions involve several assumptions. These are based on the exclusive presence of a single ozone-reactive VOC, limonene, which is more reactive than several other terpenoids found indoors. We use the Y_{SOA} value determined using limonene and styrene (rather than limonene alone) in our experiment. We do not incorporate the effect of other environmental factors including: temperature, relative humidity, co-reagent concentrations (e.g., NO_x) and level and size distribution of pre-existing aerosol particles (Donahue et al, 2005; Youssefi and Waring, 2012). Furthermore, we did not consider deposition of aerosol particles to indoor surfaces, a process sensitive to particle size and the fluid dynamics present indoors. For the UFP particle size range typical of SOA from ozone-terpene reactions, it is reasonable to assume that losses by deposition will not have a dramatic effect on the predicted indoor SOA levels (Lai and Nazaroff, 2000). This approach does not account for limonene removal by the air cleaner, either. It should also be kept in mind that UFP often contribute only a small fraction of the PM mass concentration, and mass-based comparisons can be biased.

5.4.2. Potential Health Implications

We evaluate potential health implications by comparing predicted pollutant levels in Scenarios 1 and 2 with reference exposure levels (RELs) listed by the California EPA's Office of Environmental Health Hazard Assessment (OEHHA, 2014a). Ozone levels are also compared with the State ambient air standards for 1-h and 8-h exposures (ARB, 2008), and with ARB regulation limiting the levels of ozone emitted by air cleaning devices (ARB, 2012). We also perform a similar comparison with listed Proposition 65 "safe harbor" levels for no significant risk levels (NSRLs) of carcinogens and maximum allowable dose levels (MADLs) for chemicals causing reproductive toxicity (OEHHA, 2014b). Since NSRLs and MADLs are reported in micrograms of daily intake, we converted those values to air concentrations dividing by the breathing rate of a healthy adult $VE = 16 \text{ m}^3 \text{ day}^{-1}$. This value, reported by the US EPA's Exposure Factors

Handbook (US EPA, 2011), integrates periods of resting, light, moderate and heavy activity, and averages male and female adults. Only a fraction of pollutants present in inhaled air is effectively absorbed, and that fraction varies from compound to compound. For that reason, the air concentrations calculated by this method should be considered only a first approximation. These reference concentrations are listed in Table 5.4.5.

Table 5.4.5: Health-based reference levels for pollutants studied in this study

POLLUTANT	CAL EPA REL	California ozone air quality standard		ARB regulation on air cleaners' emissions	PROP 65 NSRL, inhalatory exposure		PROP 65 MADL, inhalatory exposure	
		1-h	8-h		$\mu\text{g}\cdot\text{day}^{-1}$	$\mu\text{g}\cdot\text{m}^{-3}$	$\mu\text{g}\cdot\text{day}^{-1}$	$\mu\text{g}\cdot\text{m}^{-3}$
	$\mu\text{g}\cdot\text{m}^{-3}$	ppb ($\mu\text{g}\cdot\text{m}^{-3}$)	ppb ($\mu\text{g}\cdot\text{m}^{-3}$)	ppb ($\mu\text{g}\cdot\text{m}^{-3}$)	$\mu\text{g}\cdot\text{day}^{-1}$	$\mu\text{g}\cdot\text{m}^{-3}$	$\mu\text{g}\cdot\text{day}^{-1}$	$\mu\text{g}\cdot\text{m}^{-3}$
ozone	180 (A)	90 (180)	70 (140)	50 (100)				
hexane	7000 (C)							
benzene	60 (C)				13	0.81	49	3.1
TCE	600 (C)				50	3.1		
toluene	300 (C)						7000	438
o-xylene	700 (C)							
styrene	900 (C)							
formaldehyde	9 (C)				40	2.5		
acetaldehyde	140 (C)				90	5.6		

A: acute REL
C: chronic REL

By comparing reference levels in Table 5.4.5 with those predicted in our two model Scenarios (Tables 5.4.3 and 5.4.4), we observed that most VOCs were either emitted or removed in amounts that were far smaller than health-based exposure levels, and likely did not contribute to any major change in indoor air quality. However, we identified the following pollutants that exceeded at least in one case potentially hazardous levels:

- (1) **Ozone:** concentration increases ΔC_{ozone} predicted for PAC3 exceeded California REL acute levels, both State air quality standards (1-h and 8-h) and the ARB regulatory level for air cleaners in Scenario 2, which constitutes the most significant exposure risk evaluated in this study. Values of ΔC_{ozone} predicted for PAC3 in Scenario 1 did not exceed those reference levels, but still constitute a

considerable hazard, particularly when taking into account the negative effects of ozone-driven indoor chemistry (Weschler, 2006). Ozone emissions by PAC4, while measurable, were of a much smaller magnitude and did not exceed the reference levels in any scenario.

- (2) **Formaldehyde:** Concentration changes predicted in Scenario 1 did not exceed the California REL, nor the concentration calculated based on the Prop 65 NSRL. However, results from Scenario 2 showed devices that resulted in concentration increases $\Delta C_{\text{formaldehyde}}$ that exceeded both reference values (PAC1, PAC2 and PAC4). On the other hand, the other three devices (PAC3, PAC5 and PAC6) removed formaldehyde in amounts that were either larger or comparable to the OEHHA chronic REL of $9 \mu\text{g}\cdot\text{m}^{-3}$.
- (3) **Benzene:** Concentration changes predicted in Scenario 1 did not exceed the California REL, and in some cases were close to the (much lower) concentrations calculated based on Prop 65 NSRL and MADL. Results from Scenario 2 showed devices that resulted in concentration increases $\Delta C_{\text{benzene}}$ that exceeded NSRL and MADL (PAC2, and PAC5). The other four devices (PAC1, PAC3, PAC4 and PAC6) removed benzene in amounts that were either larger or comparable to the NSRL and MADL. In addition, PAC4 removed benzene at a rate that was slightly higher than the OEHHA chronic REL of $60 \mu\text{g}\cdot\text{m}^{-3}$.
- (4) **UFP:** Only PAC3 emitted a significant level of UFPs in the presence of ozone-reacting VOCs in Phase 2. For those conditions, levels predicted in Scenario 1 and Scenario 2 are comparable to those measured using similar instrumentation in a limited number ($n=7$) of California homes over multi-day periods (Banghar et al, 2011). In the absence of health-based guidelines for occupant exposures to UFP, we use these recently-reported values as a reference to predict whether emissions from air cleaners will cause a measurable impact. In the Banghar et al (2011) study, both indoor and outdoor sources were found to contribute to UFP levels indoors, with the largest indoor source being cooking activities. The average exposure concentration considering all homes was $14.5 \cdot 10^3$ particles per cm^3 , which is equivalent to a mass concentration of $\sim 2 \mu\text{g m}^{-3}$ (assuming a mean particle size of 64 nm and a particle density of 1 g cm^{-3}). The choice of this mean particle size is supported by other recent UFP measurements, listed in Table 5.4.6.

Table 5.4.6: Indoor and outdoor UFP particle sizes reported in recent studies

Source	Particle diameter (nm)	Reference
Outdoor (freeway)	40 – 80	Zhu et al., 2005
Gas combustion	10	Wallace et al., 2008
Electric toaster/oven	30	
Cooking	25-50	
Candles and incense	60	
SOA	60-150	Waring et al, 2011

While short-term exposures (minutes) should consider smaller average particle sizes, results from Bhangar et al suggest that the average particle number concentration used here is appropriate for a longer time period (days), accounting for the contributions from various sources and particle coagulation.

The UFP number concentration value is ~5 times higher than the UFP concentration observed in the chamber experiment for PAC3 in Phase 2 (in the order of $3 \times 10^3 \text{ \# cm}^{-3}$). It is therefore reasonable to assume that contributions from this particular air cleaner to UFPs will not be negligible. The levels predicted in Scenarios 1 and 2, in the order of the low $\mu\text{g m}^{-3}$ levels, are comparable to those reported by Bhangar et al. In the same study, emission rates from the pilot lights from gas cooking appliances were in the order of $10^{12} \text{ \# h}^{-1}$, two orders of magnitude higher than the emission rates established for PAC3 under our experimental conditions ($3 \times 10^{10} \text{ \# h}^{-1}$).

- (5) **ROS:** Our experimental methods did not allow us to measure chamber ROS concentrations, although they indirectly suggest that interaction of high ozone levels emitted by PAC3 with VOCs present in the challenge mixture (Phase 2) led to the formation of increased ROS levels. Preliminary studies carried out with PAC3 and PAC4 (reported in Section 3.6) suggest that measureable levels can be detected directly at the outlet of the device. There are no health-based guidelines associated to these reactive species, however it is likely that inhalation of air that has been enriched in ROS may lead to cause oxidative stress, irritation or inflammation of the respiratory and cardiovascular systems (Danielsen et al, 2011; Donaldson et al, 2001; Li et al, 2003).

6. SUMMARY, CONCLUSIONS AND RECOMMENDATIONS

We have investigated the primary emissions and secondary byproducts from the operation of six portable air cleaners with a significant market presence in California. Tests using a 20-m³ room-sized environmental chamber allowed us to reproduce realistic operation conditions. Levels of volatile organic compounds (VOCs), ultrafine particulate matter, ozone and ROS were determined with the air cleaners operating in clean chamber (Phase 1) air and in the presence of a challenge VOC mixture (Phase 2). We have also evaluated their removal efficiency for VOCs and particulate matter. While some devices achieved significant removal efficiencies of some indoor pollutants, others were shown to emit remarkably high levels of ozone (up to 6 mg h⁻¹) and several VOCs as primary emissions (e.g., 85 µg h⁻¹ toluene) or secondary byproducts (e.g., 16 µg h⁻¹ formaldehyde). One device (PAC3) emitting high levels of ozone also produced a significant amount of ultrafine particulate matter, reaching chamber concentrations of 3x10³ # cm⁻³, corresponding to an estimated secondary organic aerosol yield of 1-5 %. This device was not certified by ARB. It is not expected that those certified devices, which emitted no more than 50 ppb, would produce a similar impact. ROS chamber levels were below background for most devices; however, increased detection when PAC3 operated in the presence of VOCs suggests that interaction of ozone with VOCs leads to measurable levels. Also, ROS emissions determined in preliminary tests of PAC4 (plasma generator) suggest that breathing from the proximity of the device may lead to exposure to higher-than-background levels.

Chamber-derived emission rates were used to predict typical indoor levels, and to evaluate occupant exposures by comparing predicted concentrations with California reference exposure levels and Proposition 65 risk levels. Three pollutants (ozone, formaldehyde and benzene) were found to exceed those reference levels in at least one of the two scenarios considered in this study.

The study findings indicate that primary and secondary emissions from portable air cleaners may lead to poor IAQ and associated health effects for a significant number of Californians. These findings will help the State assist the public in making informed decisions when purchasing and using portable air cleaners. It will also help ARB identify which health and indoor air quality concerns associated with the new technologies investigated here need to be further addressed.

Information generated in this work will also contribute to the broader research and regulatory effort that the ARB has been carrying out in this field over the past years. It will contribute to the development of effective standard testing procedures, in concert with results from other studies carried out in recent years addressing the same and other complementary aspects of indoor air cleaning. These findings can contribute to the development of effective standard testing procedures, such as ASTM or ISO methods, which are needed to control harmful emissions and verify the validity of marketing claims. The implementation and adoption of widely accepted testing and rating methods for portable air cleaners is recommended as a tool that can enable

developing over time a comprehensive body of evidence required to support new regulation.

In addition, this research may help manufacturers develop the appropriate engineering controls to prevent harmful pollutants from being released to indoor air. Those controls are recommended in cases in which emissions are intrinsically associated with the principles of operation of the devices and may include, for example, the use of filters and/or catalysts to eliminate ozone or ROS downstream of a plasma generator. The use of ozone-generating VUV lamps should be discouraged in PCO air cleaners.

Inaccurate and/or misleading advertising describes some of these devices as ROS generators. Given the extremely low levels measured in this study, such description seems not to be supported by the evidence. In the case of PCO air cleaners, very reactive species are formed on the surface of the photocatalyst, but are not released to indoor air in measurable amounts.

This study constituted an initial effort towards describing emissions of potentially harmful pollutants and air cleaner performance. Given the reduced number of devices tested (six), the conclusions and recommendations are limited by the size of the experimental matrix. However, these results provide a basis on which subsequent studies can build and expand our knowledge base.

Another limitation of the study is associated with the fact that ROS emissions, which were likely present in PAC3, could not be accurately quantified due to the presence of high levels of ozone, which interfered with the determination.

References

- Alshawa, A., Russell, A.R., and Nizkorodov, S.A. Kinetic analysis of competition between aerosol particle removal and generation by ionization air purifiers, *Environ. Sci. Technol.*, 2007, 46, 2498-2504.
- Ao, CH, and SC Lee. Indoor air purification by photocatalyst TiO₂ immobilized on an activated carbon filter installed in an air cleaner. *Chemical Engineering Sci.*, 2005, 60, 103-109.
- ARB. Ozone and Ambient Air Quality Standards. California Environmental Protection Agency. Air Resources Board, 2008.
<http://www.arb.ca.gov/research/aaqs/caaqs/ozone/ozone.htm>
- ARB. Hazardous Ozone-Generating "Air Purifiers". California Environmental Protection Agency. Air Resources Board, 2012.
<http://www.arb.ca.gov/research/indoor/ozone.htm>
- Arellanes, C., Paulson, S.E., Fine, P.M., Sioutas, C. Exceeding of Henry's Law by hydrogen peroxide associated with urban aerosols. *Environ. Sci. Technol.*, 2006, 40, 4859-4866
- Bahrini, C.; Parker, A.; Schoemaeker, C.; Fittschen, C. Direct detection of HO₂ radicals in the vicinity of TiO₂ photocatalytic surfaces using cw-CRDS. *Applied Catalysis B – Environmental*, 2010, 99, 413-419.
- Balasubramanian, R., Husain, L. Observations of gas-phase hydrogen peroxide at an elevated rural site in New York. *J. Geophys. Res.* 1997, 102, D17, 21,209-21,220.
- Bhangar, S., Mullen, N.A., Hering, S.V., Kreisberg, N.M., Nazaroff, W.W. Ultrafine particle concentrations and exposures in seven residences in northern California. *Indoor Air* 2011, 21, 132-144.
- Boularnanti, AK, CA Korologos, and CJ Philippopoulos. The rate of photocatalytic oxidation of aromatic volatile organic compounds in the gas-phase. *Atmos. Environ* 2008, 42, 7844-7850.
- Britigan, N., Alshawa, A., and Nizkorodov, S.A. Quantification of ozone levels in indoor environments generated by ionization and ozonolysis air purifiers, *J. Air Waste Manage. Assoc.*, 2006, 56, 601-610.
- Cano-Ruiz J.A., Kong, D., Balas, R.B. and Nazaroff, W.W. Removal of reactive gases at indoor surfaces: Combining mass transport and surface kinetics. *Atmos. Environ.* 1993, Vol. 27A, (13), 2039-2050.
- Chen, W, and JS Zhang. UV-PCO device for indoor VOCs removal: Investigation on multiple compounds effect. *Building and Environment* 2008, 43, 246-252.
- Chen, X.; Hopke, P.K. A chamber study of secondary organic aerosol formation by linalool ozonolysis. *Atmos. Environ.* 2009, 43, 3935-3904.
- Chen, X.; Hopke, P.K. A chamber study of secondary organic aerosol formation by limonene ozonolysis. *Indoor Air* 2010, 20, 320-328.

- Cheng, H.H., Hsieh, C.C., Tsai, C.H. Antibacterial and regenerated characteristics of Ag-zeolite for removing bioaerosols in indoor environment. *Aerosol and Air Quality Research* 2012, 12, 409-419.
- Cheng, Y.S.; Lu, J.C.; Chen, T.R. Efficiency of a portable indoor air cleaner in removing pollens and fungal spores *Aerosol Sci. and Technol.* 1998, 29, 92-101.
- Coleman, B.K., Lunden, M. M., Destailats, H. and Nazaroff W.W. Secondary organic aerosol from ozone-initiated reactions with terpene-rich household products. *Atmos. Environ.*, 2008, 42, 8234-8245.
- Damit, B., Wu, C.Y., Yao, M.S. Ultra-high temperature infrared disinfection of bioaerosols and relevant mechanisms. *J. Aerosol Sci.* 2013, 65, 88-100.
- Danielsen, P.H., Moller, P., Jensen, K.A., Sharma, A.K., Wallin, H., Bossi, R., Autrup, H., Molhave, L., Ravanat, J-L., Briede, J.J., de Kok, T.M., Loft, S. Oxidative stress, DNA damage and inflammation induced by ambient air and wood smoke particulate matter in human A549 and THP-1 cell lines. *Chem. Res. Toxicol.* 2011, 24, 168-184.
- Destailats, H.; Lunden, M. M.; Singer, B. C.; Coleman, B. K.; Hodgson, A. T.; Weschler, C. J.; Nazaroff, W. W. Indoor secondary pollutants from household product emissions in the presence of ozone. A bench scale study. *Environ. Sci. Technol.* 2006, 40, 4421-4428.
- Destailats, H., Maddalena, R. L., Singer, B.C., Hodgson, A. T., and McKone, T.E. Indoor pollutants emitted by office equipment. A review of reported data and information needs. *Atmos. Environ.*, 2008, 42, 1371-1388.
- Destailats, H., Sleiman, M., Sullivan, D.P., Jacquiod, C., Sablayrolles, J., Molins, L. Key parameters influencing the performance of photocatalytic oxidation (PCO) air purification under realistic indoor conditions. *Applied Catalysis B: Environmental*, 2012, 128, 159-170.
- Donahue, N.M., Huff Hartz, K.E., Chuong, B., Presto, A.A., Stanier, C.O., Rosenhorn, T., Robinson, A.L., Pandis, S.N. Critical factors determining the variation in SOA yields from terpene ozonolysis: A combined experimental and computational study. *Faraday Discuss.*, 2005, 130, 295-309.
- Donaldson, K., Stone, V., Seaton, A., MacNee, W. Ambient particle inhalation and the cardiovascular system: Potential mechanisms. *Environ. Health Perspect.* 2001, 109 (Suppl 4) 523-527.
- Dusanter, S., Vimal, D., Stevens, P.S., Volkamer, R., Molina, L.T. Measurements of OH and HO₂ concentrations during the MCMA-2006 field campaign – Part 1: Deployment of the Indiana University laser-induced fluorescence instrument. *Atmos. Chem. Phys.* 2009, 9, 1665-1685.
- Forbes, P.D., Davies, R.E., D'Aloisio, L.C., Cole, C. Emission spectrum differences in fluorescent blacklight lamps. *Photochem. Photobiol.* 1976, 24, 613-615.

- Gall, E., Darling, E., Siegel, J.A., Morrison, G.C., Corsi, R.L. Evaluation of three common green building materials for ozone removal, and primary and secondary emissions of aldehydes. *Atmos. Environ.* 2013, 77, 910-918.
- Ginestet, A.; Pugnet, D.; Rowley, J.; Bull, K.; Yeomans, H. Development of a new photocatalytic oxidation air filter for aircraft cabin *Indoor Air* 2005, 15, 326-334.
- Gligorovski, S., Weschler, C.J. The oxidative capacity of indoor atmospheres. *Environ. Sci. Technol.* 2013, 47, 13905-13906.
- Hasson, A.S., Paulson, S.E. An investigation of the relationship between gas-phase and aerosol-borne hydroperoxides in urban air. *Aerosol Science* 2003, 34, 459-468.
- Hodgson, A.T.; Levin, H. *Classification of measured indoor volatile organic compounds based on noncancer health and comfort considerations*. LBNL report # 53308. http://www.inive.org/members_area/medias/pdf/Inive/LBL/LBNL-53308.pdf
- Hodgson, A. T.; Destailats, H.; Sullivan, D.; Fisk, W. J. Performance of ultraviolet photocatalytic oxidation for indoor air cleaning applications *Indoor Air* 2007a, 17, 305-316.
- Hodgson, A. T.; Destailats, H.; Hotchi, T.; Fisk, W. J. Evaluation of a Combined Ultraviolet Photocatalytic Oxidation (UVPCO) / Chemisorbent Air Cleaner for Indoor Air Applications *Report prepared to the Building Technologies Program of the U.S. Department of Energy, Contract No. DE-AC02-05CH11231. [LBNL - 62202] 2007b*.
- Hoffmann, M.R.; Martin, S.T.; Choi, W.; Bahnemann, D.W. Environmental applications of semiconductor photocatalysis. *Chem. Rev.* 1995, 95, 69-96.
- Hong, S.B., Kim, G.S., Kang, C.H., Lee, J.H. Measurement of ambient hydroperoxides using an automated HPLC system and various factors which affect variations of their concentrations in Korea. *Environ. Monit. Assess.* 2008, 147, 23-34.
- Howard-Reed, C.; Nabinger, S. J.; Emmerich, S. J. Characterizing gaseous air cleaner performance in the field *Building and Environment* 2008a, 43, 368-377.
- Howard-Reed, C.; Henzel, V.; Nabinger, S. J.; Persily, A. K. Development of a field test method to evaluate gaseous air cleaner performance in a multizone building *J. Air and Waste Manag. Assoc.* 2008b, 58, 919-927.
- Hubbard H.F., Coleman B.K., Sarwar G., and Corsi R.L. The effects of an ozone generating air purifier on indoor secondary particles in three residential dwellings, *Indoor Air*, 2005, 15, 432-444.
- Jakober, C.; Phillips, T. *Evaluation of ozone emissions from portable indoor air cleaners: electrostatic precipitators and ionizers*; Staff Technical Report to the California ARB: www.arb.ca.gov/research/indoor/esp_report.pdf, 2008.
- Ji, J.H., Bae, G.N., Yun, S.H., Jung, J.H., Noh, H.S., Kim, S.S. Evaluation of a silver nanoparticle generator using a small ceramic heater for inactivation of *S.epidermis* bioaerosol. *Aerosol Sci Technol.* 2007, 41, 786-793.

- Jung, J.H., Lee, J.E., Kim, S.S., Bae, G.N. Size reduction of aspergillus versicolor fungal bioaerols during a thermal heating process in continuous-flow system. *J. Aerosol Sci.* 2010, 41, 602-610.
- Jung, J.H., Lee, J.E., Kim, S.S. Thermal effects on bacterial bioaerosols in continuous air flow. *Sci. Total Environ.* 2009, 407, 4723-4730.
- Kibanova, D., Sleiman, M., Cervini-Silva, J., Destailats, H. Adsorption and photocatalytic oxidation of formaldehyde on a clay-TiO₂ composite. *J. Hazardous Materials*, 2012, 211-212, 233-239.
- Kibanova, D., Cervini-Silva, J., Destailats, H. Efficiency of clay-TiO₂ nanocomposites on the photocatalytic elimination of a model hydrophobic air pollutant. *Environ. Sci. Technol.* 2009, 43, 1500-1506.
- Kunkel, D.A., Gall, E.T., Siegel, J.A., Novoselac, A., Morrison, G.C., Corsi, R.L. Passive reduction of human exposure to indoor ozone. *Building and Environment* 2010, 45, 445-452.
- Lai, A.C.K., Nazaroff, W.W. Modeling indoor particle deposition from turbulent flow onto smooth surfaces. *J. Aerosol Sci.* 2000, 31, 463-476.
- Li, T-H, Turpin, B.J., Shields, H.C., Weschler, C.J. Indoor hydrogen peroxide derived from ozone/d-limonene reactions. *Environ. Sci. Technol.* 2002, 36, 3295-3302.
- Li, N., Sioutas, C., Cho, A., Schmitz, D., Misra, C., Sempf, J., Wang, M., Oberley, T., Froines, J.Nel, A. Ultrafine particulate pollutants induce oxidative stress and mitochondrial damage. *Environ. Health Perspect.* 2003, 111, 455-460.
- Liang, Y.D., Wu, Y., Sun, K., Chen, Q., Shen, F.X., Zhang, J., Yao, M.S., Zhu, T., Fang, J. Rapid inactivation of biological species in the air using atmospheric pressure nonthermal plasma. *Environ. Sci. Technol.* 2012, 46, 3360-3368.
- Linxiang, L., Abe, Y., Nagasawa, Y., Kudo, R., Usui, N., Imai, K., Mashino, T., Mochizuki, M., Miyata, N. An HPLC assay of hydroxyl radicals by the hydroxylation reaction of terephthalic acid. *Biomed. Chromatogr.* 2004, 18, 470-474.
- Maddalena, R. L.; McKone, T. E.; Destailats, H.; Russel, M. L.; Hodgson, A. T.; Perino, C. *Quantifying pollutant emissions from office equipment*, CEC/CARB University of California, Berkeley, 2009.
http://www.osti.gov/bridge/product.biblio.jsp?osti_id=918677
- Macintosh, D. L.; Myatt, T. A.; Ludwig, J. F.; Baker, B. J.; Suh, H. H.; Spengler, J. D. Whole house particle removal and clean air delivery rates for in-duct and portable ventilation systems *J. Air and Waste Manag. Assoc.* 2008, 58, 1474-1482.
- Mo, JH, YP Zhang, QJ Xu, YF Zhu, JJ Lamson, and RY Zhao. 2009. Determination and risk assessment of by-products resulting from photocatalytic oxidation of toluene. *App. Cat. B: Environ.* 2009, 89, 570-576.
- Morrison, G.C., Nazaroff, W. W. The rate of ozone uptake on carpet: Mathematical modeling. *Atmos. Environ.* 2002, 36, 1749-1756.

- Nazaroff, W.W., Gadgil, A.J., Weschler, C.J. Critique of the use of deposition velocity in modeling indoor air quality. In: Nagda, N.L. (Ed.), *Modeling Indoor Air Quality and Exposure*. ASTM STP 1205. American Society for Testing and Materials, Philadelphia, 1993. (pp. 81–84).
- Nazaroff, W. W.; Coleman, B. K.; Destailats, H.; Hodgson, A. T.; Liu, D. L.; Lunden, M. M.; Singer, B. C.; Weschler, C. *Indoor air chemistry: cleaning agents, ozone and toxic air contaminants*; Final Report. Contract # 01-336 - California Air Resources Board: <http://www.arb.ca.gov/research/abstracts/01-336.htm#Disclaimer>, 2006.
- Nishikawa, H., Nojima, H. Airborne viruses inactivation with cluster ions generated in a discharge plasma. *Sharp Technical Journal* 2003, 86, 10-15.
- OEHHA, 2014a. List of acute, 8-hour and chronic Reference Exposure Levels. <http://www.oehha.ca.gov/air/Allrels.html>
- OEHHA, 2014b. Proposition 65 No Significant Risk Levels (NSRLs) for carcinogens and Maximum Allowable Dose Levels (MADLs) for chemicals causing reproductive toxicity. <http://www.oehha.ca.gov/prop65/pdf/safeharbor081513.pdf>
- Offermann, F. J. 2009. Ventilation and Indoor Air Quality in New Homes. California Air Resources Board and California Energy Commission, PIER Energy-Related Environmental Research Program. Collaborative Report. CEC-500-2009-085. <http://www.arb.ca.gov/research/apr/past/04-310.pdf>.
- Park, J.H., Byeon, J.H., Yoon, K.Y., Hwang, J. Lab-scale test of a ventilation system including a dielectric barrier discharger and UV-photocatalyst filters for simultaneous removal of gaseous and particulate contaminants. *Indoor Air* 2008, 18, 44-50.
- Phillips, T., Jakober, C. *Evaluation of ozone emissions from portable indoor "air cleaners" that intentionally generate ozone*; Staff Technical Report to the California ARB: www.arb.ca.gov/research/indoor/o3g-rpt.pdf, 2006.
- Piazza, T.; Lee, R. H.; Hayes, J. *Survey of the use of ozone-generating air cleaners by the California public.*; Final Report prepared for the California ARB and Cal EPA, Contract 05-301: www.arb.ca.gov/research/apr/past/05-301.pdf, 2006.
- Poppendieck, D., Hubbard, H., Ward, M., Weschler, C., Corsi, R.L. Ozone reactions with indoor materials during building disinfection. *Atmos. Environ.* 2007, 41, 3166-3176.
- Quici, N.; Vera, M.L.; Choi, H.; Li Puma, G. ; Dionysiou, D.D. ; Litter, M.I. ; Destailats, H. Effect of key parameters on the photocatalytic oxidation of toluene at low concentrations in air under 254+185 nm UV irradiation. *Applied Catalysis B: Environmental* 2010, 95, 312-319.
- Salthammer, T., Mentese, S., Marutzky, R. Formaldehyde in the indoor environment. *Chem. Rev.* 2010, 110, 2536-2572.
- Shaugnessy, R. J.; Levetin, E.; Blocker, J.; Sublette, K. L. Effectiveness of portable indoor air cleaners: sensory testing results *Indoor Air* 1994, 4, 179-188.

- Shaugnessy, R. J.; Sextro, R. G. What is an effective portable air cleaning device? A review *J. Occup. Environ. Hyg.* 2006, 3, 169-181.
- Shimer, D.; Phillips, T.J.; Jenkins, P.L. 2005. *Report to the California Legislature. Indoor Air Pollution in California.*
<http://www.arb.ca.gov/research/indoor/ab1173/rpt0705.pdf>
- Shimizu, K., Blajan, M., Kuwabara, T. Removal of indoor air contaminant by atmospheric microplasma. *IEEE Trans. Ind. Appl.* 2011, 47, 2351-2357.
- Shin-Etsu Quartz Products Co. 2014. *Transparent Quartz Glass for Lamps.*
http://www.sqp.co.jp/e/seihin/catalog/pdf/e_5.pdf
- Sidheswaran, M., Destailats, H., Sullivan, D.P., Larsen, J., Fisk, W.J. Quantitative room-temperature mineralization of airborne formaldehyde using manganese oxide catalysts. *Applied Catalysis B: Environmental*, 2011, 107, 34-41.
- Singer, B.C., Coleman, B.K., Destailats, H., Hodgson, A.T., Weschler, C.J. Nazaroff, W.W. Indoor secondary pollutants from cleaning product and air freshener use in the presence of ozone. *Atmos. Environ.* 2006, 40, 6696-6710.
- Singer, B.C., Hodgson, A.T., Hotchi, H., Ming, K.Y., Sextro, R.G., Wood, E.E., Brown, N.J. Sorption of organic gases in residential rooms. *Atmos. Environ.* 2007, 41, 3251-3265.
- Sleiman, M., Destailats, H., Gundel, L.A. Solid-phase supported profluorescent nitroxide probe for the determination of aerosol-borne reactive oxygen species. *Talanta* 2013, 116, 1033-1039.
- Stephens, B., Siegel, J.A. Penetration of ambient submicron particles into single-family residences and associations with building characteristics. *Indoor Air* 2012, 22, 501-513.
- Sultan, Z.M., Nilsson, G.J., Magee, R.J. Removal of ultrafine particles in indoor air: Performance of various portable air cleaner technologies. *HVAC&R Research* 2011, 17, 513-525.
- Sun, Y.; Fang, L.; Wyon, D. P.; Wisthaler, A.; Lagercrantz, L.; Strom-Tejsten, P. Experimental research on photocatalytic oxidation air purification technology applied to aircraft cabins *Building and Environment* 2008, 43, 258-268.
- Thevenet, F., Guaitella, O., Puzenat, E., Herrmann, J-M., Rousseau, A., Guillard, C. Oxidation of acetylene by photocatalysis coupled with dielectric barrier discharge. *Catalysis Today* 2007, 122, 186-194.
- Thiebaud, J.; Thevenet, F.; Fittschen, C. OH radicals and H₂O₂ in the gas phase near TiO₂ surfaces. *J. Phys. Chem. C*, 2010, 114, 3082-3088.
- Tung, T. C. W.; Niu, J. L.; Burnett, J.; Hung, K. Determination of ozone emission from a domestic air cleaner and decay parameters using environmental chamber tests *Indoor and Built Environ.* 2005, 14, 29-37.
- US EPA. Method TO-1, Revision 1.0: Method for the determination of volatile organic compounds in ambient air using Tenax® Adsorption and gas chromatography/

- mass spectrometry (GC/MS), Center for Environmental Research Information, Office of Research and Development US Environmental Protection Agency, 1984.
- US EPA. Compendium Method TO-11A – Determination of formaldehyde in ambient air using adsorbent cartridge followed by HPLC [active sampling methodology], Office of Research and Development – US Environmental Protection Agency, Cincinnati, OH, 1999.
- US EPA. Exposure Factors Handbook: 2011 Edition. National Center for Environmental Assessment, Office of Research and Development, U.S. Environmental Protection Agency, Washington, DC 20460.
<http://www.epa.gov/ncea/efh/pdfs/efh-complete.pdf>
- Venkatachari P., Hopke, P.K. Development and laboratory testing of an automated monitor for the measurement of atmospheric particle-bound reactive oxygen species (ROS). *Aerosol Sci. Technol.* 2008, 42, 629-635.
- Voronov A. New generation of low pressure mercury lamps for producing ozone. *Ozone Sci. Eng.* 2008, 30, 395-397.
- Wallace, L., Wang, F., Howard-Reed, C., Persily, A. Contribution of gas and electric stoves to residential ultrafine particle concentrations between 2 and 64 nm: size distributions and emission and coagulation rates. *Environ. Sci. Technol.* 2008, 42, 8641-8648.
- Wang, Y., Kim, H., Paulson, S.E. Hydrogen peroxide generation from alpha- and beta-pinene and toluene secondary organic aerosols. *Atmos. Environ.* 2011, 45, 3149-3156.
- Ward, M.; Siegel, J. A.; Corsi, R. The effectiveness of standalone air cleaners for shelter-in-place *Indoor Air* 2005, 15, 127-134.
- Waring, M.S., Siegel, J.A., and Corsi, R.L. Ultrafine particle removal and generation by portable air cleaners, *Atmos. Environ.*, 2008, 42, 5003-5014.
- Waring, M.S., Wells, J.R., Siegel, J. A. Secondary organic aerosol formation from ozone reactions with single terpenoid and terpenoid mixtures. *Atmos. Environ.* 2011, 45, 4235-4242.
- Weschler, C.J., Shields, H.C. Measurements fo the hydroxyl radical in a manipulated but realistic indoor environment. *Environ. Sci. Technol.* 1997, 31, 3719-3722.
- Weschler, C.J. Ozone's impact on public health: Contributions from indoor exposures to ozone and products of ozone-initiated chemistry. *Environ. Health Perspectives* 2006, 114, 1489-1496.
- Youssefi, S., Waring, M.S. Predicting secondary organic aerosol formation from terpenoid ozonolysis with varying yields in indoor environments. *Indoor Air* 2012, 22, 415-426.
- Yu, KP, GWM Lee, WM Huang, CC Wu, and SH Yang. The correlation between photocatalytic oxidation performance and chemical/physical properties of indoor volatile organic compounds. *Atmos. Environ* 2006, 40, 375-385.

- Yu, J.G., Li, X.Y., Xu, Z.H., Xiao, W. NaOH-modified ceramic honeycomb with enhanced formaldehyde adsorption and removal performance. *Environ. Sci. Technol.* 2013, 47, 9928-9933.
- Zhang, Y., Mo, J., Li, Y., Sundell, J., Wargocki, P., Zhang, J., Little, J.C., Corsi, R., Deng, Q., Leung, M.H.K., Fang, L., Chen, W., Li, J., Sun, Y. Can commonly-used fan-driven air cleaning technologies improve indoor air quality? A literature review. *Atmos. Environ.* 2011, 45, 4329-4343.
- Zhao, J., Hopke, P.K. Concentration of reactive oxygen species (ROS) in mainstream and sidestream cigarette smoke. *Aerosol Sci. Technol.* 2012, 46, 191-197.
- Zhou, M., Diwu, Z., Panchuk-Voloshina, N., Haugland, R.P. A stable nonfluorescent derivative of resorufin for the fluorometric determination of trace hydrogen peroxide: Applications in detecting the activity of phagocyte NADPH oxidase and other oxidases. *Anal. Biochem.* 1997, 253, 162-168.
- Zhu, Y., Hinds, W.C., Krudysz, M. Kuhn, T., Froines, J., Sioutas, C. Penetration of freeway ultrafine particles into indoor environments. *Aerosol Sci.* 2005, 36, 303-322.
- Zuraimi, M.S., Nilsson, G.J., Magee, R.J. Removing indoor particles using portable air cleaners: Implications for residential infection transmission. *Building and Environment* 2011, 46, 2512-2519.

List of Publications Generated by this Study

Two journal articles are currently being prepared that will summarize the findings of this project, and will be submitted for publication during 2015:

- a) "Impact of portable air cleaners in indoor air quality"
H. Destailats, M. Sleiman, S. Cohn, M. Russell, W.J. Fisk
Manuscript in preparation, summarizing the main findings of this study.
Target journal: *Environ. Sci. Technol.* or *Atmos. Environ.*
- b) "Detection and quantification of reactive oxygen species (ROS) in indoor air"
V.N. Montesinos, M. Sleiman, S. Cohn, M.I. Litter and H. Destailats
Manuscript in preparation describing the development of ROS sampling and analytical methods.
Target journal: *Talanta* or *Anal. Chim. Acta*

In addition, two oral presentations were delivered at two international conferences in August and October 2014:

- a) "Evaluation of indoor pollutant emissions from portable air cleaners"
H. Destailats, S. Cohn, M. Sleiman.
24th Annual Meeting of the International Society for Exposure Science (ISES), Cincinnati, OH, October 2014.
- b) "Pollutant emissions from portable air cleaners relying on photocatalytic oxidation (PCO), non-thermal plasma and microbial thermal inactivation"
H. Destailats, S. Cohn, M. Sleiman.
248th National Meeting of the American Chemical Society (ACS), San Francisco, CA, August 2014.

Glossary of Terms, Abbreviations and Symbols

AuR = Amplex® ultra Red

CE = collection efficiency

C_i = pollutant chamber concentration [$\mu\text{g m}^{-3}$]

C_i^{OFF} = pollutant chamber concentration with the air cleaner turned OFF [$\mu\text{g m}^{-3}$]

C_i^{ON} = pollutant chamber concentration with the air cleaner turned ON [$\mu\text{g m}^{-3}$]

C_i^0 = pollutant concentration in clean air entering the chamber [$\mu\text{g m}^{-3}$]

C_{SF_6} = downstream SF_6 concentration [$\mu\text{g m}^{-3}$] (used in determination of F_{AC})

$C_{SF_6}^0$ = upstream SF_6 concentration [$\mu\text{g m}^{-3}$] (used in determination of F_{AC})

D_i = pollutant deposition rate [h^{-1}]

DCFH = 2',7'-dichlorofluorescein

DMSO = dimethyl sulfoxide

DNPH = dinitrophenyl hydracine

E_i^S = source strength of pollutant i [$\mu\text{g h}^{-1}$]

E_i^{AC} = air cleaner emission rate [$\mu\text{g h}^{-1}$]

F_{CH} = chamber air flow rate [$\text{m}^3 \text{h}^{-1}$]

F_{AC} = air cleaner flow rate [$\text{m}^3 \text{h}^{-1}$]

H_2DCF = 2',7'-dichlorodihydrofluorescein

H_2DCFDA = 2',7'-dichlorodihydrofluorescein diacetate

HPLC = high pressure (performance) liquid chromatography

HPR = Type VI-A horseradish peroxidase

HTPA = 2-hydroxyterephthalic acid

IAQ = indoor air quality

IR = SF_6 injection rate [$\text{m}^3 \text{h}^{-1}$] (used in determination of F_{AC})

MADL = maximum allowable dose level [μg]

m_i = mass of pollutant i formed per unit time [$\mu\text{g h}^{-1}$]

N = number of devices used in model scenario

NO_x = nitrogen oxides

NSRL = no significant risk level [μg]

PM = particulate matter

R_{AC} = air cleaner removal efficiency [$\mu\text{g h}^{-1}$]

RE = recovery efficiency

REL = reference exposure level [$\mu\text{g m}^{-3}$]

RH = relative humidity

ROS = reactive oxygen species

S^α = surface area of material α exposed to pollutant i [m^2]

SOA = secondary organic aerosol

TD/GC/MS = thermal desorption / gas chromatography / mass spectrometry

TPA = terephthalic acid

UFPs = ultrafine particles

VE = breathing rate of a healthy adult [$\text{m}^3 \text{day}^{-1}$]

V_{CH} = chamber volume [m^3]

W-CPC = water-based condensation particle counter

Y_i = yield of pollutant i (unitless)

ΔC_i = incremental concentration of pollutant i [$\mu\text{g m}^{-3}$]

λ = air exchange rate [h^{-1}]

v_i^α = deposition velocity of pollutant i on material α [m h^{-1}]

ρ = recycle ratio [unitless]

ξ = reactant conversion [%]

ω_i = chamber concentration reduction factor for pollutant i [unitless]

$\Phi_{\rho,ss}^i$ = single-pass removal efficiency for each compound i under steady-state conditions (ss) [unitless]



APPENDICES

APPENDIX 1

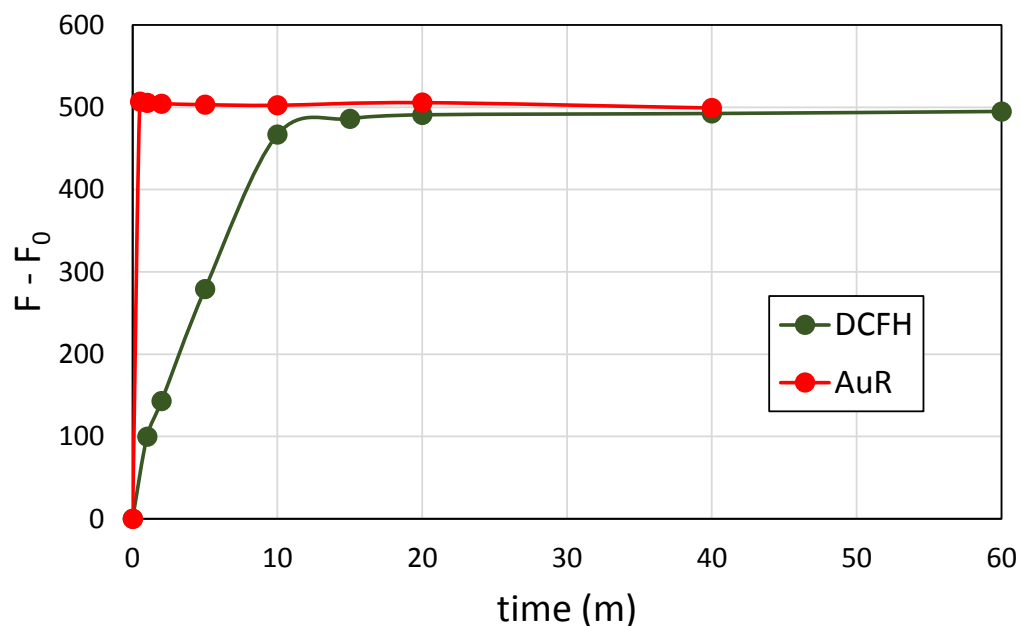
DEVELOPMENT OF SAMPLING AND ANALYTICAL METHODS FOR THE QUANTIFICATION OF ROS

A.1.1. Development of calibration curves for the three fluorescent probes

The calibrations for the DCFH and AuR methods were carried out with H₂O₂ solutions prepared by serial dilution of the 1:1000 H₂O₂ stock solution. For the DCFH method, a five-point calibration curve was prepared for H₂O₂ concentrations between 100 nM and 2000 nM. Each calibration level was prepared by addition of 400 μM H₂DCF and HPR to obtain final concentrations of 10 μM and 2 U mL⁻¹, respectively. Standards were allowed to equilibrate at room temperature in the dark for at least 20 minutes, to allow for the reaction to be completed. The intensity of fluorescence was measured before 60 minutes. The same general procedure was applied for AuR samples in the range [H₂O₂] = 10 – 500 nM, with final concentrations of AuR and HPR of 15 μM and 1 U mL⁻¹. In this case the reaction was almost instantaneous, and samples were equilibrated at room temperature in the dark for only 3 to 5 minutes. The fluorescent intensity was measured before 30 minutes, and the signal was confirmed to be stable for at least 40 minutes. Figure A.1.1 shows measurements taken at different times to determine the duration of the waiting period required for the reaction to be completed and the stability of the fluorescent signals for these two probes.

Figure A.1.1. Determination of the waiting period required for the reactions involving the probes DCFH and AuR

The fluorescent signal F is subtracted from the reactant blank signal, F_0



In the case of TPA tests, calibration curves were developed using directly the fluorescent species, HTPA. Dilutions were prepared from a stock HTPA solution of 2.5 mM, in the range 10 – 500 nM.

Figure A.1.2 presents the calibration curves prepared for each of the three fluorescent probes. The analytical and statistical parameters for these calibrations are presented in Table A.1.1.

Figure A.1.2. Calibration curves for ROS determined with the three fluorescent probes: (a) DCFH; (b) AuR; and (c) TPA

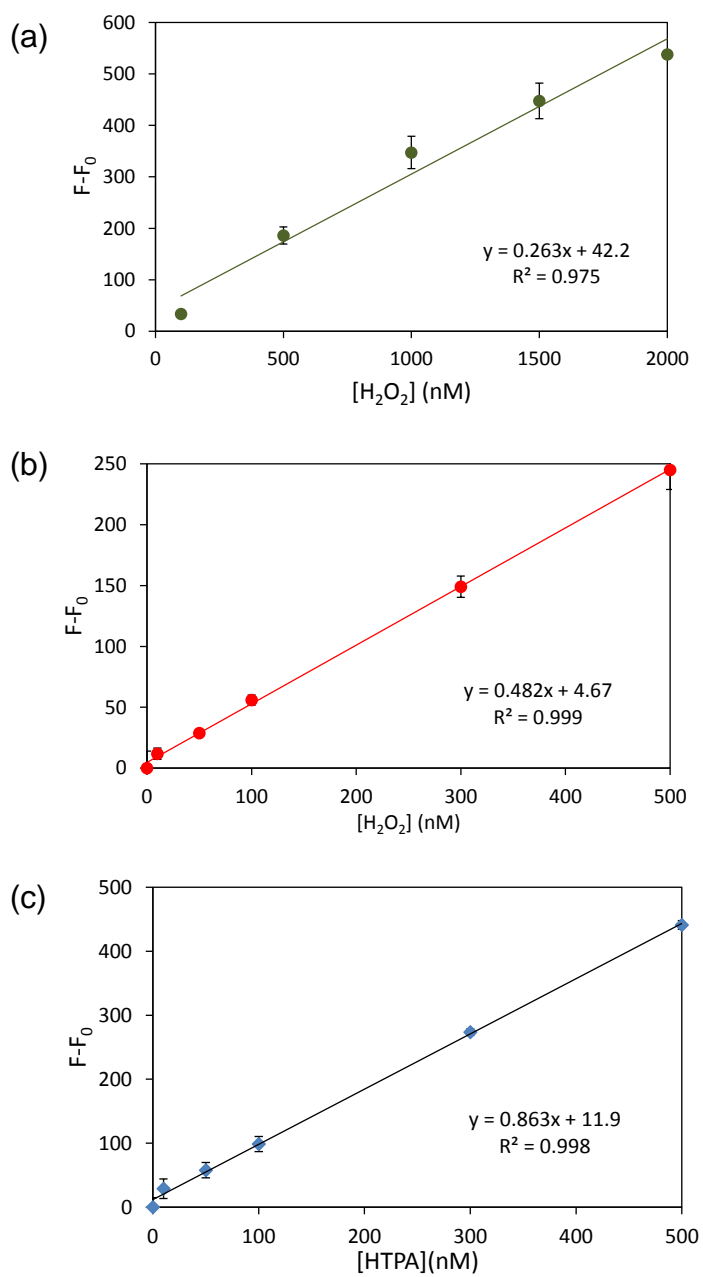


Table A.1.1. Analytical figures of merit for ROS quantification using DCFH, AuR and TPA

Probe	Slope (nM ⁻¹)	Slope Relative Standard Deviation, RSD (%)	Detection Limit, DL (nM)	Quantification Limit, QL (nM)	Lowest calibration level
DCFH	0.27	2.9	9.1	15.2	100 nM H ₂ O ₂
AuR	0.48	6.4	13.2	22.0	10 nM H ₂ O ₂
TPA	0.86	3.0	10.9	18.3	10 nM HTPA

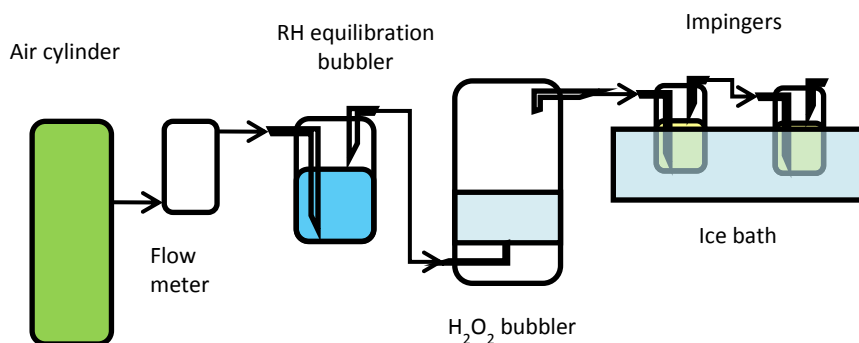
All calibration curves were successfully adjusted by a linear correlation with $R^2 \geq 0.98$. The method's detection (DL) and quantification (QL) limits were calculated for each probe, based on instrumental response. The instrumental limits were calculated as three (DL) or five (QL) times the standard deviation of a blank solution prepared using all the reactants except the fluorescent probe. In all cases, detection and quantification limits obtained were in good agreement with those showed in prior studies using the same probes. The good reproducibility for each method is reflected in the low relative standard deviation of the slopes, which were in all cases lower than 7%, as determined in at least three replicates. Finally, we observed that the reaction time of AuR was significantly faster than that of DCFH, and the fluorescent product was more stable.

A.1.2. Development of the ROS sampling method

Prior to sampling from chamber air, we performed tests in the laboratory using a stable ROS source to characterize the accuracy of the determination and the collection efficiency. We collected each ROS sample by bubbling air into two impingers in series containing the corresponding buffer used for analysis of each fluorescent probe. The ROS source consisted on a bubbler containing a known amount of H₂O₂ (aq), in equilibrium with the corresponding partial pressure of H₂O₂ (g). The peroxide generator and ancillary sampling equipment are illustrated in Figure A.1.3. A controlled flow of clean air ("zero" quality, Praxair, CA) was bubbled first through a water column to achieve saturation, and then through a gas sparger consisting in a glass column provided with a porous frit base that was filled with 250 mL of an H₂O₂ aqueous solution of known concentration (in the range 1 – 13 mM). For the evaluation of the DCFH and AuR methods, gas phase H₂O₂ was collected in two 25-mL Midget Impingers (SKC®, CA) in series filled with 10 mL of 50 mM phosphate buffer (pH 7.2) kept in an ice bath at a constant temperature of 3°C to maximize peroxide capture and prevent ROS decomposition in aqueous solution. After collection, a 3 mL aliquot from each impinger

was placed in a 5-mL volumetric flask, the reactants (including the fluorescent probe) were added immediately after sampling, and the fluorimetric assays were carried out following the same procedure described above for the calibration standards. For the TPA test, 10 mL of 0.5 mM TPA in 50 mM phosphate buffer (pH 7.2) solution was placed in each impinger. In this case the fluorimetric determination was carried out without further dilution of the collected sample. In all cases the corresponding blanks were prepared by bubbling “zero quality” clean air into the impingers containing the corresponding probes. A calibration curve for each probe was also prepared and analyzed simultaneously.

Figure A.1.3. Experimental setup used to develop the ROS sampling method



Assuming that the gas/liquid partitioning was achieved instantaneously, we used the Henry’s law constant to estimate the expected H₂O₂ concentrations in the gas phase. The experimental conditions are indicated in Table A.1.2. Collection flow rates and peroxide concentration inside the sparger [H₂O₂]_{aq} were adjusted to fit in the linear range of each technique when using a sampling time of approximately 30 min. Tests were carried out for the AuR, DCFH and TPA methods, to evaluate the overall recovery efficiency of gas phase H₂O₂ by the sampling system and to calculate the collection efficiency at the first impinger (*CE*) determined as

$$CE = 100 \times \left[1 - \frac{[H_2O_2]_{gas}^2}{[H_2O_2]_{gas}^1} \right] \quad (3.1)$$

where $[H_2O_2]_{gas}^1$ and $[H_2O_2]_{gas}^2$ are the H_2O_2 gas phase concentrations determined with data from the first and in second impinger, respectively. Results reported in Table A.1.2 show that, for DCFH and AuR, the collection efficiency was $CE = 100\%$, indicating that there was no breakthrough of analyte to the second impinger under the working conditions. Furthermore, the tests also showed excellent recovery efficiency (RE) for both probes, as determined by

$$RE = 100 \times \left[\frac{\text{measured } [H_2O_2]_{gas}}{\text{expected } [H_2O_2]_{gas}} \right] \quad (3.2)$$

The H_2O_2 gas phase concentrations were within the expected values calculated with the Henry's law constant in the case of DCFH (i.e., $RE = 100\%$). For AuR, the measured value was slightly lower than the expected range of concentration, consistent with a recovery of $RE = 73\%$. One possible reason for the incomplete recovery may be the fact that this test was carried out with H_2O_2 concentrations that were ten times lower than those used for DCFH tests, and the determination involved larger uncertainties (the relative error for DCHF was $\sim 3\%$ and for AuR was 35%). Blank samples for both probes showed no fluorescent signal. The test performed with TPA did not generate any measureable amount of HTPA, as expected since this probe is not sensitive to H_2O_2 . The negative result obtained with TPA confirmed that this probe is not sensitive to peroxides.

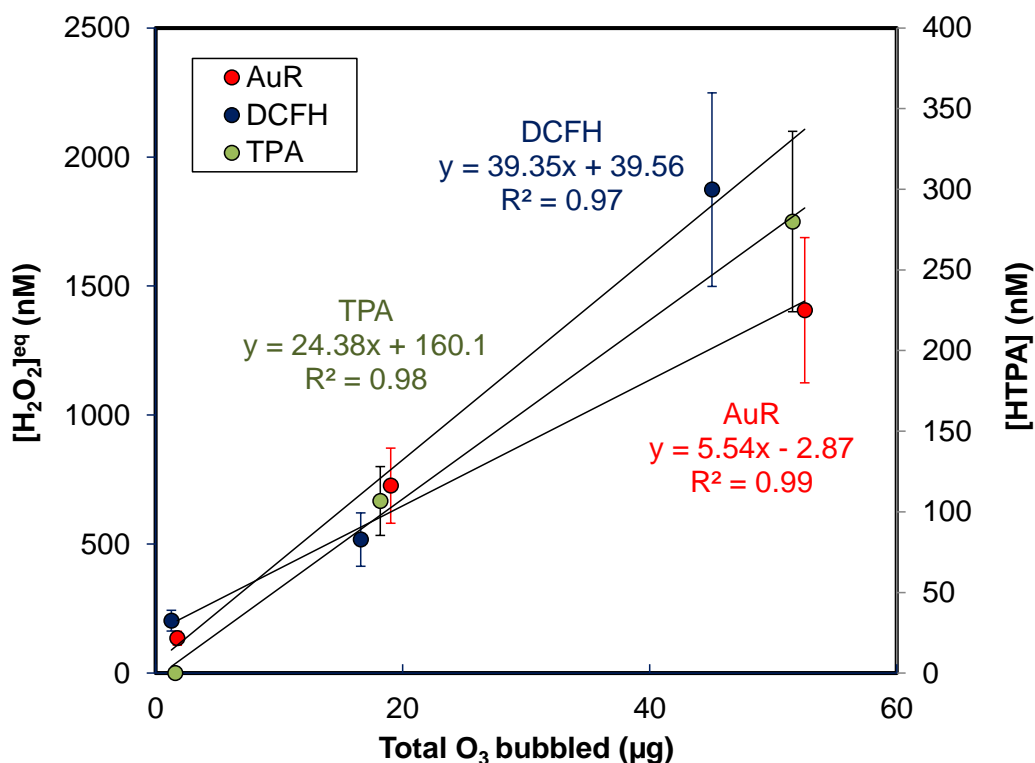
Table A.1.2. Experimental conditions and results for H_2O_2 collection efficiency with each fluorescent probe

Probe	T (°C)	$[H_2O_2]_{aq}$ (mM)	Sample time (min)	Sampling flow rate (L min ⁻¹)	Expected $[H_2O_2]_{gas}$ (ppb)	Measured $[H_2O_2]_{gas}$ (ppb)	Collection efficiency, CE (%)	Recovery efficiency, RE (%)
DCFH	12-14	12.7	23	0.70	35 – 49	42 ± 1	100	100
AuR	12-14	1.27	30	0.75	3.8 – 4.7	3.1 ± 1.1	100	73
TPA	12-14	12.7	30	0.70	35 – 49	n.d.	N/A	0

A.1.3. Effect of ozone on ROS sampling

Some of the tested air cleaners are ozone emitters. For that reason, we evaluated potential sampling artifacts due to the presence of ozone. Experiments were carried out for each of the three probes. In each case, two impingers in series containing the corresponding sampling buffers were connected downstream of an OG-2 ozone generator (UVP, Upland CA), which was fed with “zero” quality clean air to produce controlled concentrations of O₃ in the range 13 – 470 ppbv. The low-end of this range corresponded to typical indoor values, and the high-end to levels that may be reached in a small indoor space with a commercial ozone generating air cleaning device. In all cases, 50 – 60 L samples were collected by drawing air at rates of 0.75 – 0.85 L min⁻¹. Ozone concentrations were determined using a photometric ozone analyzer (Advanced Pollution Instrumentation Inc., San Diego CA), and ROS were quantified fluorometrically in duplicate determinations following the above-described protocol. The results of these tests are illustrated in Figure A.1.4.

Figure A.1.4. Equivalent H₂O₂ and HTPA concentrations determined in the presence of ozone



Ozone has a complex chemistry in aqueous solution that, under most conditions, leads to the formation of hydroxyl radicals, peroxides and superoxides. These species can react with one or more of the fluorometric probes and cause sampling interferences leading to over-reporting ROS concentrations. A simplified scheme illustrating these processes is shown in Figure A.1.5.

In Figure A.1.4, the total amount of O_3 bubbled from an ozone generator is plotted against the equivalent aqueous hydrogen peroxide concentration, $[H_2O_2]^{eq}$, measured in the sampling solutions at the end of the DCFH and AuR tests (represented in the left y-axis). Results from the TPA tests are plotted in terms of aqueous HTPA concentrations (in the right y-axis). In all cases, linear trends were observed, suggesting that the measured signal is proportional to the amount of ozone circulated through the aqueous medium. DCFH showed the highest response for the same amount of O_3 bubbled, in good agreement with the fact that it can detect a broad variety of ROS including dissolved O_3 . Instead, AuR and TPA reacted with peroxides and OH^\bullet , respectively. We assume that AuR reacted primarily with the main stable peroxide generated by O_3 in water, H_2O_2 . In the case of TPA, it detected the OH^\bullet radicals generated during that process.

It is well known that H_2O_2 and peroxides are present in secondary organic aerosol particles formed in the ozonolysis of terpenoids (Wang et al, 2011). However, the effect of ozone observed in our experiments was equally present in Phase 1, in the absence of terpenoids and other ozone-reacting VOCs.

Further evidence of the role played by dissolved ozone in ROS sampling artifacts was obtained from carrying out similar determinations at different sampling temperatures, in the range 3 – 18 °C. Ozone solubility decreased with increasing temperature of the sampling buffer, leading to a reduction in the amount of ROS detected. The total amount of ROS captured, expressed in equivalent H_2O_2 aqueous concentration, $[H_2O_2]^{eq}$, was measured in each case with the DCFH method and correlated with the expected decrease in ozone solubility, as shown in Figure A.1.6. In each of these three tests, the concentration of ozone in the air circulated through the impingers was 470 ppb, and the volume of air sampled in each case over approximately one hour was 50 L. We observed a marked effect of the buffer temperature, suggesting that ozone dissolution was the main factor driving the formation of ROS in the system. When temperature decreased, the total amount of ozone dissolved increased and, with it, the amount of ROS generated into the impingers.

Figure A.1.5. Schematic representation of chemical processes in aqueous solution leading to formation of ROS from ozone decomposition

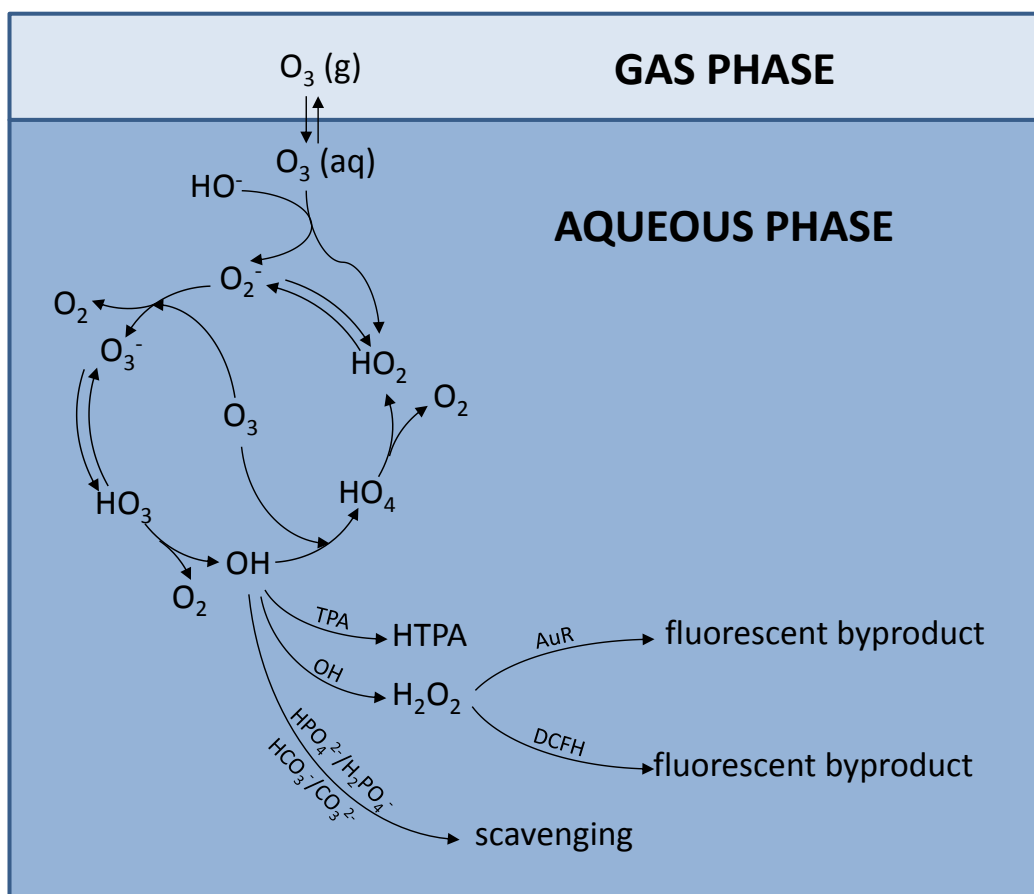
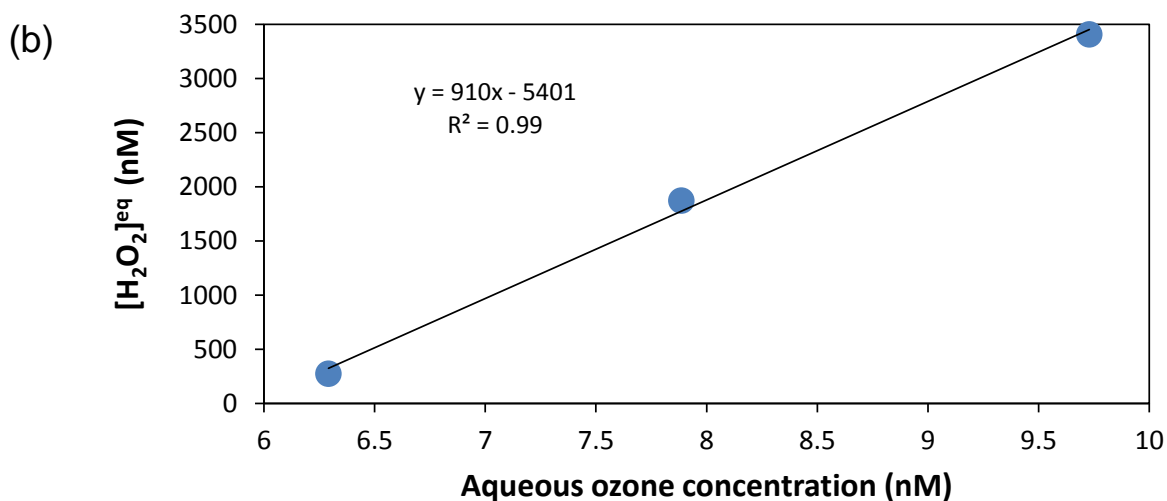
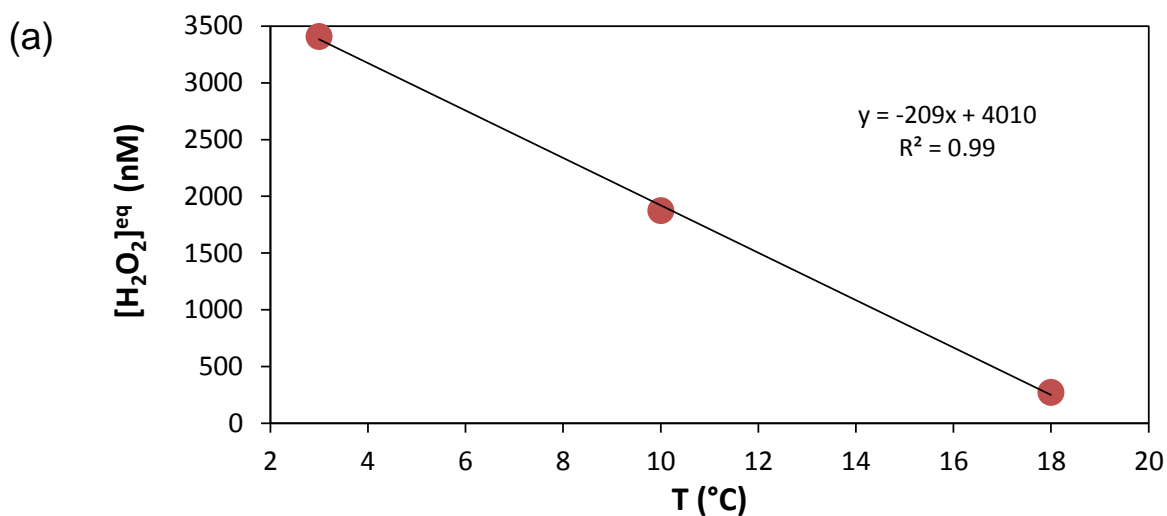


Figure A.1.6: Equivalent H_2O_2 determined with the DCFH method at three collection temperatures, by sampling 50 L of air containing 470 ppb O_3 (g)

(a) Effect of temperature;

(b) effect of O_3 (aq) concentration calculated with the Henry's law constant in the same tests.



APPENDIX 2

SUMMARY OF MEASUREMENTS OF EXPERIMENTS DESCRIBED IN SECTION 4

We present as appendices Tables A.2.1 to A.2.7, containing the pollutant concentrations determined in experiments described in Section 4, which were used in the models described in Section 5.

Table A.2.1: Pollutant concentrations measured in PAC1 experiments

PAC1	PHASE 1		PHASE 2	
	OFF	ON	OFF	ON
VOCs (ppb)				
ethanol	3.5	1.74	8.3	8.3
hexane	0.11	0.06	56.5	38.6
butanal	0.10	0.06	5.1	3.1
benzene	1.2	0.95	9.7	8.5
TCE	n.d.	n.d.	7.2	6.3
toluene	0.33	0.15	17.1	14.9
pyridine	n.d.	n.d.	5.2	4.8
o-xylene	0.09	0.06	8.5	7.6
styrene	0.15	0.08	2.6	2.4
d-limonene	0.06	0.03	4.6	4.4
formaldehyde	3.3	2.1	38.0	40.9
acetaldehyde	1.27	0.54	0.59	0.50
acetone	3.7	1.6	1.5	2.0
UFP (# cm⁻³)	324	315	443	491
O₃ (ppb)	1.4	1.7	1.2	1.6
air exchange rate (h⁻¹)	0.57	0.54	0.44	0.48
duration (h)	40	30	90	45

UFP and O₃ concentrations listed in this table, as well as the air exchange rate values, correspond to the average over the whole ON or OFF periods. The duration of each period is reported in the table.

The VOC concentrations correspond to an integrated 1-h period at the end of each ON and OFF period.

Table A.2.2: Pollutant concentrations measured in PAC2 experiments

PAC2	PHASE 1		PHASE 2	
	OFF	ON	OFF	ON
VOCs (ppb)				
ethanol	0.55	0.65	1.0	1.6
hexane	0.21	0.23	37.6	45.6
butanal	0.09	0.11	4.5	4.7
benzene	2.2	1.8	8.0	8.4
TCE	n.d.	n.d.	5.0	6.13
toluene	0.44	2.68	12.1	15.5
pyridine	n.d.	n.d.	3.8	4.0
o-xylene	0.14	0.15	3.1	3.8
styrene	0.12	0.11	1.5	1.8
d-limonene	0.09	0.10	2.4	2.5
formaldehyde	0.62	0.91	15.4	17.5
acetaldehyde	0.40	0.52	0.25	0.34
acetone	1.1	1.3	1.1	0.88
UFP (# cm⁻³)	886	148	572	58
O₃ (ppb)	2.4	2	2.3	2.5
air exchange rate (h⁻¹)	0.53	0.56	0.58	0.58
duration (h)	20	25	20	50

UFP and O₃ concentrations listed in this table, as well as the air exchange rate values, correspond to the average over the whole ON or OFF periods. The duration of each period is reported in the table.

The VOC concentrations correspond to an integrated 1-h period at the end of each ON and OFF period.

Table A.2.3: Pollutant concentrations measured in PAC3 experiments

PAC3	PHASE 1		PHASE 2	
	OFF	ON	OFF	ON
VOCs (ppb)				
ethanol	0.99	0.00	1.2	0.79
hexane	0.06	0.02	17.7	12.0
butanal	0.08	0.00	5.6	3.2
benzene	0.95	0.18	7.2	5.1
TCE	n.d.	n.d.	7.9	5.5
toluene	0.15	0.28	25.8	17.9
pyridine	n.d.	n.d.	12.3	8.8
o-xylene	0.03	0.04	10.6	6.9
styrene	0.13	0.01	5.5	0.12
d-limonene	0.03	0.01	8.7	0.24
formaldehyde	1.5	2.7	25.8	20.8
acetaldehyde	0.28	0.58	0.38	0.68
acetone	1.7	1.8	1.1	7.4
benzaldehyde	0.03	3.3	0.15	4.6
UFP (# cm⁻³)	716	491	496	3167
O₃ (ppb)	1	165	2.2	162
air exchange rate (h⁻¹)	0.48	0.33	0.28	0.3
duration (h)	43	24	45	20

UFP and O₃ concentrations listed in this table, as well as the air exchange rate values, correspond to the average over the whole ON or OFF periods. The duration of each period is reported in the table.

The VOC concentrations correspond to an integrated 1-h period at the end of each ON and OFF period.

Table A.2.4: Pollutant concentrations measured in PAC4 experiments

PAC4	PHASE 1		PHASE 2	
	OFF	ON	OFF	ON
VOCs (ppb)				
ethanol	n.d.	n.d.	34.3	14.1
hexane	0.01	0.03	38.5	28.1
butanal	n.d.	0.03	6.3	5.1
benzene	0.54	0.79	12.7	9.8
TCE	n.d.	n.d.	11.3	9.2
toluene	0.11	0.10	25.8	19.4
pyridine	n.d.	n.d.	8.7	6.2
o-xylene	0.03	0.02	5.3	4.1
styrene	0.09	0.08	1.9	1.5
d-limonene	n.d.	n.d.	2.0	1.7
formaldehyde	0.99	1.0	7.5	9.4
acetaldehyde	0.26	0.28	0.29	0.32
acetone	0.92	0.87	1.1	1.0
UFP (# cm⁻³)	619	401	846	410
O₃ (ppb)	1.6	3.5	1.0	4.8
air exchange rate (h⁻¹)	0.31	0.37	0.54	0.58
duration (h)	26	25	26	22

UFP and O₃ concentrations listed in this table, as well as the air exchange rate values, correspond to the average over the whole ON or OFF periods. The duration of each period is reported in the table.

The VOC concentrations correspond to an integrated 1-h period at the end of each ON and OFF period.

Table A.2.5: Pollutant concentrations measured in PAC5 experiments with heating and ionizer

PAC5 heating + ionizer	PHASE 1		PHASE 2	
	OFF	ON	OFF	ON
VOCs (ppb)				
ethanol	0.35	0.32	0.18	0.44
hexane	0.18	0.17	12.0	16.7
butanal	0.12	0.13	2.8	5.8
benzene	1.5	1.8	3.0	4.1
TCE	n.d.	n.d.	0.8	1.4
toluene	0.49	0.64	8.1	11.8
pyridine	0.09	0.14	1.0	2.2
o-xylene	0.13	0.23	6.5	9.8
styrene	0.15	0.25	4.6	7.1
d-limonene	0.15	0.22	14.4	23.2
formaldehyde	3.4	4.6	35.5	20.3
acetaldehyde	0.35	0.55	0.87	1.1
acetone	0.95	1.3	2.5	5.6
UFP (# cm⁻³)	341	792	352	420
O₃ (ppb)	N.D.	N.D.	N.D.	N.D.
air exchange rate (h⁻¹)	0.66	0.66	0.61	0.62
duration (h)	15	10	35	10

UFP and O₃ concentrations listed in this table, as well as the air exchange rate values, correspond to the average over the whole ON or OFF periods. The duration of each period is reported in the table.

The VOC concentrations correspond to an integrated 1-h period at the end of each ON and OFF period.

Table A.2.6: Pollutant concentrations measured in PAC5 experiments with only ionizer

PAC5 only ionizer	PHASE 1		PHASE 2	
	OFF	ON	OFF	ON
VOCs (ppb)				
ethanol	0.42	0.49	22.2	29.5
hexane	0.22	0.26	35.5	44.6
butanal	0.15	0.21	4.4	4.5
benzene	1.8	2.9	4.6	5.7
TCE	n.d.	n.d.	3.3	4.0
toluene	0.59	0.99	14.6	16.6
pyridine	0.11	0.22	4.5	4.9
o-xylene	0.16	0.36	12.3	13.6
styrene	0.19	0.39	8.7	9.5
d-limonene	0.18	0.34	22.4	23.9
formaldehyde	0.78	1.28	34.3	31.1
acetaldehyde	0.14	0.50	1.2	1.2
acetone	0.26	1.4	4.5	4.4
UFP (# cm⁻³)	N.D.	N.D.	N.D.	N.D.
O₃ (ppb)	3.0	2.2	1.2	2.1
air exchange rate (h⁻¹)	0.66	0.66	0.61	0.62
duration (h)	25	24	16	13

UFP and O₃ concentrations listed in this table, as well as the air exchange rate values, correspond to the average over the whole ON or OFF periods. The duration of each period is reported in the table.

The VOC concentrations correspond to an integrated 1-h period at the end of each ON and OFF period.

Table A.2.7: Pollutant concentrations measured in PAC6

PAC6	PHASE 1		PHASE 2	
	OFF	ON	OFF	ON
VOCs (ppb)				
ethanol	n.d.	n.d.	1.2	1.6
hexane	0.19	0.21	56.3	53.8
butanal	0.12	0.13	6.5	4.9
benzene	0.95	2.0	18.7	18.0
TCE	n.d.	n.d.	16.1	15.6
toluene	0.43	0.63	36.2	34.7
pyridine	0.29	0.13	15.7	11.9
o-xylene	0.22	0.19	18.0	14.6
styrene	0.21	0.21	8.5	7.4
d-limonene	0.22	0.18	7.8	7.2
formaldehyde	0.42	0.72	6.2	5.3
acetaldehyde	0.30	0.50	0.35	0.32
acetone	0.56	0.91	0.69	0.79
UFP (# cm⁻³)	318	407	290	120
O₃ (ppb)	2.5	3.3	3.0	4.3
air exchange rate (h⁻¹)	0.31	0.37	0.54	0.58
duration (h)	18	22	40	25

UFP and O₃ concentrations listed in this table, as well as the air exchange rate values, correspond to the average over the whole ON or OFF periods. The duration of each period is reported in the table.

The VOC concentrations correspond to an integrated 1-h period at the end of each ON and OFF period.

APPENDIX 3

CHAMBER CONCENTRATION REDUCTION FACTORS ω_i AND SINGLE-PASS REMOVAL EFFICIENCY $\phi_i^{p,ss}$ DESCRIBED IN SECTION 5

Table A.3.1: VOC removal efficiency parameters corresponding to four air cleaners that showed net VOC elimination

VOCs	PAC1		PAC3		PAC4		PAC6	
	$\phi_i^{p,ss}$	ω_i	$\phi_i^{p,ss}$	ω_i	$\phi_i^{p,ss}$	ω_i	$\phi_i^{p,ss}$	ω_i
ethanol	n.d.	n.d.	0.29	0.33	>1	0.59	n.d.	n.d.
hexane	0.031	0.32	0.28	0.32	0.52	0.27	0.12	0.04
butanal	0.042	0.39	0.45	0.43	0.34	0.19	0.88	0.25
benzene	0.009	0.12	0.24	0.29	0.40	0.22	0.11	0.04
TCE	0.010	0.13	0.26	0.30	0.31	0.18	0.08	0.03
toluene	0.010	0.13	0.26	0.30	0.46	0.25	0.11	0.04
pyridine	0.005	0.07	0.24	0.29	0.56	0.29	0.83	0.24
o-xylene	0.008	0.11	0.31	0.34	0.45	0.24	0.60	0.19
styrene	0.005	0.07	>1	0.98	0.47	0.25	0.39	0.13
d-limonene	0.002	0.04	>1	0.97	0.28	0.17	0.23	0.08
formaldehyde	emitted		0.14	0.20	emitted		0.42	0.14
acetaldehyde	0.013	0.16	emitted		emitted		0.26	0.09
acetone	emitted		emitted		0.12	0.08	emitted	

Table A.3.2: UFP removal efficiency parameters corresponding to two air cleaners that showed net elimination of particulate matter

UFP	PAC2		PAC4	
	$\phi_i^{p,ss}$	ω_i	$\phi_i^{p,ss}$	ω_i
Phase 1	0.27	0.83	0.77	0.35
Phase 2	0.49	0.90	>1	0.52